

CARBON PUMPS IN THE  
BENGUELA CURRENT UPWELLING SYSTEM

Dissertation zur Erlangung des Doktorgrades  
an der Fakultät für Mathematik, Informatik und Naturwissenschaften  
Fachbereich Geowissenschaften  
der Universität Hamburg

vorgelegt von

Anita Flohr

Hamburg, 2014

Als Dissertation angenommen

vom Fachbereich Geowissenschaften der Universität Hamburg

auf Grund der Gutachten von

Prof. Dr. Kay-Christian Emeis

und

Dr. Tim Rixen

Tag der Disputation: 13.01.2015

The study has been realised from April 2009 to September 2014 at the Leibniz Center for Tropical Marine Ecology in Bremen in the frame of the GENUS programme (Geochemistry and Ecology of the Namibian Upwelling System). This project has been funded by the German Federal Ministry of Education and Research (03F0497D-ZMT) and is an endorsed project of the Integrated Marine Biogeochemistry and Ecosystem Research (IMBER).



## CONTENT

Summary.....	1
Zusammenfassung .....	4
1. Scientific background and objectives.....	7
1.1. The marine carbon cycle.....	7
1.1.1. Significance in global carbon cycling.....	7
1.1.2. Chemical basis - The carbonate system of seawater.....	9
1.2. Drivers, strength and efficiency of marine CO <sub>2</sub> sequestration .....	12
1.3. Relevance of eastern boundary upwelling systems in marine carbon cycling.....	14
1.3.1. The Benguela Current upwelling system .....	15
1.4. Objectives and outline.....	18
2. Outline of publications .....	22
3. Chapter I.....	25
4. Chapter II .....	51
5. Chapter III.....	69
6. Chapter IV.....	81
7. Synoptic discussion and conclusion.....	97
7.1. Aspects of carbon pumping in the Benguela Current upwelling system.....	97
7.2. Impacts of climate change .....	104
8. Perspectives.....	106
Figure captions .....	108
Table captions.....	117
References .....	119
List of co-author publications.....	135
Curriculum Vitae.....	137
Danksagung .....	138
Erklärung .....	141





---

## ABBREVIATIONS

$A_T$	see TA
BUS	Benguela Current upwelling system
C	carbon
$\text{CaCO}_3$	calcium carbonate
cm	centimetre
$C_T$	see DIC
$\text{CO}_2$	carbon dioxide
d	day
$\delta^{13}\text{C}_{\text{CT}}$	stable isotope ratio of dissolved inorganic carbon
DIC, $C_T$	dissolved inorganic carbon
$\delta^{15}\text{N}_{\text{NO}_3^-}$	stable isotope ratio of dissolved nitrate
DOC	dissolved organic carbon
EBUS	eastern boundary upwelling system
ESACW	Eastern South Atlantic Central Water
$f\text{CO}_2$	fugacity of $\text{CO}_2$
g	gram
GENUS	Geochemistry and Ecology of the Namibian Upwelling System
$\text{H}_2\text{S}$	hydrogen sulphide
$\text{km}^2$	square kilometre
l	litre
$\text{m}^2$	square meter
N	fixed nitrogen ( $\text{NO}_3^-$ , $\text{NO}_2^-$ , $\text{NH}_4^+$ )
$\text{N}_2$	di-nitrogen gas
$\text{N}^*$	deviation of fixed nitrogen with respect to phosphate; based on the Redfield ratio of N/P = 16/1
NatMIRC	National Marine Information and Research Centre in Swakopmund
NBUS	northern Benguela upwelling system
$\text{NH}_4^+$	ammonium
$\text{NO}_3^-$	nitrate
$\text{NO}_2^-$	nitrite
$\text{O}_2$	oxygen
OM	organic matter
$\Omega_A$	saturation state of aragonite in seawater

---

$\Omega_C$	saturation state of calcite in seawater
P*	deviation of phosphate with respect to N; based on the Redfield ratio of N/P = 16/1
PIC, C <sub>CaCO3</sub>	particulate inorganic carbon
P, PO <sub>4</sub> <sup>3-</sup>	phosphate
PO <sub>4</sub> <sup>0</sup>	preformed phosphate
pCO <sub>2</sub>	partial pressure of CO <sub>2</sub>
POC, C <sub>org</sub>	particulate organic carbon
SACW	South Atlantic Central Water
Si(OH) <sub>4</sub>	silicate
SBUS	southern Benguela upwelling system
TA, A <sub>T</sub>	total alkalinity
yr	year
%	percent
°C	degree Celsius

## FACTORS

P	peta	10 <sup>15</sup>
T	terra	10 <sup>12</sup>
G	giga	10 <sup>9</sup>
M	mega	10 <sup>6</sup>
k	kilo	10 <sup>3</sup>
m	milli	10 <sup>-3</sup>
μ	micro	10 <sup>-6</sup>
n	nano	10 <sup>-9</sup>



## SUMMARY

The biological carbon (C) pump influences the flux of carbon dioxide (CO<sub>2</sub>) between the ocean and the atmosphere by carbon assimilation during the photosynthesis of particulate organic carbon (POC) and the precipitation of calcium carbonate particles (PIC). Regions of intense biological carbon pumping are eastern boundary upwelling systems, among which the Benguela upwelling system (BUS) is the most productive but the least studied one.

This work is based on data obtained during several research cruises between 2009 and 2011 in the framework of the GENUS project (Geochemistry and Ecology of the Namibian Upwelling System). GENUS is a multi-disciplinary programme that aims to improve our understanding of the complex interaction between biological, biogeochemical and physical processes within the BUS and their response to climate change.

The main objective of this thesis is to investigate the functioning of the biological carbon pump in the northern BUS (NBUS), to assess whether the BUS is a net source or sink for carbon and to give basis for evaluating potential responses of the BUS to global change.

Dissolved inorganic nutrient and carbonate chemistry data was raised and used to study the spatio-temporal variability of the remineralisation ratios of C, nitrogen (N) and phosphate (P) (C/N/P) with emphasis on the variability of N deficiency, which is a major factor that limits the production of POC. Records of annual particle fluxes along with hydrographical data were obtained by a mooring on the shelf off Walvis Bay. In conjunction with meteorological records, these data were used to investigate the influence of upwelling on the particle fluxes with a focus on the factors that control the export of POC and PIC on the shelf. Furthermore, carbonate chemistry data allow to determine the variability of the carbonate saturation state ( $\Omega$ ) which influences calcification, growth and survival in many marine calcifying organisms. Along with patterns of air-sea CO<sub>2</sub> fluxes, these results were used to evaluate the C source-sink function of the BUS.

The results show that the release of C, N and P in the course of organic matter decomposition follows the Redfield stoichiometry of C/N/P of 106/16/1 in the oxygenated

water column. However, N loss and P input, which occur in sub- and anoxic bottom waters overlying the mud belt of the Namibian shelf, lower the N/P to  $<16$  in upwelling intermediate water. Together, these processes result in an N deficiency ( $-N^*$ ), equivalent to a relative P excess ( $+P^*$ ), which surfaces and extends to the adjacent hemipelagic ocean. Around 300 km offshore,  $P^*$  ranged between  $P^* \sim 0.007 \mu\text{mol kg}^{-1}$  in 2008 and  $P^* \sim 0.3 \mu\text{mol kg}^{-1}$  in 2010/2011. The results suggest that the magnitude of exported  $P^*$  is not only controlled by the degree of local  $\text{O}_2$  deficiency on the shelf, but as well by the amount of remotely supplied  $N^*$  excess ( $N/P >16$ ,  $+N^*$ ). This  $+N^*$  is carried along with South Atlantic Central Water (SACW) to the NBUS shelf and varied between  $N^* \sim 12 \mu\text{mol kg}^{-1}$  in 2008 and  $N^* \sim 3-4 \mu\text{mol kg}^{-1}$  in 2009/2011 off Kunene. The findings point to a mechanism which replenishes the  $N^*$  deficiency on the NBUS shelf and thereby counteracts the N limitation that hampers the N-driven  $\text{CO}_2$  drawdown of the biological carbon pump in the NBUS.

The combined results of hydrographical, meteorological and particle flux data show that even comparatively weak upwelling of high SACW fractions fuels higher POC fluxes ( $>91 \text{ g POC m}^{-2} \text{ yr}^{-1}$ ) than intense upwelling of Eastern South Atlantic Central Water (ESACW). This reflects the higher nutrient inventory of SACW compared to ESACW, among other factors. The results further indicate that the POC export on the shelf is dominated by diatom productivity. The decomposition of the basically diatomaceous organic matter causes very low  $\Omega$  ( $\Omega_{\text{Amin}} = 0.7$ ,  $\Omega_{\text{Cmin}} = 1.2$ ) and high silicate concentrations in ascending sub-thermocline waters. This corrosive water reduces the PIC formation in the surface and its export ( $11 \text{ g PIC m}^{-2} \text{ yr}^{-1}$ ) on the Namibian shelf, relative to the high, diatom-dominated POC formation and export ( $66 \text{ g POC m}^{-2} \text{ yr}^{-1}$ ). This results in a high POC/PIC ratio of 6 in sinking matter, pointing to an efficient  $\text{CO}_2$  uptake by the coastal biological carbon pump. Towards the slope and the open ocean, an increasing contribution of PIC to POC export is enabled by rising  $\Omega$  and depleted silicate concentrations, providing an ecological advantage for carbonate producers. As indicated by the results of  $P^*$  in offshore waters, the biological pump's efficiency in the offshore sector of the upwelling system is hampered by N limitation, thus lowering the N-driven  $\text{CO}_2$  drawdown. In terms of nutrient stoichiometry, the unused  $P^*$  constitutes a leakage of potential C export that accounts for  $\sim 25\%$  of the total N-driven potential export fluxes of  $\sim 98 \text{ Tg C yr}^{-1}$  of the NBUS. Clearly,

NBUS productivity suffers from the impact of N loss or P gain incurred from suboxic conditions on the shelf.

The CO<sub>2</sub> emission patterns reveal that the NBUS is a CO<sub>2</sub> source in the order of 13.6 Tg C yr<sup>-1</sup>, likely reflecting the N deficit in upwelling subsurface water. The southern BUS (SBUS) is a significant sink of -3.4 Tg C yr<sup>-1</sup> and reflects the higher contribution of biologically unused, preformed nutrients in upwelling source waters of the SBUS compared to the NBUS.

Adding the combined POC and PIC export sink of (-66 and -11 g C m<sup>-2</sup> yr<sup>-1</sup>) to the CO<sub>2</sub> emissions of the NBUS (+71 g C m<sup>-2</sup> yr<sup>-1</sup>) indicates that the NBUS is a small net sink of -6 g C m<sup>-2</sup> yr<sup>-1</sup>.

## ZUSAMMENFASSUNG

Die biologische Kohlenstoffpumpe beeinflusst den Austausch von Kohlenstoffdioxid ( $\text{CO}_2$ ) zwischen dem Ozean und der Atmosphäre durch die Photosynthese von partikulärem organischem Kohlenstoff (POC) sowie durch die Bildung von partikulärem Kalziumcarbonat (PIC). Regionen mit intensivem biologischem Kohlenstoffumsatz sind die Hauptauftriebsgebiete an den Ostseiten der Ozeanbecken. Das Benguela Auftriebsgebiet (BUS) ist das produktivste der vier Hauptauftriebsgebiete, über dessen Kohlenstoff-Kreislauf bisher dennoch relativ wenig bekannt ist.

Diese Doktorarbeit basiert auf Daten, die während diverser Schiffsexpeditionen zwischen 2009 und 2011 im Rahmen des GENUS Projektes (Geochemistry and Ecology of the Namibian Upwelling System) erhoben wurden. GENUS ist ein inter-disziplinäres Projekt, das darauf abzielt die komplexen Wechselwirkungen zwischen biologischen, biogeochemischen und physikalischen Prozessen im Benguela Auftriebssystem zu verstehen, sowie deren Reaktionen auf den Klimawandel abzuschätzen.

Das Hauptziel dieser Doktorarbeit ist es, die Funktionsweise der biologischen Kohlenstoffpumpe im nördlichen Benguela Auftriebsgebiet (NBUS) zu untersuchen, um Rückschlüsse auf die Kohlenstoffquellen- bzw. Kohlenstoffsinkenfunktion des Benguela Auftriebsgebietes zu ziehen. Zudem soll diese Doktorarbeit Anhaltspunkte liefern, anhand derer die Reaktionen des Systems auf den Klimawandel abgeschätzt werden können.

Gelöste, anorganische Nährstoffe und Parameter des Karbonatsystems wurden erhoben, um die räumliche und zeitliche Variabilität der C/N/P-Remineralisierungsverhältnisse zu bestimmen. Dabei wurde der Fokus auf die Dynamik von Stickstoffdefiziten ( $-\text{N}^*$ ) sowie die Variabilität der Karbonatsättigung ( $\Omega$ ) gerichtet, die beide die Bildung von POC und PIC beeinflussen. Mit Hilfe einer Verankerung wurden auf dem Namibischen Schelf vor Walvis Bay ein Jahr lang hydrographische Messungen gemacht und absinkendes partikuläres Material eingefangen. Zusammen mit meteorologischen Daten wurden diese Messreihen ausgewertet, um den Einfluss des Auftriebs auf die Menge und relative Zusammensetzung des Partikelflusses zu bestimmen. Darüber hinaus wurden Unterwegsmessungen des  $\text{CO}_2$  Partialdrucks ( $\text{pCO}_2$ ) im Oberflächenwasser durchgeführt,

um das Ausmaß der CO<sub>2</sub>-Flüsse zwischen der Meeresoberfläche und der Atmosphäre zu quantifizieren.

Die Ergebnisse zeigen, dass die Freisetzung von biologisch verfügbarem Stickstoff (N) und Phosphat (P) während des aeroben Abbaus von organischem Material der Redfield Stöchiometrie von C/N/P = 106/16/1 folgt. In sub- und anoxischem Bodenwasser, das den Schlammgürtel auf dem Namibischen Schelf bedeckt, werden die N/P Verhältnisse durch den Einfluss von N-Reduktion und P-Freisetzung stark verringert. Dies zeigt sich in einem N-Defizit (-N\*), gleichbedeutend mit einem P-Überschuss (+P\*), das aufgetrieben und in der Oberflächenströmung auf den offenen, nährstoffarmen Südatlantik transportiert wird. Ungefähr 300 km von der Küste entfernt, schwankte P\* zwischen 0.007 µmol kg<sup>-1</sup> in 2008 und 0.3 µmol kg<sup>-1</sup> in den Jahren 2010/2011. Die Ergebnisse weisen darauf hin, dass die Veränderlichkeit des P\*-Exportes nicht nur durch das Ausmaß des Sauerstoff-Defizites auf dem Schelf, sondern zusätzlich durch die Menge an extern zugeführtem N-Überschuss (+N\*) kontrolliert wird. Dieser N-Überschuss gelangt zusammen mit dem Südatlantischen Zentralwasser (SACW) in das NBUS und schwankte zwischen N\* = ~12 µmol kg<sup>-1</sup> in 2008 und N\* = ~3-4 µmol kg<sup>-1</sup> in den Jahren 2009/2011. Die Ergebnisse weisen auf einen Mechanismus hin, der zu einem Ausgleich des N\*-Mangels beiträgt, und damit der N-Limitierung entgegenwirkt, die die CO<sub>2</sub> Aufnahmefähigkeit der biologischen Pumpe im NBUS abschwächt.

Ein erhöhter Einstrom des SACW aus dem Norden auf den Schelf des NBUS findet bei geringer Auftriebsaktivität im Südsommer statt. Die Ergebnisse hydrographischer und meteorologischer Aufzeichnungen, sowie des Partikelflusses zeigen, dass geringer Auftrieb von hohen SACW-Anteilen zu einem höheren POC-Export (>91 g POC m<sup>-2</sup> yr<sup>-1</sup>) führt, als intensiver Auftrieb von hohen Anteilen des Östlichen Südatlantischen Zentralwassers (ESACW). Dies spiegelt unter anderem den hohen Nährstoffgehalt des SACW im Vergleich zum ESACW wider. Die qualitativen Analysen ergaben, dass der POC-Export auf dem Schelf von Diatomeen dominiert wird. Der Abbau des Diatomeen-dominierten organischen Materials verursacht geringe Karbonatsättigungen ( $\Omega_{\text{Amin}} = 0.7$ ,  $\Omega_{\text{Cmin}} = 1.2$ ), sowie hohe Silikatkonzentrationen im auftreibenden Wasser. Die geringen  $\Omega$ -Werte führen zu einer Verringerung der PIC Bildung in der Oberfläche und damit zu einem geringen PIC-Export von 11 g C m<sup>-2</sup> yr<sup>-1</sup> verglichen mit dem vielfach höheren POC-Export von 66 g

$\text{C m}^{-2} \text{ yr}^{-1}$ . Dies spiegelt sich in einem hohen POC/PIC Verhältnis von  $\sim 6$  in absinkendem partikulärem Material wider, das auf eine effiziente  $\text{CO}_2$  Aufnahme der biologischen Pumpe schließen lässt. Mit zunehmender Entfernung von der Küste nimmt  $\Omega$  im Oberflächenwasser zu und die Silikat-Konzentration ab, und bietet damit bessere Voraussetzung für Entwicklung von kalzifizierenden planktischen Organismen. Die Effizienz der biologischen Pumpe in küstenfernen Regionen wird durch das zuvor erwähnte  $\text{N}^*$ -Defizit geschwächt, das im NBUS rund 25 % des gesamten N-getriebenen potentiellen POC-Exportes von  $\sim 98 \text{ Tg C yr}^{-1}$  ausmacht. Damit wird deutlich, dass das  $\text{N}^*$ -Defizit signifikant zur Verringerung der Produktivität des NBUS beiträgt.

Die  $\text{CO}_2$  Emissionen im BUS weisen eine räumliche Teilung auf, die unter den Hauptauftriebsgebieten eine Besonderheit darstellt. Das NBUS ist eine  $\text{CO}_2$  Quelle von  $+13.6 \text{ Tg C yr}^{-1}$  für die Atmosphäre, und ist das Resultat der ausgeprägten N-Reduktion im Auftriebswasser. Im Gegensatz zum NBUS ergaben die Messungen im SBUS eine  $\text{CO}_2$  Aufnahme von  $-3.4 \text{ Tg C yr}^{-1}$ , wonach das SBUS eine Senke für atmosphärisches  $\text{CO}_2$  darstellt. Die Ergebnisse weisen darauf hin, dass die Ursache für die räumliche Teilung der  $\text{CO}_2$ -Flüsse im BUS auf den Anteil biologisch ungenutzter Nährstoffe, sogenannter *preformed nutrients*, im Quellwasser zurückzuführen ist.

Die Gegenüberstellung der  $\text{CO}_2$ -Quelle des NBUS von  $+71 \text{ g C m}^{-2} \text{ yr}^{-1}$  und der kombinierten POC und PIC-Export Senke von  $-66$  und  $-11 \text{ g C m}^{-2} \text{ yr}^{-1}$  zeigt, dass das NBUS eine geringe Netto-Kohlenstoffsенke von  $-6 \text{ g C m}^{-2} \text{ yr}^{-1}$  darstellt.

## 1. SCIENTIFIC BACKGROUND AND OBJECTIVES

### 1.1. THE MARINE CARBON CYCLE

#### 1.1.1. SIGNIFICANCE IN GLOBAL CARBON CYCLING

The oceanic carbon reservoir, mainly in the form of dissolved inorganic carbon (DIC), exceeds the atmospheric carbon dioxide (CO<sub>2</sub>) reservoir by a factor of ~50 and emphasises the strong potential impact that changes in the oceanic carbon fluxes can exert on atmospheric CO<sub>2</sub> concentrations and thus on earth's climate (Falkowski et al., 2000; Sigman and Boyle, 2000; Sabine et al., 2004). Marine carbon cycling affects the atmospheric CO<sub>2</sub> concentration through physical (solubility pump) and biological (biological pump) processes that reduce the surface concentration of DIC relative to the deep ocean (Volk and Hoffert, 1985) (Fig. 1.1.).

The solubility pump influences the flux of CO<sub>2</sub> between the ocean and the atmosphere via the interplay of two processes: high CO<sub>2</sub> solubility in cold, relatively fresh seawater in combination with the ocean's thermohaline circulation. This leads to the subduction of cold, CO<sub>2</sub> laden water at polar latitudes into the deep ocean which effectively prevents CO<sub>2</sub> from re-equilibrating with the atmosphere for long time scales ranging from decades to >1000 years. The solubility pump is assumed to account for 10-35 % of the vertical DIC gradient in the ocean (Toggweiler et al., 2003; Sarmiento and Gruber, 2006).

The biological carbon pump contributes 65-90 % to the vertical DIC gradient. It regulates the flux of CO<sub>2</sub> between the ocean and the atmosphere via the biologically mediated removal of DIC in the sunlit surface mixed layer by the photosynthetic production of particulate organic carbon (POC) (soft tissue pump) and particulate inorganic carbon (PIC) in the form of carbonate shells (carbonate counter pump). Organic and inorganic C particles sink into the ocean's interior and are subsequently remineralised and/or dissolved to DIC below the thermocline. Most of the organic carbon fixed in the upper ocean, representing 40-60 Pg C yr<sup>-1</sup> (Longhurst et al., 1995; Behrenfeld and Falkowski, 1997; Carr et al., 2006), is consumed by bacteria and higher trophic levels and respired to DIC in the mixed layer. Only a small fraction of ~6-15 % of the POC sinks into

the ocean interior below the euphotic zone (Lutz et al., 2002; Dunne et al., 2007; Henson et al., 2011) and <1 % to below 1000 m water depth (Lutz et al., 2002) and is sequestered there on long time scales equivalent to ocean turnover times.

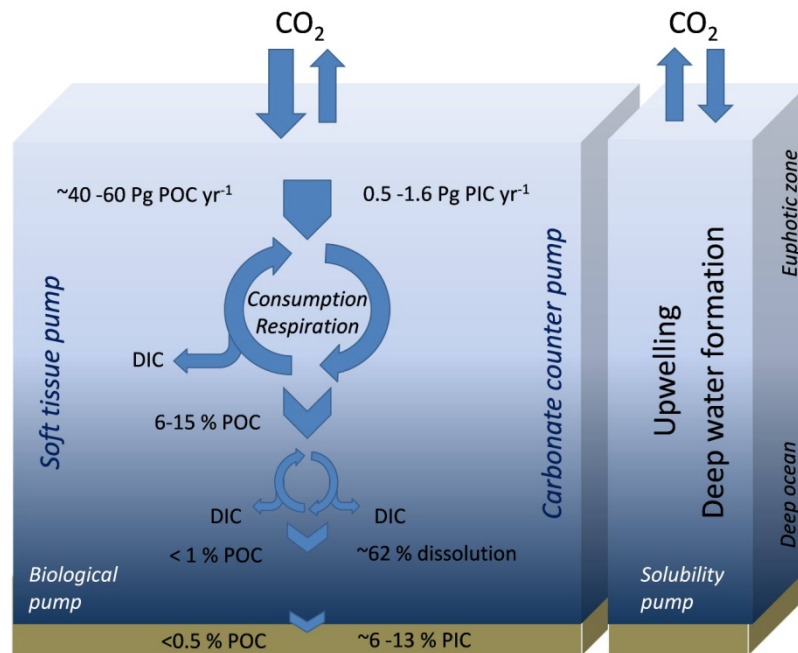


Fig. 1.1.: General schematic of the biological (left) and solubility pump (right) (adapted and modified from Chisholm (2000)) that maintain a DIC gradient between the atmosphere and the deep ocean.

Additionally, many phytoplankton and zooplankton species use DIC to build their  $\text{CaCO}_3$  shells. That way  $0.5 - 1.6 \text{ Pg PIC yr}^{-1}$  sink into the ocean's interior. Around 62 % of the PIC produced in the surface water dissolves, either in the water column or in the sediments (Berelson et al., 2007) and thereby contribute  $\sim 20 \text{ %}$  to the vertical DIC gradient in the ocean (Toggweiler et al., 2003; Sarmiento and Gruber, 2006). Only a small fraction of  $\sim 6 - 13 \text{ %}$  of the PIC is buried permanently (Sarmiento et al., 2002; Berelson et al., 2007). Although the precipitation of  $\text{CaCO}_3$  lowers the DIC concentration in the surface, it is associated with an increase of the  $\text{CO}_2$  partial pressure in seawater ( $p\text{CO}_{2\text{sw}}$ ) (Zeebe and Wolf-Gladrow, 2001). This highlights that the net  $\text{CO}_2$  uptake efficiency of the biological pump critically depends on the relative contribution of the soft tissue and carbonate counter pump (Heinze et al., 1991).

The oceans therefore play an important role in modulating atmospheric CO<sub>2</sub> concentrations at present by acting as net sink for anthropogenic CO<sub>2</sub> (Sabine et al., 2004; Takahashi, 2004; Le Quéré et al., 2014) and on glacial-interglacial time scales (Broecker, 1982; Sigman and Boyle, 2000; Sigman et al., 2010).

### 1.1.2. CHEMICAL BASIS - THE CARBONATE SYSTEM OF SEAWATER

The magnitude and direction of diffusive CO<sub>2</sub> air-sea gas exchange depends on the gradient between the pCO<sub>2</sub> in the surface water (pCO<sub>2sw</sub>) and the atmosphere (pCO<sub>2atm</sub>), among other factors. The burning of fossil fuel, cement production and land use change have contributed to a rise of pCO<sub>2atm</sub> of ~150 ppm as compared to the pCO<sub>2atm</sub> of preindustrial times (250 ppm) (Le Quéré et al., 2014). The higher pCO<sub>2atm</sub> results in an invasion of anthropogenic CO<sub>2</sub> into surface and sub-thermocline waters of the ocean (Sabine et al., 2004).

Apart from temperature and pressure, the pCO<sub>2</sub> in seawater is governed by the total amount of DIC and total alkalinity (TA). As mentioned before, the immense carbon reservoir of the ocean consists to >90 % of DIC (Falkowski et al., 2000; Rhein et al., 2013). The fundamental basis for the high DIC inventory of the ocean arises from the fact that CO<sub>2</sub> not only dissolves in but also reacts with seawater, and forms aqueous CO<sub>2</sub> (CO<sub>2aqua</sub>) and carbonic acid (H<sub>2</sub>CO<sub>3</sub>), summarised as H<sub>2</sub>CO<sub>3</sub>\* which dissociates to bicarbonate (HCO<sub>3</sub><sup>-</sup>) and carbonate (CO<sub>3</sub><sup>2-</sup>) ions:



DIC refers to the sum of all the dissolved inorganic carbon species with HCO<sub>3</sub><sup>-</sup> and CO<sub>3</sub><sup>2-</sup> accounting for ~97 % of the ocean's DIC pool (Zeebe and Wolf-Gladrow, 2001):

$$\text{DIC} = [\text{H}_2\text{CO}_3^*] + [\text{HCO}_3^-] + [\text{CO}_3^{2-}] \quad (2)$$


  
 ~ 0.5 % : 86.5 % : 13 %

The charge of major cations (e.g.  $\text{Ca}^{2+}$ ,  $\text{Mg}^{2+}$ ) in seawater slightly exceeds that of anions ( $\text{Cl}^-$ ,  $\text{SO}_4^{2-}$ ,  $\text{NO}_3^-$ ) and create a small charge imbalance which is mainly compensated for by shifts in the charges of the anions of predominantly carbonic and boric acid, referred to as total alkalinity (TA) (Broecker, 1982; Zeebe and Wolf-Gladrow, 2001):

$$\text{TA} = [\text{HCO}_3^-] + 2 [\text{CO}_3^{2-}] + [\text{OH}^-] - [\text{H}^+] + [\text{B}(\text{OH})_4^-] + \text{minor bases} \quad (3)$$

where  $[\text{OH}^-]$  and  $[\text{B}(\text{OH})_4^-]$  are the concentrations of hydroxide and borate ions, respectively. The TA is alternatively defined as the excess of bases (proton acceptors) over acids (proton donors) and is determined by titration with an acid (Dickson, 1981; Zeebe and Wolf-Gladrow, 2001). In general, the higher the TA at a given DIC concentration, the higher the contribution of  $\text{CO}_3^{2-}$  to total DIC, i.e. the more the equilibrium (Equ. 1) is shifted to the less acidic right hand side.

The invasion of anthropogenic  $\text{CO}_2$  into surface and sub-thermocline waters of the ocean is associated with a shift in the carbonate system from  $\text{CO}_3^{2-}$  towards  $2 \text{HCO}_3^-$ , which does not affect TA because the overall charge balance does not change. However, the shift towards the more acidic (i.e. protonated) side is associated with a reduction of the pH, also referred to as *ocean acidification* (e.g. Caldeira and Wickett, 2003; Doney et al., 2009), and a reduction of the carbonate saturation state ( $\Omega$ ) which both affect marine organisms on different levels (e.g. Hofmann et al., 2010; Doney et al., 2012; Kroeker et al., 2013).

The  $\Omega$  of the biologically important  $\text{CaCO}_3$  minerals calcite ( $\Omega_C$ ) and aragonite ( $\Omega_A$ ) is an important determinant for the ability of calcifying organisms to build their shells. The  $\Omega$  is a measure of observed  $\text{Ca}^{2+}$  and  $\text{CO}_3^{2-}$  ion concentrations in seawater ( $[\text{CO}_3^{2-}]_{\text{sw}}, [\text{Ca}^{2+}]_{\text{sw}}$ ) relative to their concentration at saturation ( $[\text{CO}_3^{2-}]_{\text{sat}}, [\text{Ca}^{2+}]_{\text{sat}}$ ):

$$\Omega = [\text{CO}_3^{2-}]_{\text{sw}} [\text{Ca}^{2+}]_{\text{sw}} / [\text{CO}_3^{2-}]_{\text{sat}} [\text{Ca}^{2+}]_{\text{sat}} \quad (4)$$

with values of  $\Omega > 1$  expressing that the seawater is supersaturated and  $\text{CaCO}_3$  precipitation is favoured, and conversely  $\Omega < 1$  expressing that the seawater is undersaturated with respect to the solubility product of  $\text{CaCO}_3$ , leading to the dissolution of  $\text{CaCO}_3$  shells.

Since seawater is in excess of  $[\text{Ca}^{2+}]$ , the numerator of equation 4 (i.e. the observed  $[\text{CO}_3^{2-}]_{\text{sw}}$  and  $[\text{Ca}^{2+}]_{\text{sw}}$  ion concentrations) is mainly controlled by  $[\text{CO}_3^{2-}]_{\text{sw}}$  which in turn is influenced by diverse processes:

The physical invasion of  $\text{CO}_2$  into seawater results in a shift from  $\text{CO}_3^{2-}$  towards  $2\text{HCO}_3^-$  which raises DIC at the expense of  $[\text{CO}_3^{2-}]$  reflected in a reduction of  $\Omega$  and vice versa, an emission of  $\text{CO}_2$  results in an increase of  $\Omega$ . The uptake of DIC and nutrients at specific stoichiometric ratios (Chapter 1.2) during photosynthesis decreases DIC and increases TA (TA/DIC = 17/-106) (Goldman and Brewer, 1980; Wolf-Gladrow et al., 2007) elevating  $[\text{CO}_3^{2-}]$  and thus  $\Omega$ . Vice versa, aerobic remineralisation elevates DIC and reduces TA due to nutrient release (TA/DIC = -17/106), thus lowering  $[\text{CO}_3^{2-}]$ . The formation of biogenic carbonate, in principle, reduces DIC in the surface water but the  $[\text{CO}_3^{2-}]_{\text{sw}}$  reduction in the seawater during carbonate production also reduces TA (TA/DIC = 2/1) which in turn leads to an increase of  $\text{pCO}_2$  and hence to  $\text{CO}_2$  emission if  $\text{pCO}_{2\text{sw}} > \text{pCO}_{2\text{atm}}$ . Accordingly, the biological pump's  $\text{CO}_2$  uptake efficiency depends on the relative contribution of organic and inorganic (carbonate) matter formation, referred to as rain ratio.

However, the denominator in equation 4 (i.e. the  $[\text{CO}_3^{2-}]$  and  $[\text{Ca}^{2+}]$  ion concentrations at saturation of calcite and aragonite) is a function of pressure and temperature because the  $\text{CaCO}_3$  solubility increases with increasing pressure and decreasing temperature. Additionally, the remineralisation of organic matter enriches the water with DIC and lowers TA. Both these processes raise  $[\text{CO}_3^{2-}]_{\text{sat}}$  and  $[\text{Ca}^{2+}]_{\text{sat}}$  required to reach saturation with increasing depth. Because  $[\text{CO}_3^{2-}]_{\text{sw}}$  is progressively undersaturated with depth, sinking  $\text{CaCO}_3$  particles are dissolved downwards of depth levels governed by the DIC inventory of the water (e.g. Feely et al., 2002; Chung et al., 2003). The dissolution of  $\text{CaCO}_3$  in the deep ocean is associated with a release of  $\text{CO}_3^{2-}$  and hence with an increase of TA which in turn decreases the  $\text{pCO}_2$ . This process is thought to be a major driver of glacial/interglacial atmospheric  $\text{CO}_2$  variability (Broecker, 1982; Sigman et al., 2010).

## 1.2. DRIVERS, STRENGTH AND EFFICIENCY OF MARINE CO<sub>2</sub> SEQUESTRATION

The biological pump accounts for the majority of the downward DIC transport. Besides the availability of light and micronutrients such as dissolved iron (dFe), the biological pump is both driven and limited by the availability of the two ‘major’ universally required macronutrients, fixed nitrogen (N = NH<sub>4</sub><sup>+</sup>, NO<sub>2</sub><sup>-</sup>, NO<sub>3</sub><sup>-</sup>) and phosphate (P), (Watson et al., 2000; Behrenfeld et al., 2006b). Macronutrients are required in specific stoichiometric ratios for the photosynthetic production of organic matter traditionally termed the Redfield ratio of C/N/P = 106/16/1 (Redfield et al., 1963), although it varies with growth rate, taxonomy, ambient CO<sub>2</sub> concentrations and nutrient availability (e.g. Arrigo, 2005; Riebesell et al., 2007). On a global scale the ratio of remineralised C, N, P and consumed oxygen (-O<sub>2</sub>) (C/N/P/-O<sub>2</sub>) are essentially constant with depth and in good agreement with the Redfield ratio for the photosynthetic production of organic matter (Redfield et al., 1963; Takahashi et al., 1985; Anderson and Sarmiento, 1994). Variations of the C/N/P/-O<sub>2</sub> remineralisation ratios, for example with depth, have been suggested to indicate differences in remineralisation rates of sinking organic matter on the one hand (Takahashi et al., 1985; Li and Peng, 2002; Schneider et al., 2003; Brea et al., 2004), and an impact of N loss and P efflux from sediments occurring in oxygen minimum zones (OMZ) on the other hand (Gruber and Sarmiento, 1997; Tyrrell and Law, 1997). The simple amount of nutrient supply is hence only one control on the potential strength of the biological pump, i.e. the magnitude of the downward carbon export (Lutz et al., 2002; Lutz et al., 2007). The other is the relative nutrient contribution and the Redfield concept emphasises the strong potential that deviations of the C/N/P ratio in organic matter formation and degradation have on the overall CO<sub>2</sub> sequestration efficiency of the biological pump (Heinze et al., 1991) in which nutrient limitation plays a crucial role (Moore et al., 2013).

The impact of micronutrient limitation is visible in the upwelling areas of the world, e.g. the eastern boundary upwelling systems (EBUS), the Southern Ocean and North Pacific which all are characterised by high supply of macronutrients to the surface (e.g. Sarmiento et al., 2004; Messié et al., 2009). In the Southern Ocean upwelling region, also termed as HNLC (high nutrient low chlorophyll) area, the biological production is limited by the lack of dFe (e.g. Boyd et al., 2000) despite optimal supply of macronutrients. This is in contrast

to the EBUS where iron is supplied via aeolian input (Mahowald et al., 2009) and sediments (Bruland et al., 2005; Chase et al., 2005; Noble et al., 2012), so that an optimal supply of macronutrients sustains an intense biological productivity and carbon export (Lutz et al., 2002; Carr and Kearns, 2003). In HNLC regions, macronutrients are not depleted due to light or micronutrient limitation, and CO<sub>2</sub> equilibrates with to the atmosphere, so that these waters typically have C/N <6.6 and C/P <106 ratios. This signature, referred to as *preformed nutrients*, implies an excess of macronutrients over carbon, and thus the potential to take up additional carbon (Sarmiento et al., 2004; Ito and Follows, 2005; Weber and Deutsch, 2010). Such waters are subducted into the sub-thermocline water in the course of mode water formation at high southern latitudes and enhance the nutrient driven CO<sub>2</sub> uptake efficiency in regions where these waters are upwelled again, e.g. off California (Hales et al., 2005).

A major process that lowers the ocean's ability to sequester CO<sub>2</sub> from the atmosphere is the loss of fixed N (NH<sub>4</sub><sup>+</sup>, NO<sub>2</sub><sup>-</sup>, NO<sub>3</sub><sup>-</sup>) through heterotrophic denitrification and autotrophic anammox occurring in the pelagic and coastal oxygen minimum zones (OMZ's) (e.g. Lam and Kuypers, 2010) and in anoxic sediments (Devol, 1991; Middelburg and Levin, 2009). These processes lower the N/P signature to <16 (Gruber and Sarmiento, 1997) and raise C/N >6.6 in the water column, which if being upwelled to the sunlit surface, lowers the potential N-driven CO<sub>2</sub> drawdown in these regions (Rixen et al., 2005). On the other hand, newly fixed N is introduced to the marine N cycle via N<sub>2</sub> fixation. This process is carried out by diazotrophic cyanobacteria preferentially under warm stratified conditions and availability of P along with micronutrients, e.g. dFe; such conditions prevail in the subtropical northern Atlantic and Pacific (Mahaffey et al., 2005; Sohm and Capone, 2011; Zehr, 2011). High N/P (34-125) and C/P ratios (464-779) in organic matter of diazotrophs, especially under P exhaustion (Bertillon et al., 2003; Sañudo-Wilhemly et al., 2004; Karl et al., 2012), illustrate efficient C sequestration by the biological pump under conditions differing from the overall Redfield stoichiometry of phytoplankton and thus enhance the ocean's ability to sequester CO<sub>2</sub> from the atmosphere (Rixen and Ittekkot, 2005). The subsequent remineralisation of diazotrophic organic matter is expressed in N/P >16 in sub-thermocline water (Gruber and Sarmiento, 1997; Mahaffey et al., 2003; Singh et al., 2013) and is assumed to counterbalance the N loss; this view, however, is challenged

by global estimates on N loss ranging between 275 and 482 Tg N yr<sup>-1</sup> while overall sources add up to 265-294 Tg N yr<sup>-1</sup> (Gruber and Sarmiento, 1997; Codispoti et al., 2001). However, methodological improvements (Mohr et al., 2010; Großkopf et al., 2012) and the broadening range of identified species involved in N<sub>2</sub> fixation (Moisander et al., 2010; Zehr, 2011) suggest that rates and regions of N<sub>2</sub> fixation may have been considerably underestimated so far.

In addition to the availability of light and nutrients, the carbonate counter pump is impacted by the saturation states ( $\Omega$ ) of the biologically important CaCO<sub>3</sub> minerals aragonite ( $\Omega_A$ ) and calcite ( $\Omega_C$ ) in the seawater. Pelagic carbonate (PIC) production is dominated by calcite producing coccolithophorids and foraminifera (Schiebel, 2002) and, at present, is particularly impacted by ocean acidification (Riebesell et al., 2000; Barker and Elderfield, 2002; Beaufort et al., 2011) thus influencing the strength of the carbonate counter pump.

### 1.3. RELEVANCE OF EASTERN BOUNDARY UPWELLING SYSTEMS IN MARINE CARBON CYCLING

Eastern boundary upwelling systems (EBUS) are driven by persistent equatorward winds along the eastern boundaries of the Atlantic and the Pacific Ocean. The interaction of the coastal boundary and earth's rotation (Coriolis force) generate a wind-driven offshore directed surface Ekman transport, which is replaced by a compensation flow of CO<sub>2</sub>- and nutrient-enriched subsurface water that causes CO<sub>2</sub> emission and intense biological production along the coast (Carr, 2002; Chen and Borges, 2009). Although the EBUS cover 0.3 % of the ocean's surface area they account for ~2 % (~1 Pg C yr<sup>-1</sup>) of global primary production (Carr, 2002; Carr et al., 2006) supporting a significant share of marine resources, e.g. ~20 % of global fish catch (Ryther, 1969; Pauly and Christensen, 1995; Chavez and Messié, 2009).

In contrast to the CO<sub>2</sub> flux estimates of the open ocean, which are consistently confirming a mean oceanic CO<sub>2</sub> uptake between 1.2-2.2 Pg C yr<sup>-1</sup> (Gruber et al., 2009; Takahashi et al., 2009; Le Quéré et al., 2014), the CO<sub>2</sub> flux estimates for the coastal ocean are subject to large uncertainties mainly arising from the relatively low data coverage with

respect to the high variability in space and time. Overall, EBUS are small CO<sub>2</sub> sources of ~0.037 Pg C yr<sup>-1</sup> (Chen and Borges, 2009; Larouelle et al., 2010), which is argued to be compensated by a high POC export arising from the high primary productivity along with high new production (Muller-Karger et al., 2005). However, CO<sub>2</sub> flux estimates most extensively studied in the California Current upwelling system suggest that upwelling systems can be both, substantial sources but also sinks for atmospheric CO<sub>2</sub> (Friederich et al., 2002; Hales et al., 2005; Fassbender et al., 2011). Air-sea exchange fluxes in EBUS are largely unquantified, yet essential to understand the role of these highly productive systems to the global carbon cycle. Additionally, coastal surface water of upwelling systems is naturally eutrophied, O<sub>2</sub>-depleted, DIC-enriched and acidified, which makes them natural “labs” to study the functioning of the biological and physical pump under scenarios which are, among others, projected as main threats in the future (Rhein et al., 2013). However, it is also suggestive of a higher vulnerability to anthropogenic impacts, which are already reflected in warming (Di Lorenzo et al., 2005), acidification (Feely et al., 2008; Hauri et al., 2009) and deoxygenation (Bograd et al., 2008) emphasising the importance to study these systems also in the light of their economic importance.

### 1.3.1. THE BENGUELA CURRENT UPWELLING SYSTEM

The Benguela Current upwelling system (BUS) roughly stretches from ~16° S to ~35° S (Fig. 1.2.) and is bordered to the south by the Agulhas Current (AgC) and to the north by the Angola Benguela Frontal Zone (ABFZ). Persistent equatorward winds at the eastern flank of the South Atlantic Gyre feed the trade winds and drive the Benguela Current. Coastal upwelling is eminently pronounced where the shelf narrows at 17 °S, 26 °S and 34 °S (Shillington et al., 2006; Hutchings et al., 2009). The strong Lüderitz upwelling cell (~26 °S) which accounts for ~35-50 % of total upwelled water establishes an environmental barrier that separates the BUS into a northern and southern subsystem (N- and SBUS) (Shannon, 1985; Duncombe Rae, 2005) of which the NBUS receives 80 % of the upwelling flux (Monteiro, 2010). The Lüderitz cell also marks the boundary of two central water mass regimes that cause distinct differences in biogeochemical properties of

upwelling waters. Upwelling in the SBUS entrains Eastern South Atlantic Central Water (ESACW) into the offshore Ekman drift (Duncombe Rae, 2005; Mohrholz et al., 2008). Between the ABFZ and the Lüderitz cell, the ESACW mixes with an Angola Gyre subtype of the South Atlantic Central Water (SACW) which enters the Namibian shelf from the north. This Angola Gyre subtype is older and thus strongly enriched in nutrients and depleted in  $O_2$  compared to the ESACW (Poole and Tomczak, 1999; Mohrholz et al., 2008).

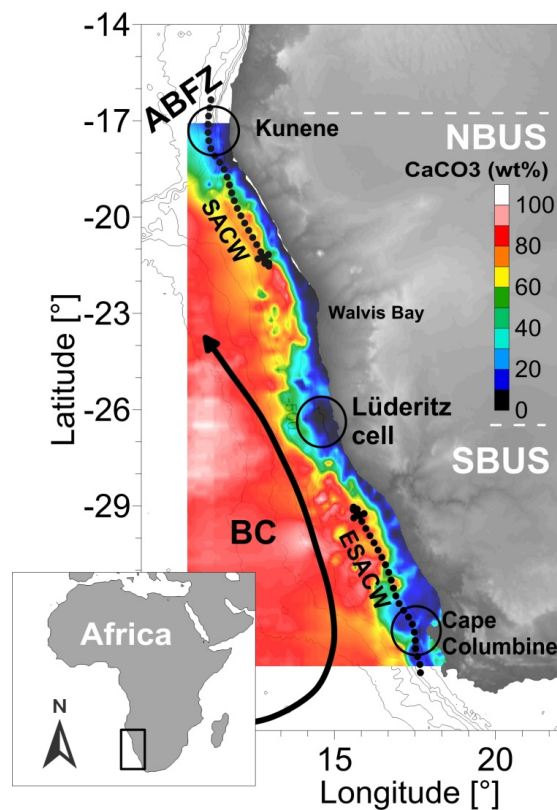


Fig. 1.2.: Schematic overview of the Benguela Current upwelling system located at the southwest African coast. BC, Benguela Current; ESACW, Eastern South Atlantic Central Water; NBUS, northern Benguela upwelling system; SACW, South Atlantic Central Water; SBUS, southern Benguela upwelling system. The  $CaCO_3$  content (wt %, colour coded) of the surface sediments illustrates the low  $CaCO_3$  content on the shelf.  $CaCO_3$  data provided by Inthorn et al. (2006).

Increased inflow of SACW into the NBUS during austral summer preconditions the development of an oxygen minimum zone (OMZ) and anoxic events over the Namibian shelf and upper slope (Weeks et al., 2002; Monteiro et al., 2006; Mohrholz et al., 2008).

The dominance of the O<sub>2</sub>-depleted and nutrient-enriched SACW in the NBUS (Duncombe Rae, 2005; Hutchings et al., 2009; Monteiro, 2010) as compared to the SBUS makes the NBUS being particularly vulnerable to deoxygenation, and is visible by a shoaling of the 2.5 ml l<sup>-1</sup> O<sub>2</sub> iso-surface (~110 μmol l<sup>-1</sup>) during the last 50 years (Ekau et al., 2010).

N loss in the anoxic and hypoxic (<10 μmol l<sup>-1</sup> O<sub>2</sub>) water column and sediments caused by anammox and denitrification (Kuypers et al., 2005; Nagel et al., 2013) along with P release from sediments, mediated by sulphur bacteria (Schulz and Schulz, 2005), result in an N deficit of ~2.5 Tg N yr<sup>-1</sup> (Nagel et al., 2013) and is reflected in non-standard nutrient ratios (N/P <16) in upwelling water (Dittmar and Birkicht, 2001; Tyrrell and Lucas, 2002). The N deficiency in surface water is not stimulating N<sub>2</sub> fixation in the central BUS and the South East Atlantic (Staal et al., 2007; Sohm et al., 2011), which is attributed to the overall low supply of dissolved dFe (Moore et al., 2009; Sohm and Capone, 2011) resulting from low aeolian dust input to the Eastern South Atlantic (Chester et al., 1972; Sarthou et al., 2003). Low rates of N<sub>2</sub> fixation have been observed under nutrient replete conditions at the ABFZ (Sohm et al., 2011) but overall N loss exceeds estimates on N<sub>2</sub> fixation suggesting that the BUS acts as net sink for fixed N (Nagel et al., 2013).

However, among the four major EBUS the BUS is the most productive upwelling system accounting for 40 % (~0.37 Pg C yr<sup>-1</sup>) of the total EBUS potential primary production estimate (Carr, 2002). The potential nitrate driven new production estimates of 517 g C m<sup>-2</sup> yr<sup>-1</sup> (0.14 Pg C yr<sup>-1</sup>) (Chavez and Messié, 2009; Messié et al., 2009) are comparatively low suggesting that the primary production is driven by a high fraction of locally regenerated productivity (Dittmar and Birkicht, 2001; Füssel et al., 2011). Phytoplankton communities of the BUS are dominated by diatoms and dinoflagellates near the coast in freshly upwelled water (Barlow et al., 2006; Barlow et al., 2009), while nanoflagellates and calcite forming coccolithophorids are usually more abundant in mature water, e.g. at the rims of upwelling cells (Mitchell-Innes and Winter, 1987; Pitcher et al., 1992; Giraudeau et al., 1993; Henderiks et al., 2012). High fractions of POC export accounting for ~1.75 % of surface production to depths below 1000 m (Fischer et al., 2000) are driven by carbonate producers, mainly coccolithophorids and foraminifera, which dominate offshore PIC fluxes (Wefer and Fischer, 1993; Giraudeau et al., 2000; Romero et al., 2002) and create to the carbonate-rich surface sediments (Giraudeau, 1993;

Boeckel and Baumann, 2004). In contrast, over the BUS shelf, where highest accumulation of POC occurs, the surface sediment record shows no considerable PIC deposition (Bremner, 1981; Mollenhauer et al., 2002 ) (Fig. 1.2.) but high opal contribution (Bremner and Willis, 1993; Inthorn et al., 2006). In light of corrosive waters surfacing along the Californian coast (Feely et al., 2008), the question is raised whether this carbonate-depleted zone solely results from low PIC production in the surface and which role carbonate dissolution might play. However, this is unknown due to an absence of qualitative particle flux records and a lack of the vertical and spatial variability of  $\Omega$  on the shelf.

Estimates of air-sea CO<sub>2</sub> fluxes reveal that the NBUS is a CO<sub>2</sub> source of 0.2 Tg C yr<sup>-1</sup> and the SBUS a CO<sub>2</sub> sink of -2.7 Tg C yr<sup>-1</sup> (González-Dávila et al., 2009). Although these fluxes are based on pCO<sub>2</sub> measurements with high temporal resolution, they were obtained far offshore, particularly in the NBUS sector. Hence, they do not capture the coastal variability, and likely underestimate the CO<sub>2</sub> emissions in the NBUS sector.

#### 1.4. OBJECTIVES AND OUTLINE

Coastal ecosystems are important contributors to global marine carbon cycling (Muller-Karger et al., 2005; Chen and Borges, 2009). Nevertheless, they are highly undersampled in spite of their pronounced spatial and temporal variability. The BUS is a divided system with the NBUS being particularly rich in macronutrients and deoxygenated indicative of diverse processes that influence the strength and efficiency of the biological pump. The drivers and the magnitude of organic carbon export on the shelf, the current state of  $\Omega$  and coastal pCO<sub>2</sub> fluxes in the upwelling zone are largely unknown especially in the NBUS but are crucial to better understand the functioning of the carbon cycling.

The overall aim of this thesis is to investigate parameters indicative of the strength and efficiency of carbon cycling in the NBUS. More specifically, a focus is given on examining the variability of N deficiency and carbonate saturation states and their effects on the magnitude and composition of the particle export on the shelf. I combine these

results with patterns of air-sea CO<sub>2</sub> fluxes to contribute to a better understanding of the C source-sink function of the BUS.

The thesis addresses the following detailed objectives:

### **Objective I**

**To determine the C/N/P/-O<sub>2</sub> remineralisation patterns in the NBUS with emphasis on the spatial and temporal variability of N deficiency.**

The ratios of remineralised C, N, P and consumed oxygen (-O<sub>2</sub>) (C/N/P/-O<sub>2</sub>) are characteristic of the coupled nutrient and carbon cycling in the oceans, but are poorly constrained in the subsurface waters of the NBUS. Oxygen, nutrient and carbonate chemistry data from different seasons are expected to reveal variations in spatio-temporal patterns of nutrient supply, nutrient utilisation, and the variability of the carbonate saturation state, which all impact the strength and efficiency of the biological carbon pump.

### **Objective II**

**To quantify the particle fluxes on the shelf with a focus on the factors that control the magnitude of POC and PIC export.**

Contrary to the adjacent South Atlantic, offshore regions where the export of POC is dominated by calcifying plankton, most of the NBUS shelf area is characterised by low carbonate deposits. Furthermore, qualitative estimates of particle fluxes on the NBUS shelf are lacking. A mooring deployed on the shelf, which was equipped with hydrographic sensors and a sediment trap, will provide data on the magnitude and the ratio of POC and PIC export on the shelf and will monitor the strength and efficiency of the biological pump. Data on the variability of the carbonate saturation states will, along with the findings of nutrient variability, serve as basis to interpret the flux patterns.

### **Objective III**

**To quantify air-sea CO<sub>2</sub> fluxes with emphasis on the coastal regions of the NBUS.**

Available pCO<sub>2</sub> measurements from the Benguela Current system do not capture the intense temporal and spatial variability, and underestimate CO<sub>2</sub> emissions especially in the NBUS sector. Underway pCO<sub>2</sub> measurements within the coastal realm and during different seasons will provide more robust data accounting for the coastal and seasonal variability. Moreover, these measurements will serve as basis to assess the C source-sink function of the NBUS, along with the results on carbon export.

To address these objectives, the following specific key aspects are discussed in 4 separate chapters of this thesis:

- Chapter I: Dissolved inorganic nutrient and carbonate chemistry data is used to study the spatio-temporal variability of C/N/P/-O<sub>2</sub> ratios to identify sources of DIC and detect spatial and temporal patterns of N and P supply. Particular focus was set on the variability of N deficiency as major factor lowering the productivity of the system.
- Chapter II: Carbonate chemistry along with nutrient data was used to investigate the state of  $\Omega$  as a major factor influencing calcification, growth and survival of many marine calcifying organisms and, upon death and sinking, the burial of carbonate shells in the sediments. A key aspect is to differentiate between the processes that control the variability of  $\Omega$  on the shelf.
- Chapter III: Records of annual particle fluxes along with hydrographical data obtained by a mooring on the shelf off Walvis Bay, in conjunction with meteorological data, are used to investigate the influence of upwelling on particle fluxes with a focus on the factors that influence the export of POC to the shelf.

Chapter IV: Air-sea CO<sub>2</sub> flux estimates based on underway measurements of surface pCO<sub>2</sub> distribution in the coastal regions of the BUS, along with calculations on potential nutrient supply, are used to investigate the impact of preformed nutrient contribution to the CO<sub>2</sub> sink-source dynamics of the BUS and were applied to other major upwelling systems.

To address these objectives and key aspects, sampling was carried out during four research cruises to the BUS and a suite of methods was applied onboard the research vessels and subsequently after the cruises. For detailed information about the methods used the reader is referred to the *Material and Methods* and *Supplement* sections of Chapter I – IV. Data presented in this thesis refers to measurements conducted in the GENUS I phase from 2009 – 2012, except for the MSM7/3 cruise in 2008.

This thesis was realised in the framework of the GENUS project (Geochemistry and Ecology of the Namibian Upwelling System; <http://genus.zmaw.de>), which is a multi-disciplinary programme aiming to improve our understanding of the complex interactions between biological, biogeochemical and physical processes of the Benguela upwelling system and their response to climate change.

## 2. OUTLINE OF PUBLICATIONS

The following list of publications gives an overview of the first and co-author publications, my contribution to each manuscript and their current status. The general idea for this PhD project, which is embedded in the GENUS project (Geochemistry and Ecology of the Namibian Upwelling System), was developed by Dr. T. Rixen and supervised by Dr. Tim Rixen, Prof. Dr. K.-C. Emeis, and Dr. Anja K. van der Plas (NatMIRC, Swakopmund).

### Chapter I

#### **Spatio-temporal patterns of C/N/P ratios in the northern Benguela upwelling system**

Flohr, A., van der Plas, A. K., Emeis, K.-C., Mohrholz, V., Rixen, T.

Current status: published in February 2014 in *Biogeosciences*.

Contributions: Anita Flohr and Tim Rixen designed the study and took part in nutrient field sampling. Anita Flohr conducted the field sampling and the data analysis of carbonate chemistry data, and wrote the manuscript with scientific and editorial advice by the co-authors.

---

### Chapter II

#### **Alkalinity production buffers the carbonate saturation state in the Benguela Current upwelling system**

Flohr, A., Rixen, T., Mohrholz, V., Neumann, A., Emeis, K.-C.

Current status: to be submitted

Contributions: Anita Flohr and Tim Rixen designed the study. Anita Flohr conducted the field sampling and the data analysis of carbonate chemistry data, and wrote the manuscript with scientific and editorial advice by the co-authors.

### Chapter III

#### **Upwelling lowering carbon export in the Benguela upwelling system off Namibia**

Rixen, T. \*, Flohr, A. \*, Lahajnar, N., Schmidt, M., Mohrholz, M., van der Plas, A., Gaye, B., Eggert, A., Emeis, K.-C.

\*authors contributed equally to the manuscript

Current status: to be submitted

Anita Flohr and Tim Rixen designed the study and conducted the field sampling together with Volker Mohrholz and Martin Schmidt who deployed and recovered the mooring and provided the hydrographical data. The meteorological data was provided by Anja van der Plas. Anita Flohr, Tim Rixen and Niko Lahajnar analysed the sediment trap material. Tim Rixen and Anita Flohr wrote the manuscript with scientific and editorial advice by the co-authors.

---

### Chapter IV

#### **Carbon and nutrient balances of the Benguela upwelling system**

Rixen, T., Flohr, A., Lahajnar, N., van der Plas, A., Emeis, K.-C.

Current status: to be submitted

Contributions: Anita Flohr participated in pCO<sub>2</sub> field sampling during Afr258 and D356, conducted pCO<sub>2</sub> field sampling during MSM17/3 and MSM18/4 cruises and contributed to the manuscript with scientific and editorial advice.



## 3. CHAPTER I

SPATIO-TEMPORAL PATTERNS OF C/N/P RATIOS IN THE  
NORTHERN BENGUELA UPWELLING SYSTEM

Anita Flohr<sup>1</sup>, Anja van der Plas<sup>2</sup>, Kay-Christian Emeis<sup>3,4</sup>,

Volker Mohrholtz<sup>5</sup>, and Tim Rixen<sup>1,4</sup>

[1] Leibniz Centre for Tropical Marine Ecology (ZMT), Fahrenheitstraße 6, 28359 Bremen, Germany

[2] National Marine Information and Research Centre, Ministry of Fisheries & Marine Resources, PO Box 912 Swakopmund, Namibia

[3] Helmholtz-Centre for Materials and Coastal Research Geesthacht, Max-Planck-Straße 1, 21502 Geesthacht, Germany

[4] Institute for Biogeochemistry and Marine Chemistry, University of Hamburg, Bundesstraße 55, 20146 Hamburg, Germany

[5] Leibniz-Institute for Baltic Sea Research, Seestraße 15, 18119 Rostock, Germany

Corresponding author: A. Flohr, Leibniz Centre for Tropical Marine Ecology (ZMT), Fahrenheitstraße 6, 28359 Bremen, Tel.: ++49 421 2380047, Fax: ++49 421 2380030, (anita.flohr@zmt-bremen.de)

Published in *Biogeosciences* (2014)



## ABSTRACT

On a global scale the ratio of fixed nitrogen (N) and phosphate (P) is characterised by a deficit of N with regard to the classical Redfield ratio of N/P = 16/1 reflecting the impact of N loss occurring in the oceanic oxygen minimum zones. The northern Benguela upwelling system (NBUS) is known for losses of N and the accumulation of P in sub- and anoxic bottom waters and sediments of the Namibian shelf resulting in low N/P ratios in the water column. To study the impact of the N/P anomalies on the regional carbon cycle and their consequences for the nutrient export from the NBUS into the oligotrophic subtropical gyre of the South Atlantic we measured dissolved inorganic carbon ( $C_T$ ), total alkalinity ( $A_T$ ), oxygen ( $O_2$ ) and nutrient concentrations in February 2011. The results indicate increased P concentrations over the Namibian shelf due to P efflux from sediments resulting in a C/N/P/ $-O_2$  ratio of 106/16/1.6/138. N reduction further increases C/N and reduces N/P ratios in those regions where  $O_2$  concentrations in bottom waters are  $<20 \mu\text{mol kg}^{-1}$ . However, off the shelf along the continental margin, the mean C/N/P/ $-O_2$  ratio is again close to the Redfield stoichiometry. Additional nutrient data measured during 2 cruises in 2008 and 2009 imply that the amount of excess P, which is created in the bottom waters on the shelf, and its export into the subtropical gyre after upwelling varies through time. The results further reveal an inter-annual variability of excess N within the South Atlantic Central Water (SACW) that flows from the north into the NBUS with highest N values observed in 2008. It is postulated that the N excess in SACW occurred due to the impact of remineralised organic matter produced by  $N_2$  fixation and that the magnitude of excess P formation and its export is governed by inputs of excess N along with SACW flowing into the NBUS. Factors controlling  $N_2$  fixation north of the BUS need to be addressed in future studies to better understand the NBUS' role as P source and N sink in the coupled C, N, and P cycles.

## INTRODUCTION

The biological carbon pump is the term used for the production of organic carbon from dissolved carbon dioxide ( $CO_2$ ) in the surface mixed layer of the ocean and its transport into the large  $CO_2$  reservoir of the ocean beneath the mixed layer. It is both driven and

limited by the availability of macronutrients, such as fixed nitrogen (N) and phosphate (P), as well as micronutrients such as iron (Watson et al., 2000; Behrenfeld et al., 2006b). Macronutrients are required in specific stoichiometric ratios for the photosynthetic production of organic matter traditionally termed as Redfield ratio of C/N/P = 106/16/1 (Redfield et al., 1963). Nevertheless, on a more regional scale phytoplankton C/N/P ratios vary with growth rate, taxonomy, ambient CO<sub>2</sub> concentrations and nutrient availability (e.g. Arrigo, 2005; Riebesell et al., 2007). Especially upon exhaustion of the nutrients, changes in the nutrient uptake ratios could strongly influence the marine productivity and the oceans' ability to sequester CO<sub>2</sub> from the atmosphere (McElroy, 1983; Heinze et al., 1991; Falkowski, 1997).

The ratios of remineralised C, N, P and consumed oxygen (-O<sub>2</sub>) (C/N/P/-O<sub>2</sub>) are useful to characterise the coupled nutrient and carbon cycling in the oceans. On a global scale the mineralisation of nutrients is essentially constant with depth and in good agreement with the traditional Redfield ratio for the photosynthetic production of organic matter (Redfield et al., 1963; Takahashi et al., 1985; Anderson and Sarmiento, 1994). However, depending also on the methods used, variations of the C/N/P/-O<sub>2</sub> mineralisation ratios, e.g. with depth have been suggested indicating elemental fractionation during the mineralisation of sinking organic matter (Takahashi et al., 1985; Li and Peng, 2002; Schneider et al., 2003; Brea et al., 2004) and an impact of N loss occurring in oxygen minimum zones (OMZ) (Gruber and Sarmiento, 1997; Tyrrell and Law, 1997).

Eastern boundary upwelling systems (EBUS) are regions of high CO<sub>2</sub> concentrations (Boehme et al., 1998; Torres et al., 1999) and intense biological production and export of carbon (Carr, 2002). They as well play an important role in supplying nutrients to the surface mixed layer of adjacent oligotrophic subtropical gyres where nutrient supply is limited by stable thermal stratification (Behrenfeld et al., 2006a). The Benguela upwelling system (BUS) is a coastal upwelling system known for non-standard nutrient (N/P) ratios in upwelling waters (Dittmar and Birkicht, 2001; Tyrrell and Lucas, 2002) caused by N loss (anammox and/or denitrification) and P release from sediments in low O<sub>2</sub> environments (Kuypers et al., 2005; Nagel et al., 2013). The C/N/P remineralisation ratios in the subsurface waters are poorly constrained but are crucial in order to characterise the cycling of C in the BUS.

We analysed nutrient ( $\text{NO}_3^-$ ,  $\text{NO}_2^-$ , P) and dissolved  $\text{O}_2$  data in conjunction with data on dissolved inorganic carbon ( $C_T$ ) and total alkalinity ( $A_T$ ) produced during an expedition in 2011, and complemented these with nutrient data from 2 other expeditions staged in 2008 and 2009. Our objectives were to investigate C/N/P/ $\text{O}_2$  mineralisation ratios of the NBUS to study the spatial and temporal impact of N reduction and the associated consequences for the nutrient export from the eutrophic upwelling system into the oligotrophic subtropical gyre.

## MATERIAL AND METHODS

### STUDY AREA

The BUS spans along the southwest coast of Africa, covering the western South African and Namibian coastline roughly from Cape Agulhas (~34 °S) to the Angola Benguela Frontal Zone (ABFZ) (Hutchings et al., 2009) (Fig. 3.1.). At the ABFZ, which is centred between 14 °S and 16 °S (Meeuwis and Lutjeharms, 1990) but is highly dynamic in terms of shape and location, the cold Benguela current system converges with warm tropical waters of the Angola Current (AC). To the south, the system is bordered by the Agulhas Current that reverses and partly converges with the South Atlantic water resulting in the formation of eddies (Agulhas Rings, AR) and filaments (Hall and Lutjeharms, 2011).

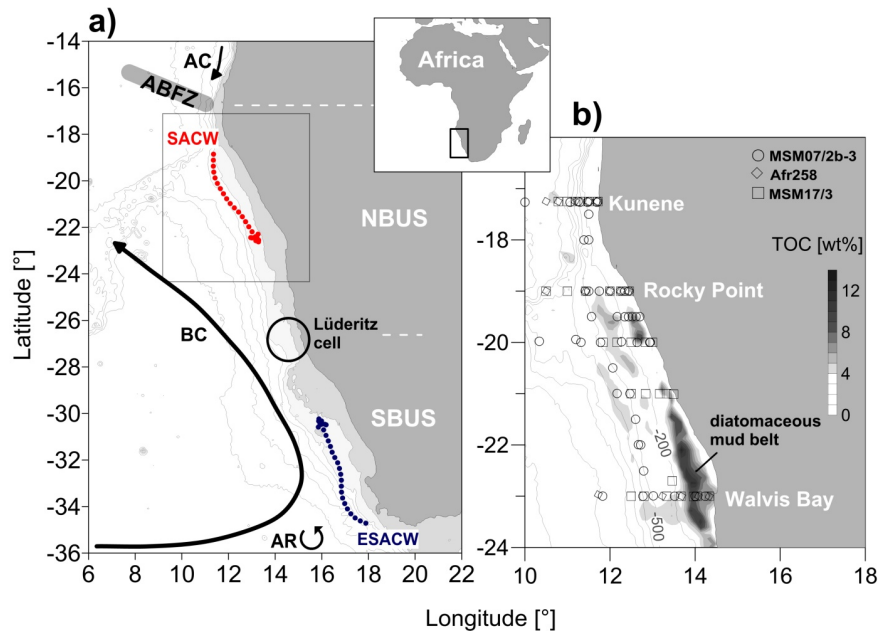


Fig. 3.1.: (a) Schematic overview of the the Benguela upwelling system located at the southwest African coast. Surface currents are represented by solid und subsurface currents by dotted lines. AC, Angola Current; ABFZ, Angola Benguela Frontal Zone; AR, Agulhas Rings; BC, Benguela Current; ESACW, Eastern South Atlantic Central Water; NBUS, northern Benguela upwelling system; SACW, South Atlantic Central Water; SBUS, southern Benguela upwelling system. (b) Stations sampled during the cruises: MSM07/2b-3 (circles), Afr258 (diamonds) and MSM17/3 (squares). The grey shading refers to the TOC content (wt %) of the surface sediments representing the diatomaceous mud belt (TOC data taken from Inthorn et al. (2006)/10.1594/PANGAEA.351146).

Along the coast of southwest Africa, the interaction of southerly trade winds with coastal topography forces upwelling, which is strongest at 3 distinct upwelling cells (Shillington et al., 2006; Hutchings et al., 2009). The Lüderitz upwelling cell ( $\sim 26^\circ\text{S}$ ) accounts for roughly 50 % of physical upwelling and separates the upwelling region into a northern and a southern subsystem (Shannon, 1985; Duncombe Rae, 2005). In the southern region (south of  $26^\circ\text{S}$ ) the trade winds are seasonal and upwelling maximises during austral spring and summer. The northern region (from  $26^\circ\text{S}$  to the ABFZ) is characterised by perennial alongshore winds and upwelling along the coast (Shannon, 1985).

The Lüderitz cell also marks the boundary of two central water regimes that cause distinct differences in biogeochemical properties of upwelling waters. Upwelling in the southern BUS entrains Eastern South Atlantic Central Water (ESACW) into the offshore Ekman drift (Duncombe Rae, 2005; Mohrholz et al., 2008). The ESACW is a central water

mass that forms in the Indian Ocean and enters the South Atlantic Ocean by Agulhas Current intrusions (Poole and Tomczak, 1999; Stramma and England, 1999). Between the ABFZ and the Lüderitz cell, the ESACW mixes with an Angola Gyre subtype of the South Atlantic Central Water (SACW). This subtype of SACW originates in the subtropical Angola Gyre and enters the Namibian shelf and continental margin in a poleward undercurrent via the Angola Current (Duncombe Rae, 2005; Mohrholz et al., 2008). The SACW originally forms in the Brazil-Malvinas Confluence off South America (Gordon, 1981), flows eastward with the South Atlantic Current and is then diverted northwards along with the Benguela Current towards the equatorial current system. Here, a branch spreads eastwards and flows into the Angola Gyre (Poole and Tomczak, 1999). This Angola Gyre subtype is older and thus strongly enriched in nutrients and depleted in O<sub>2</sub> compared to the ESACW (Poole and Tomczak, 1999; Mohrholz et al., 2008). Increased inflow of SACW into the NBUS preconditions the development of an oxygen minimum zone (OMZ) and anoxic events over the Namibian shelf and upper slope (Weeks et al., 2002; Monteiro et al., 2006; Mohrholz et al., 2008).

On the shelf at low O<sub>2</sub> concentrations (<20 µM O<sub>2</sub>) fixed nitrogen (N) is reduced by denitrification and/or anammox (Lam and Kuypers, 2010). The loss of fixed N to anammox within the OMZ on the shelf has been estimated to ~1.4 Tg N yr<sup>-1</sup> (Kuypers et al., 2005; Kalvelage et al., 2011) and the loss to denitrification to ~2.5 Tg N yr<sup>-1</sup> (Nagel et al., 2013). However, N loss exceeds estimates on N<sub>2</sub> fixation (Sohm et al., 2011) suggesting that the BUS acts as net sink for fixed N. Furthermore, the BUS shelf is a region of modern phosphorite deposition (Glenn et al., 1994; Föllmi, 1996) associated with a massive organic-rich diatomaceous mud belt that roughly follows the Namibian coast between 50 and 200 m water depth (Fig. 3.1.) and covers an area of ~18,000 km<sup>2</sup> (Bremner, 1980; Bremner and Willis, 1993; Emeis et al., 2004). The mud belt surface is settled by consortia of large sulphur bacteria (including *Thiomargarita namibiensis*) that release phosphate (P) into the anoxic pore water (Nathan et al., 1993; Schulz and Schulz, 2005; Goldhammer et al., 2010) and thereby enrich pore waters to ~1000 µM PO<sub>4</sub><sup>3-</sup> (van der Plas et al., 2007).

## WATER SAMPLING, LABORATORY WORK AND DATA ANALYSIS

Nutrient samples were collected during three cruises in austral summer and early autumn (Fig. 3.1.): MSM07/2b-3 (RV M.S. Merian, 09 March – 17 April 2008), Afr258 (RV Africana, 1-17 December 2009) and the MSM17/3 (RV M.S. Merian, 31 January-8 March 2011). Sampled transects perpendicular to the coast stretched from the shelf, over the continental slope and into the open ocean. At least five stations per transect were sampled off Kunene (17.25 °S), Rocky Point (19.00 °S), Terrace Bay (20.00 °S), Toscanini (20.80 °S) and Walvis Bay (23.00 °S). Transects off Kunene, Rocky Point and Walvis Bay were sampled during all of the three cruises. Samples were collected by CTD casts using a rosette system equipped with 10 L Niskin bottles. The upper water column was sampled at fixed depth levels (5, 10, 15, 20, 30, 50, 100, 200 m). From 200 m downwards the depth levels were extended to 100-300 m intervals depending on the bottom depth and e.g. the O<sub>2</sub> profile. The analysed parameters presented in this study comprise dissolved inorganic carbon ( $C_T$ ), total alkalinity ( $A_T$ ) and dissolved nutrients (NO<sub>x</sub> = nitrate (NO<sub>3</sub><sup>-</sup>) + nitrite (NO<sub>2</sub><sup>-</sup>) and phosphate (PO<sub>4</sub><sup>3-</sup>)). The apparent oxygen utilisation (AOU) was calculated from O<sub>2</sub> concentrations using the equations for O<sub>2</sub> saturation according to Weiss (1970).

*DIC and TA*

The  $C_T$  and  $A_T$  samples were taken during the MSM17/3 cruise. Transects off Kunene (17.25 °S), Rocky Point (19.00 °S), Terrace Bay (20.00 °S), Toscanini (20.80 °S) and Walvis Bay (23.00 °S) were sampled. For  $C_T$  and  $A_T$  analysis the samples were filled in 250 ml borosilicate bottles using silicone tubes (Tygon). The bottles were rinsed twice and filled from the bottom to avoid air bubbles. Periodically duplicate samples were taken. The samples were fixed with mercury (II) chloride solution (250 µl of a 35 g l<sup>-1</sup> HgCl<sub>2</sub> solution) directly after collection and analysed on board using the VINDTA 3C system (Mintrop, 2005). The  $A_T$  was determined on the basis of a semi-closed cell titration principle. The samples were titrated with a fixed volume of hydrochloric acid (HCl, 0.1 N).  $C_T$  was quantified by the coulometric method (Coulometer CM 5015, precision of 0.1 %) after extracting the CO<sub>2</sub> out of the acidified water samples. Certified Reference Material

(CRM, batch #101 and #104, provided by A. Dickson (Scripps Institution of Oceanography, La Jolla, CA, USA)) was used to calibrate the VINDTA 3C system. The  $C_T$  and  $A_T$  measurements of duplicate samples agreed to  $\pm 2 \mu\text{mol kg}^{-1}$ . In the following  $A_T$  is reported as the salinity corrected value ( $A_T = A_{T\text{meas}} \cdot 35 / S_{\text{meas}}$ ).

### *Dissolved nutrients*

The nutrient samples were filtered through disposable syringe filters (0.45  $\mu\text{m}$ ) immediately after sampling, filled in pre-rinsed 50 ml PE bottles and frozen ( $-20 \text{ }^\circ\text{C}$ ). Samples collected during the MSM07/2b-3 cruise were measured on board, whereas samples taken during Afr258 and MSM17/3 cruises were analysed in the shore-based laboratory subsequently to the expedition. Dissolved nutrients were measured by a continuous flow injection system (Skalar SAN plus System) according to methods described by Grasshoff et al. (1999). The detection limits were:  $\text{NO}_x = 0.08 \mu\text{M}$  and  $\text{PO}_4^{3-} = 0.07 \mu\text{M}$  according to DIN 32645. Ammonium ( $\text{NH}_4^+$ ) concentrations were usually  $< 2.5 \mu\text{mol kg}^{-1}$  and are not discussed in this paper. In the following N = nitrate ( $\text{NO}_3^-$ ) + nitrite ( $\text{NO}_2^-$ ) and P =  $\text{PO}_4^{3-}$  will be used throughout the paper.

### *Elemental stoichiometry*

To calculate the deviation from the classical Redfield ratio (N/P = 16/1) (Redfield et al., 1963) we used the tracer  $\text{N}^*$  (Gruber and Sarmiento, 1997):

$$\text{N}^* = ([\text{NO}_3^-] - 16 \cdot [\text{PO}_4^{3-}] + 2.9) \cdot 0.87 \quad (6)$$

where  $[\text{NO}_3^-]$  and  $[\text{PO}_4^{3-}]$  are the concentrations of nitrate and phosphate in  $\mu\text{mol kg}^{-1}$ , respectively. The constants drive the global mean  $\text{N}^*$  value of  $-2.9 \mu\text{mol kg}^{-1}$  to zero. Positive and negative  $\text{N}^*$  are indicative of an excess and deficit of  $\text{NO}_3^-$  relative to  $\text{PO}_4^{3-}$ , respectively (Gruber and Sarmiento, 1997). To quantify the  $\text{PO}_4^{3-}$  anomaly ( $\text{P}^*$ ) from Redfield we use the concept of Deutsch et al. (2007):

$$P^* = [\text{PO}_4^{3-}] - [\text{NO}_3^-] / 16 \quad (7)$$

$N^*$  and  $P^*$  are a measure for the deviation from the Redfield ratio and are arbitrary values rather than definite concentrations.

### *Characterisation of central water masses*

The potential temperature ( $T_{\text{pot}}$ ) and salinity ( $S$ ) characteristics were used to differentiate between SACW and ESACW contributions. Their definitions were adopted from Mohrholz et al. (2008), who identified an Angola Gyre subtype of SACW. This subtype is characterised by  $\text{O}_2$  concentrations ranging between 22-68  $\mu\text{mol l}^{-1}$  in contrast to the ESACW that shows  $\text{O}_2$  values of 249-300  $\mu\text{mol l}^{-1}$  in the Cape Basin (Poole and Tomczak, 1999; Mohrholz et al., 2008). The SACW and ESACW are defined by a line in  $T_{\text{pot}}-S$  space that can be described by the following equations:

$$T_{\text{pot ESACW}} = 9.4454 \cdot S_{\text{ESACW}} - 319.03 \quad (1)$$

$$T_{\text{pot SACW}} = 8.5607 \cdot S_{\text{SACW}} - 289.08 \quad (2)$$

The above equations were transformed to calculate the respective proportions of SACW and ESACW:

$$S_{\text{SACW}} = (T_{\text{pot}} + 289.08) / 8.5607 \quad (3)$$

$$S_{\text{ESACW}} = (T_{\text{pot}} + 319.03) / 9.4454 \quad (4)$$

$$S_{\text{measured}} = a \cdot S_{\text{SACW}} + b \cdot S_{\text{ESACW}}, \text{ whereby } a + b = 1 \quad (5)$$

Data derived from water depths above 100 m were excluded from this mixing analysis due to the non-conservative behaviour of  $T_{\text{pot}}$  and  $S$  at shallow water depths. The relative contributions are reported in percentage (%). The  $T_{\text{pot}}-S$  range used to calculate the relative contribution of SACW and ESACW is shown in Fig. 3.2. at the example of the MSM17/3 cruise.

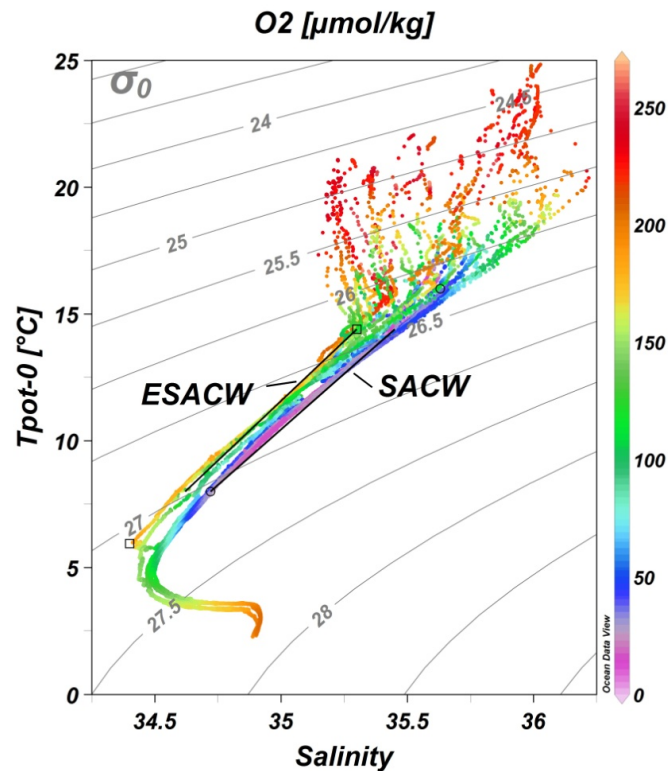


Fig. 3.2.:  $T_{\text{pot}}-S$  diagram of vertical water column profiles measured in the NBUS region during the MSM17/3 cruise. The  $\text{O}_2$  concentration ( $\mu\text{mol kg}^{-1}$ ) is indicated by colour shading and isopycnals ( $\text{kg m}^{-3}$ ) are given by the grey lines. The end points of Eastern South Atlantic Central Water (ESACW, open squares) and South Atlantic Central Water (SACW, open circles) specify the definition source water types given in the text. The  $T_{\text{pot}}-S$  range used to calculate their relative contribution in water samples from  $>100$  m depth is indicated by the black lines.

## RESULTS AND DISCUSSION

On a global scale the distribution of N/P is characterised by a deficit of N towards P with regard to the Redfield ratio (Gruber and Sarmiento, 1997; Tyrrell and Law, 1997). The loss of fixed N is caused by heterotrophic denitrification and anammox occurring in the oceanic OMZs (Lam and Kuypers, 2010) but also in shallow coastal OMZs, e.g. on the Namibian shelf. Here, N loss (Kuypers et al., 2005; Nagel et al., 2013) along with the accumulation of P in sub- and anoxic bottom waters (Goldammer et al., 2010) result in extremely low N/P ratios in the water column. In the following the C/N/P/- $\text{O}_2$  remineralisation patterns observed in 2011 are discussed with regard to their spatial variability and are

complemented by results on the temporal variability of N/P anomalies recorded in 2008 and 2009.

### C/N/P/AOU STOICHIOMETRY

The N and P concentrations of the NBUS scatter to both sides of the reference Redfield slope and characterise the NBUS as a system that produces both positive and negative deviations from Redfield expressed in positive and negative  $N^*$  anomalies (Fig. 3.3.). Major negative anomalies were apparent at shelf sites. Tyrrell and Lucas (2002) attributed low N/P (LNP) data ( $N/P < 3$  and  $P > 1.5 \mu\text{mol kg}^{-1}$ ) in waters of the BUS to nutrient trapping and denitrification that leads to a relative accumulation of P.

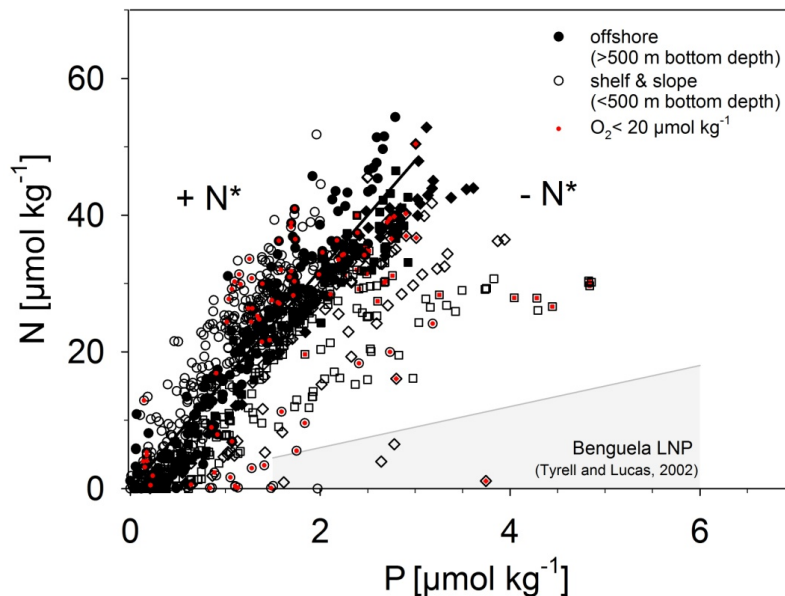


Fig. 3.3.: Composite of N versus P ( $\mu\text{mol kg}^{-1}$ ) data of the MSM07/2b-3 cruise (circles), Afr258 cruise (diamonds) and MSM17/3 cruise (squares). The data were separated into shelf & slope stations ( $< 500$  m bottom depth) indicated by open symbols and offshore stations ( $> 500$  m bottom depth) indicated by black filled symbols. The red filling corresponds to data points associated with  $O_2$  concentrations  $\leq 20 \mu\text{mol kg}^{-1}$ . Positive and negative deviations from the expected N/P correlation of 16/1 (black line) are expressed in  $+N^*$  and  $-N^*$  (Gruber and Sarmiento, 1997). The grey shaded area refers to the range of low N/P (LNP) defined by Tyrrell and Lucas (2002).

Figure 5.4. illustrates the relationships between apparent oxygen utilisation (AOU), N, P,  $A_T$  and  $C_T$  of the water samples in 2011 (MSM17/3). The observed average  $C_T/AOU$  ratio of 0.76 ( $r^2 = 0.89$ ) is close to that expected from a mineralisation C/-O<sub>2</sub> ratio of 106/-138 (Fig. 3.4. a). Exclusion of the O<sub>2</sub> <20  $\mu\text{mol kg}^{-1}$  data gave no mentionable differences between the shelf ( $C_T/AOU = 0.77$ ,  $r^2 = 0.88$ ) and offshore sites ( $C_T/AOU = 0.75$ ,  $r^2 = 0.89$ ). The scattering of the data in Fig. 3.4. is likely due to the fact that the shelf system is not truly closed and that O<sub>2</sub> is introduced into the subsurface water masses on the shelf through mixing (Ito et al., 2004).

The increase of  $C_T$  at  $AOU > 230 \mu\text{mol kg}^{-1}$  corresponding to O<sub>2</sub> <20  $\mu\text{mol kg}^{-1}$  implies  $C_T$  input from anaerobic respiration, such as denitrification and is evident from decreasing N associated with increasing  $C_T$  concentrations (Fig. 3.4. b). At O<sub>2</sub> concentrations <20  $\mu\text{mol kg}^{-1}$ , both anammox and denitrification increased  $A_T$  through the consumption of N (Fig. 3.4. d). However, a decrease in  $C_T$  indicating a dominance of anammox over heterotrophic denitrification is not visible in our data (Fig. 3.4. b) likely due to the low C/N stoichiometry of anammox (C/N = -0.07/-1.3) compared to that of denitrification (C/N ~106/-104) (Koeve and Kähler, 2010). A loss of N by 20  $\mu\text{mol kg}^{-1}$  would result in a  $C_T$  decrease of -1  $\mu\text{mol kg}^{-1}$  due to anammox and a  $C_T$  increase of +21  $\mu\text{mol kg}^{-1}$  during denitrification. At higher O<sub>2</sub> the overall average  $C_T/N = 6.1$  ( $r^2 = 0.86$ ) is similar to the Redfield ratio of 6.6 with slightly lower values in the open ocean (5.5,  $r^2 = 0.89$ ) than on the shelf (6.8,  $r^2 = 0.86$ ). The slope of  $A_T/C_T = -0.15$  (Fig. 3.4. d) observed in the paired data with >20  $\mu\text{mol kg}^{-1}$  O<sub>2</sub> agrees with the expected effect of aerobic organic matter remineralisation ( $A_T/C_T = -16 : 106$ ) (Broecker and Peng, 1982) and implies that carbonate dissolution hardly affected the  $C_T$  and  $A_T$  concentrations.

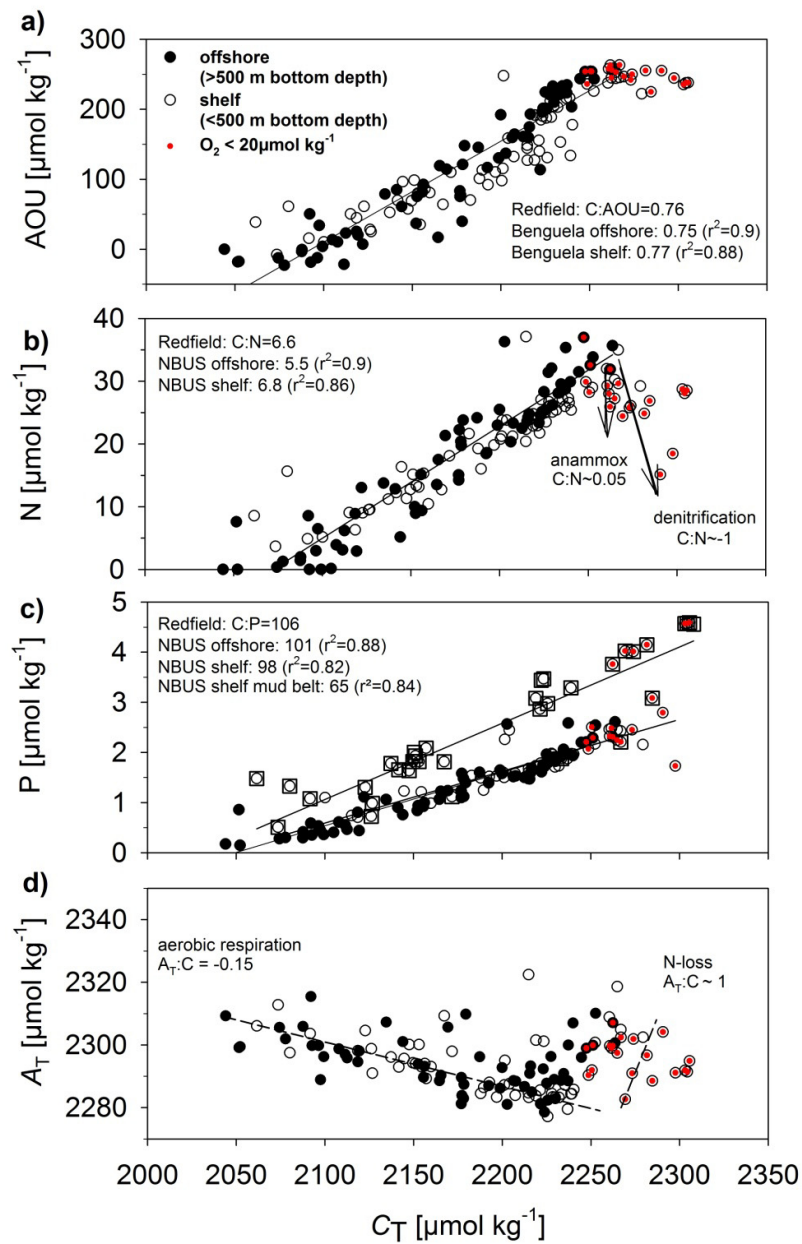


Fig. 3.4.: (a) AOU, (b) N, (c) P and (d)  $A_T$  versus  $C_T$  (all in  $\mu\text{mol kg}^{-1}$ ) as measured within the range of 30–500 m water depth during the MSM17/3 cruise. The data were separated into shelf stations (<500 m bottom depth, open circles) and offshore stations (>500 m bottom depth, black circles). The red filling corresponds to data points associated with  $O_2 \leq 20 \mu\text{mol kg}^{-1}$ . The correlations observed for the Benguela are given and indicated by the black line. The reported ratios in panel (a) and (b) are derived by excluding the  $\leq 20 \mu\text{mol kg}^{-1}$  data. The open squares in panel (c) represent data from the mud belt region. (d) The dashed black lines indicate the expected correlation caused by aerobic mineralisation  $A_T/C = -16/106 = -0.15$  (Redfield et al., 1963) and N loss, e.g. due to denitrification  $A_T/C = 104/106 = \sim 1$  (Gruber and Sarmiento, 1997).

A source of P besides the mineralisation of organic matter in the water column is suggested by the spread of the  $C_T/P$  data in Fig. 3.4. c. Open ocean sites had an average  $C_T/P$  ratio of 101/1 that is similar to the global mean C/P ratio of 106/1 (Redfield et al., 1963; Anderson and Sarmiento, 1994). The  $C_T/P$  correlation of the shelf data splits in 2 groups. One group reveal a slope of the regression line of  $\sim 98/1$  ( $r^2 = 0.82$ ) that is slightly lower but similar to those seen in the offshore samples. The remaining samples suggest a much lower average  $C_T/P$  ratio of  $\sim 65$  ( $r^2 = 0.84$ ) and are related to the mud belt region where even lower C/P ratios of 33-48 were measured in pore waters near the sediment water interface (Goldhammer et al., 2011). The low  $C_T/P$  occurring exclusively at shelf sites indicate an impact of pore water P effluxes from the anoxic mud sediments mediated by consortia of sulphur bacteria (Schulz and Schulz, 2005). This is in line with previous hypotheses that the stoichiometric N deficit in waters over the Namibian shelf is, next to the impact of N reduction, in part caused by P fluxes across the sediment water interface (Bailey and Chapman, 1991; Nagel et al., 2013). Accordingly, the impact of N loss and benthic P fluxes on the suboxic bottom layer should be observable by a spatial decoupling of the N and P maxima, i.e.  $N_{\max}$  would be expectable outside the OMZ while  $P_{\max}$  would be expectable inside the OMZ. This is in agreement with our observations of N and P maxima along the Namibian shelf and slope (Fig. 3.5.; exemplary for the MSM17/3 cruise in February 2011). The OMZ was positioned between 300 and 400 m water depth off Kunene (17.25 °S) (Fig. 3.5. a) stretching from the slope towards the open ocean. The maxima of N ( $= 45 \mu\text{mol kg}^{-1}$ ) and P ( $= 2.8 \mu\text{mol kg}^{-1}$ ) were observed at the same depth ranges slightly below the OMZ. In contrast, the OMZ was restricted to the shallow shelf region off Walvis Bay (23 °S) (Fig. 3.5. b) overlying the diatomaceous mud belt where the large sulphur bacteria occur that release P to the anoxic pore water (Goldhammer et al., 2011). In fact,  $P_{\max}$  was strongly elevated ( $= 4.8 \mu\text{mol kg}^{-1}$ ), and coincided with the OMZ, while  $N_{\max}$  had decreased to  $35 \mu\text{mol kg}^{-1}$  and was observed outside the OMZ. This increase of P relative to N is reflected in a pronounced N/P deviation from Redfield as indicated by strongly decreased  $N^*$  values over the shelf and shelf break off Walvis Bay (23 °S) compared to Kunene (17.25 °S). Although the N loss likely contributes to the overall N decrease, it also reflects the gradual increase of the ESACW fraction towards the

south. This water mass is characterised by lower nutrient concentrations than SACW (Poole and Tomczak, 1999; Mohrholz et al., 2008).

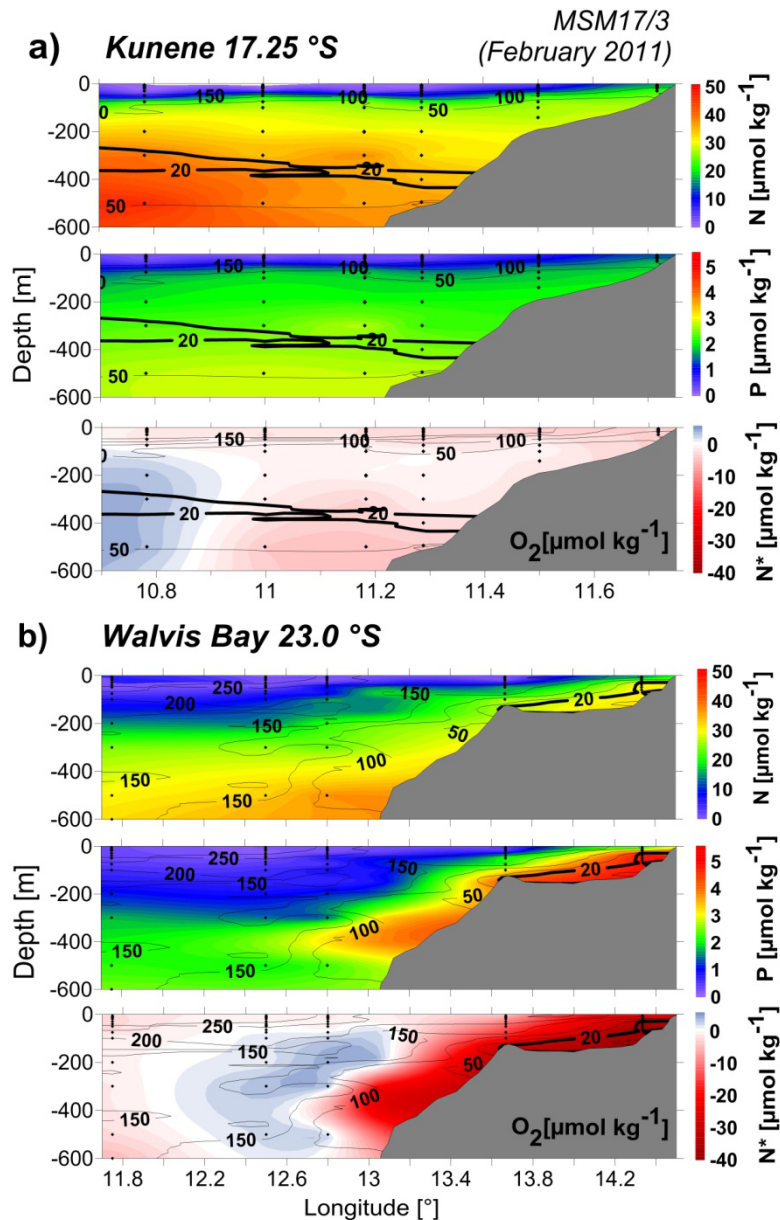


Fig. 3.5.: Cross-shelf transects off (a) Kunene (17.25 °S) and (b) Walvis Bay (23.0 °S) during MSM17/3 cruise showing the spatial decoupling of N and P maxima expressed in  $N^*$ . The N, P and  $N^*$  concentrations (colour shading, in  $\mu\text{mol kg}^{-1}$ ) are overlain by the  $\text{O}_2$  concentrations (contoured at  $50 \mu\text{mol kg}^{-1}$  intervals, black isolines). The area of low  $\text{O}_2$  concentration ( $\leq 20 \mu\text{mol kg}^{-1}$ ) is marked by the bold black line. The sampled stations used for gridding are indicated by black circles; areas of no data were extrapolated (kriging method).

Concluding, C/N/P/-O<sub>2</sub> ratios at offshore sites are 101/16/1/138 and are close to Redfield ratios. Over the Namibian shelf, in particular related to the mud belt region, increased P concentrations result in a C/N/P/-O<sub>2</sub> ratio of 106/16/1.6/138. In regions with O<sub>2</sub> concentrations <20 μmol kg<sup>-1</sup>, denitrification further increases C/N and denitrification along with anammox further lower N/P ratios.

### SPATIAL AND TEMPORAL VARIABILITY

Inter-annual differences in upwelling conditions during austral summer expeditions were well reflected in the distribution of sea surface temperatures (SST). The SST patterns, measured continuously by thermo-salinographs at 5 m water depth, indicate that upwelling was most intense in December 2009 (Afr258) (Fig. 3.6.), when minimum SST (15 °C) occurred along the entire coast and temperatures <20 °C were measured far offshore. In contrast, most of the NBUS had SST >20 °C during February 2011 (MSM17/3).

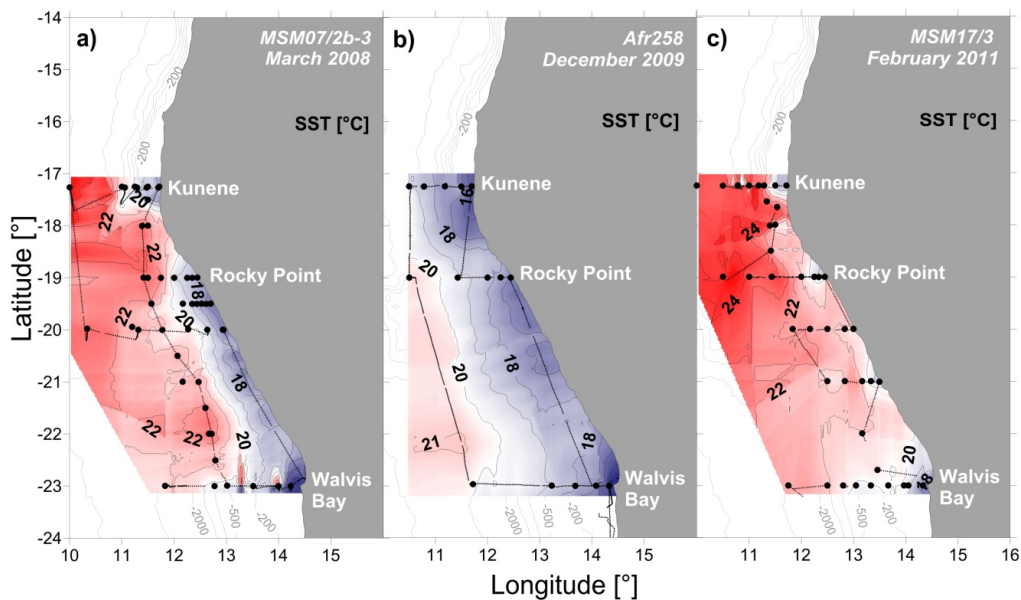


Fig. 3.6.: Distribution of sea surface temperature (SST) (contoured at 1 °C intervals) at 5 m depth continuously measured along the cruise track during (a) MSM07/2b-3, (b) Afr258 and (c) MSM17/3. Sampled stations (black circles) and cruise track (black line) were used for gridding; areas of no data were extrapolated (kriging method).

In March 2008 (MSM07/2b-3) SST outline an intermediate upwelling intensity in a coastal band of low temperatures. Stronger or weaker upwelling is also associated with distinct distributions of the central water masses on the shelf. Mohrholz et al. (2008) found that vigorous cross shelf circulation during phases of strong upwelling suppresses the along-shelf poleward undercurrent of SACW from the north. Weak upwelling phases, such as that in February 2011, permit SACW to protrude far southward as indicated by the high SACW contribution (70 %) off Walvis Bay (23 °S) (Fig. 3.7. d-f).

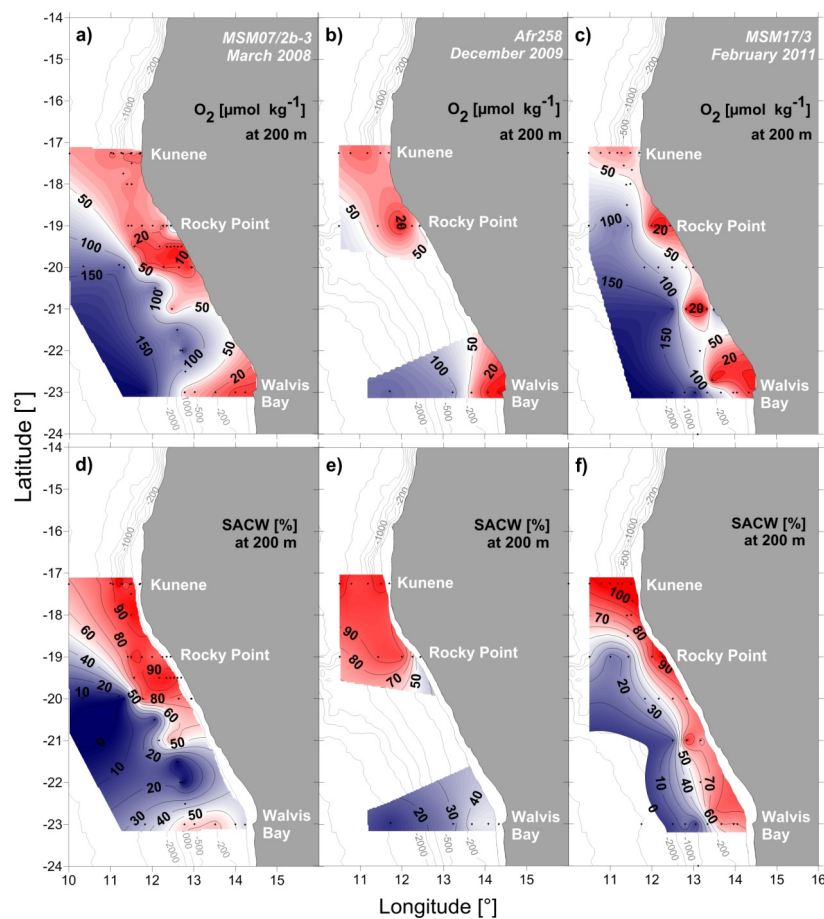


Fig. 3.7.: (a-c) Distribution of O<sub>2</sub> (μmol kg<sup>-1</sup>) and (d-f) contribution of SACW and ESACW (%) at 200 m water depth. Note: shelf stations with bottom depths shallower than 200 m were included in the O<sub>2</sub> interpolation and stations with deeper than 100 m were included in the SACW interpolation. The sampled stations used for gridding are marked by black circles; areas of no data were extrapolated (kriging method). 0% SACW is equivalent to 100% ESACW.

SACW is characterised by much lower  $O_2$  concentrations than ESACW (Mohrholz et al., 2008) which is also evident from our data (Fig. 3.2.). In fact, the dominance of SACW was reflected in mid-water  $O_2$ -deficits, so that samples with  $\geq 80\%$  SACW were associated with  $\leq 50 \mu\text{mol kg}^{-1} O_2$  (Fig. 3.7.). However, during strong and weak upwelling alike and regardless of the SACW contribution, the  $O_2$  concentrations on the shelf off Walvis Bay were  $< 20 \mu\text{mol kg}^{-1}$  during all cruises. It reflects the strong  $O_2$  demand caused by the organic-rich mud belt area and is in line with previous studies showing that SACW sets the precondition for anoxia in bottom waters off Walvis Bay but that the local sedimentary  $O_2$  demand plays a decisive role as well (Monteiro et al., 2006; van der Plas et al., 2007). The N/P deviation from Redfield varied during the different expeditions and upwelling states (Fig. 3.8.).

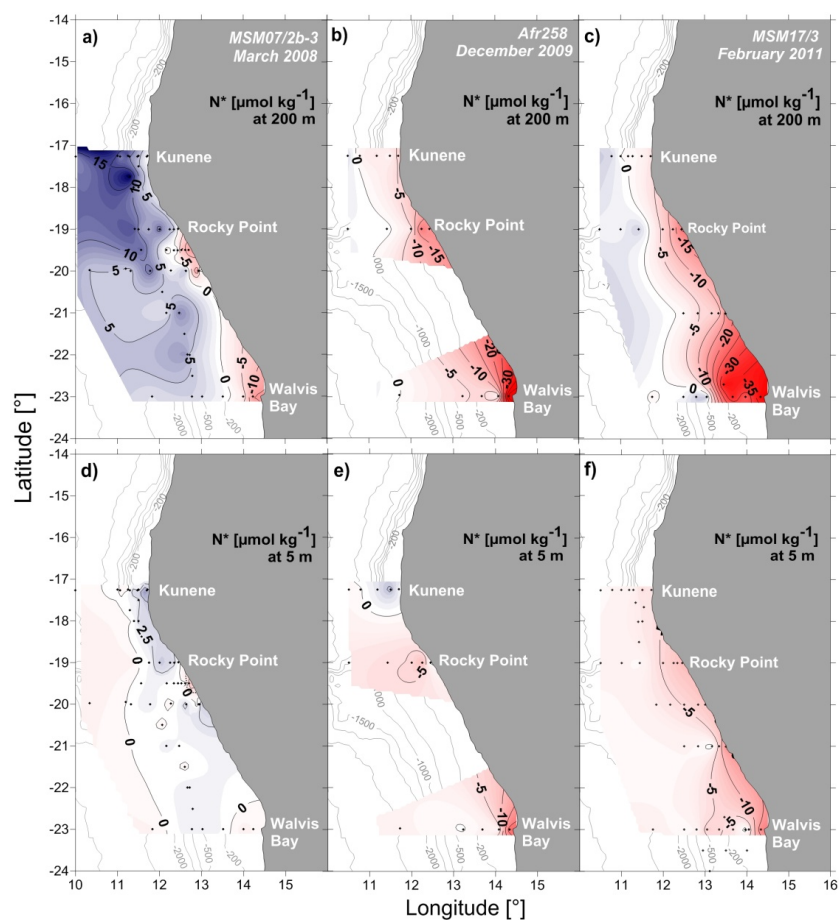


Fig. 3.8.: Distribution of  $N^*$  ( $\mu\text{mol kg}^{-1}$ ) (a-c) at 200 m and (d-e) at 5 m water depth (contoured at  $5 \mu\text{mol kg}^{-1}$  intervals). Note: shelf stations with bottom depths shallower than 200 m were included in the  $N^*$  interpolation. The sampled stations used for gridding are marked by black circles; areas of no data were extrapolated (kriging method).

Pronounced negative  $N^*$  concentrations were observed in coastal bottom waters in particular off Rocky Point and Walvis Bay (Fig. 3.8. a-c) and are comparable with reported values (Tyrrell and Lucas, 2002; Nagel et al., 2013). Elevated  $N^*$  was observed at offshore sites and differed strongly in magnitude especially offshore of Kunene (17.25 °S) where SACW dominates (Fig. 3.9. d-f) indicating that the  $N^*$  signature of SACW differs.

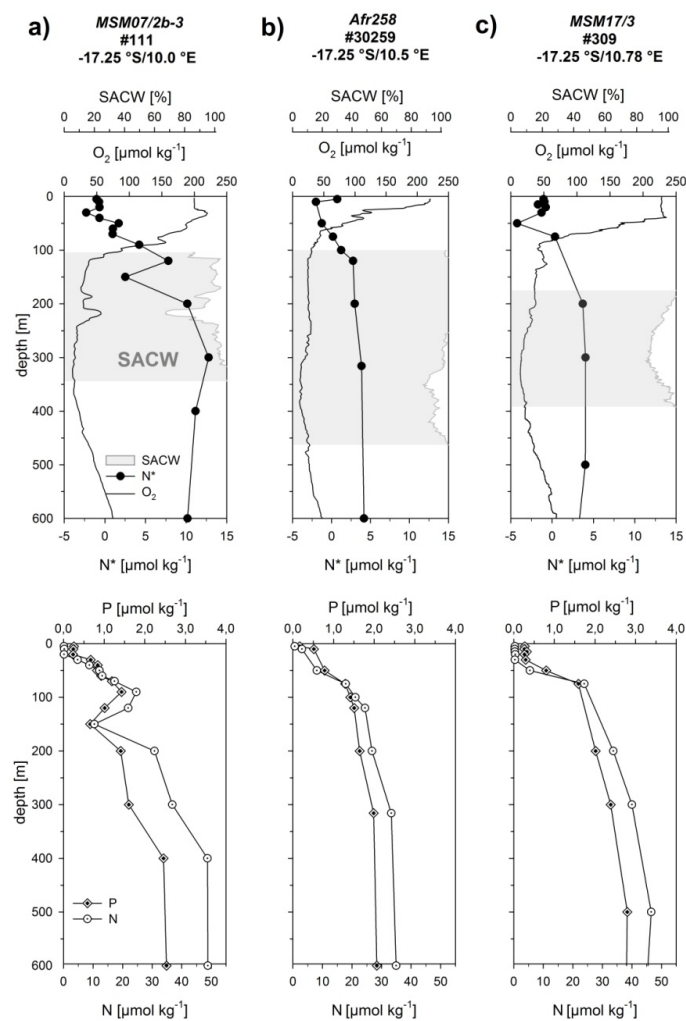


Fig. 3.9.: Vertical profiles of SACW (%),  $O_2$ ,  $N^*$ , P and N (all in  $\mu\text{mol kg}^{-1}$ ) during (a) MSM07/2b-3, (b) Afr258 and (c) MSM17/3 at offshore stations with comparable location offshore of Kunene (17.25 °S). The contribution of SACW is indicated by the grey shading.

From the temporal variability of  $N^*$  in the hemipelagic OMZ offshore of Kunene it is apparent that  $N^*$  in the SACW water mass varied significantly between years (Fig. 3.9.). During March 2008 (MSM07/2b-3),  $N^*$  was 3 fold increased within the OMZ ( $N^* = \sim 12 \mu\text{mol kg}^{-1}$ ) compared to December 2009 and February 2011 ( $N^* = \sim 3-4 \mu\text{mol kg}^{-1}$ ). This positive  $N^*$  anomaly was imported to the NBUS in 2008 along with SACW, so that water masses on the shelf were less  $N^*$ -deficient (Fig. 3.8. a-c) despite similarly low  $O_2$  concentrations in 2009 and 2011 (Fig. 3.7. a-c). Strong local sedimentary  $O_2$  demand caused by the organic-rich mud belt area is suggested by low  $N^*$  observed, e.g. off Rocky Point in 2008 despite high SACW contribution (Fig. 3.7., 5.8. a). In contrast to the situation in March 2008 (MSM07/2b-3), most of the NBUS area revealed negative  $N^*$  concentrations in December 2009 (Afr258) and February 2011 (MSM17/3) and strongest  $N^*$ -deficits ( $N^* = -35 \mu\text{mol kg}^{-1}$ ) off Walvis Bay exceeded the  $N^*$ -deficits in March 2008 by a factor of  $>2$ . The results suggest that the considerable variability in nutrient ratios of SACW controls the inter-annual variability of  $N^*$  in the NBUS. The impact of ESACW entering the NBUS from the south is difficult to assess from our data due to a lack of ESACW samples from the southern BUS. The ESACW sampled in the NBUS is characterised by lower  $O_2$  concentrations ( $\sim 150-200 \mu\text{mol kg}^{-1}$ ) (Fig. 3.2.) than reported for ESACW from the southern BUS region ( $250-300 \mu\text{mol l}^{-1}$ ) (Poole and Tomczak, 1999) indicating that ESACW is modified by aerobic mineralisation on its way from the SBUS to the NBUS region. Following the nutrient signature of ESACW given by Poole and Tomczak (1999),  $N^*$  ranges between  $-5.45$  and  $-0.762 \mu\text{mol l}^{-1}$ . Assuming mineralisation according to the Redfield stoichiometry under these oxygenated conditions and further assuming absence of  $N_2$  fixation in the SBUS implies that the  $N^*$  signature of ESACW should not be further altered on its way towards the NBUS. An intrusion of ESACW would therefore rather contribute to the negative  $N^*$  signal observed over the NBUS shelf. On the contrary, off the western South African coast,  $N^*$  was shown to vary between  $0-5 \mu\text{mol kg}^{-1}$  along the  $\sigma_\theta = 26.50$  and  $27.1 \text{ kg m}^{-3}$  surfaces (Gruber and Sarmiento, 1997) referring to a depth range where ESACW occurs. However, it suggests that comparable to SACW, the  $N^*$  signature in ESACW might vary but this aspect is not further addressed owing to the low density of ESACW data.

Positive  $N^*$  anomalies in subsurface waters are commonly attributed to the mineralisation of organic matter produced by  $N_2$ -fixing organisms (Gruber and Sarmiento, 1997) that have N/P ratios of up to 150 (Krauk et al., 2006). The impact of mineralisation is reflected in minimum  $O_2$  concentrations that coincided with maximum  $N^*$  values within the SACW fraction (Fig. 3.9.). Positive  $N^*$  anomalies in the tropical and subtropical North Atlantic are  $\sim 4 \mu\text{mol kg}^{-1}$  at  $\sigma_\theta = 26.5 \text{ kg m}^{-3}$  (Gruber and Sarmiento, 1997; Mahaffey et al., 2005). Here, intensive blooms of *Trichodesmium* spp. (Carpenter, 1983; Tyrrell et al., 2003; Capone et al., 2005) and high N/P (of up to 35) have been reported (Mahaffey et al., 2003) and are consistent with  $N_2$  fixation as a significant input source, which can raise  $N^*$  to  $\sim 20 \mu\text{mol kg}^{-1}$  (Mahaffey et al., 2003). In contrast, the South Atlantic gyre has low positive  $N^*$  (Gruber and Sarmiento, 1997), in line with low rates of  $N_2$  fixation (Mahaffey et al., 2005).  $N_2$  fixation is facilitated by P and the availability of micronutrients, e.g. iron (Fe) (Mills et al., 2004). The low  $N_2$  fixation in the South Atlantic has been attributed to a lack of Fe supply rather than P availability (Moore et al., 2009). This is supported by the negative  $N^*$  observed in the surface water offshore of Kunene (Fig. 3.9.) caused by P concentrations that ranged between  $0.17\text{-}0.28 \mu\text{mol kg}^{-1}$  and exceeded N concentrations resulting in surface water  $N^*$  deficits. The very low N concentrations further suggest that atmospheric deposition that is assumed to be another significant N source to the ocean (Duce et al., 2008; Baker et al., 2013) is negligible. However, Sohm et al. (2011) observed  $N_2$  fixation within the ABFZ ( $\sim 13\text{-}15^\circ\text{S}$ ) coinciding with decreased thermocline  $\delta^{15}\text{N}_{\text{NO}_3^-}$  values and elevated dissolved Fe and cobalt surface concentrations (Noble et al., 2012) that are important micronutrients for marine diazotrophic cyanobacteria (Saito et al., 2002; Saito et al., 2004). The studies of Sohm et al. (2011) and Noble et al. (2012) were performed from November-December 2007 and hence  $\sim 4$  months prior to the MSM07/2b-3 expedition in March 2008 that found the positive  $N^*$  anomaly in SACW. This time period is comparable to the time lag of  $\sim 2$  months that was observed between the occurrence of *Trichodesmium* and the response in  $N^*$  (Singh et al., 2013). Although the  $N_2$  fixation rates were relatively low ( $22\text{-}85 \mu\text{mol N m}^{-2} \text{ d}^{-1}$ ) (Sohm et al., 2011), it was proven that  $N_2$  fixation occurs north of the ABFZ, even with high nitrate concentrations ( $\sim 20 \mu\text{mol l}^{-1}$ ) in surface water. This finding seems to challenge the traditional paradigm of high  $N_2$  fixation activity being restricted to oligotrophic regions. However, there is

growing evidence based on laboratory and field studies showing that  $N_2$  fixation occurs under nutrient-rich conditions (Sohm et al., 2011; Knapp, 2012; Knapp et al., 2012; Subramaniam et al., 2013). It suggests that Fe might be the factor limiting  $N_2$  fixation at the ABFZ. In contrast to the Sahara dust plumes influencing the North Atlantic, the eastern South Atlantic experiences much lower aeolian input (Jickells et al., 2005; Mahowald et al., 2009). Dust plumes off Namibia are channelled by dry river beds and appear to be much more restricted to near shore regions (Eckardt and Kuring, 2005). However, dust transport from southern Africa to the South Atlantic has been reported for austral spring (Swap et al., 1996; Sarthou et al., 2003) further supported by Tyson et al. (1996) who found that the main air mass transport to the South Atlantic peaks during austral spring and summer indicating that  $N_2$  fixation initiated by atmospheric Fe input is expectable during this time of the year in line with the results of Sohm et al. (2011). Although not as pronounced as in March 2008,  $N^*$  was also elevated during December 2009 and February 2011 within the SACW fraction, suggesting  $N_2$  fixation is apparent albeit of lower magnitude. Alternatively to atmospheric Fe-sources, hypoxic bottom waters of the Angolan and Namibian shelf reveal high concentrations of dissolved and particulate Fe (Bowie et al., 2002; Noble et al., 2012). It suggests that upwelling of these bottom waters along the Angolan and Namibian coast serves as Fe-source analogue to the California and Peru upwelling system (Johnson et al., 2001; Bruland et al., 2005). In view of the findings on diazotrophy under nutrient-rich conditions, we assume that  $N_2$  fixation is a feasible input source that caused the observed N excess in the SACW in 2008. Furthermore, methodological improvements (Mohr et al., 2010; Großkopf et al., 2012) and the broadening range of identified species involved in  $N_2$  fixation (Moisander et al., 2010; Zehr, 2011) suggest that rates and regions of  $N_2$  fixation may have been considerably underestimated so far.

#### NBUS – A $P^*$ - SOURCE FOR THE SOUTH ATLANTIC

Upwelling of N-deficient water in 2009 and 2011 caused lowest  $N^*$  at 5 m depth close to the coast (Fig. 3.8. d-f) indicating that a relative P surplus surfaces and is advected offshore into the open ocean with modified upwelling water. This should stimulate  $N_2$  fixation in

the adjacent hemipelagic ocean (Deutsch et al., 2007), but experimentally determined rates of  $N_2$  fixation in the NBUS were very low to not detectable (N. Wasmund, pers. comm., 2012). We calculated the P excess ( $P^*$ ) within the euphotic zone (0-20 m) that is exported offshore for the Walvis Bay ( $23^\circ S$ ) transect (Fig. 3.10.). Roughly 300 km offshore, beyond the continental slope,  $P^*$  was close to zero in March 2008 ( $P^* = 0.007 \pm 0.09 \mu\text{mol kg}^{-1}$ ), suggesting that the NBUS at that time was not a regional source of P for the oligotrophic subtropical South Atlantic. During the other cruises, the NBUS was a relative P source with  $P^*$  values of  $0.3 \pm 0.01 \mu\text{mol kg}^{-1}$ .

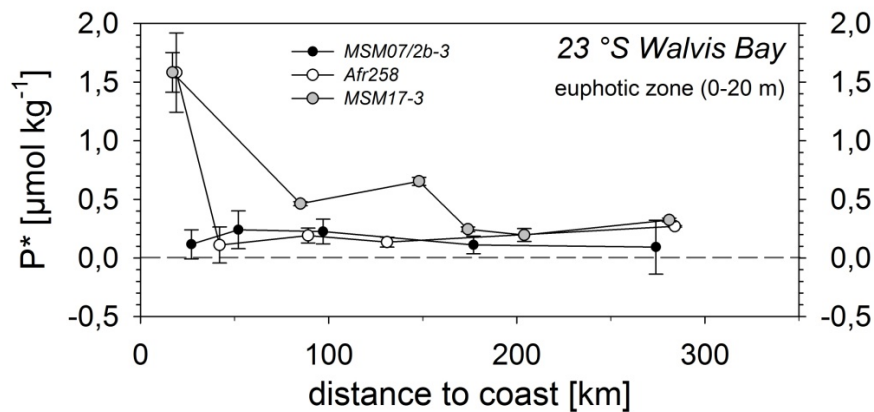


Fig. 3.10.: Averaged  $P^*$  ( $\mu\text{mol kg}^{-1}$ ) of the euphotic zone (0-20 m) versus distance to the coast (km) during MSM07/2b-3 (black circles), Afr258 (open circles) and MSM17/3 (grey circles) along the Walvis Bay transect ( $23^\circ S$ ).

These observations are in line with Staal et al. (2007) and Moore et al. (2009) who reported surface  $P^* = 0.15\text{-}0.30 \mu\text{mol kg}^{-1}$  within areas of the subtropical gyre that are influenced by the advection of water masses transported by the Benguela Current. Along with our findings, it implies that the coastal upwelling system over the shelf is a  $P^*$ -source to the South Atlantic most of the time. As shown before, the bottom water off Walvis Bay was low in  $O_2$  independent of the upwelling situation (Fig. 3.8.) leading to strongly elevated P and reduced N maxima off Walvis Bay (Fig. 3.5.). It implies that especially the mud belt of the shallow central Namibian shelf is a region of continuous  $+P^*$  generation via N loss and P efflux. We assume that the inter-annual variability of  $P^*$  in the surface (Fig. 3.10.)

depends mainly on the magnitude of  $+N^*$  in the SACW that is produced probably by  $N_2$  fixation north of the ABFZ. We further presume that  $N_2$  fixation in this region is, in turn, linked to the NBUS by the export of  $+P^*$  into the South Atlantic ocean and its advection along with the major surface currents to the Angola Gyre and ABFZ region (Fig. 3.11.).

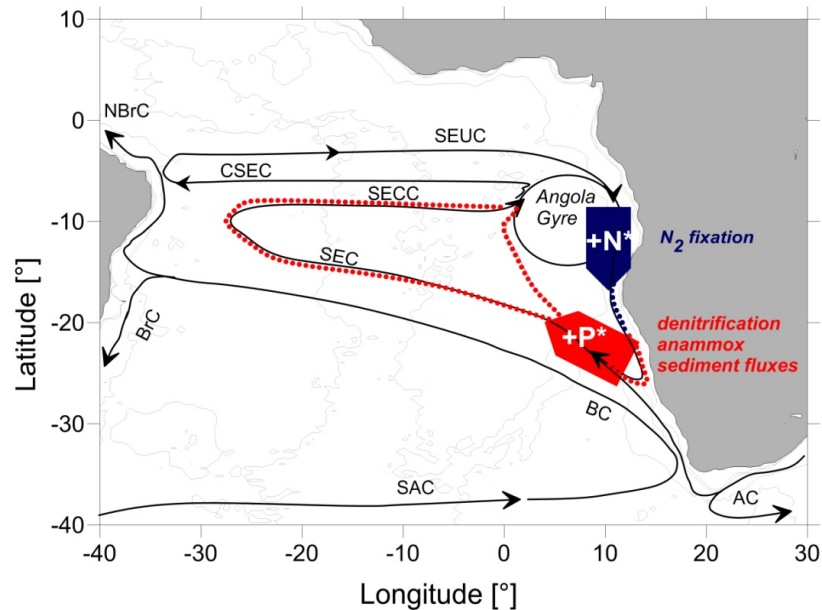


Fig. 3.11.: Map of the wind driven large scale circulation (upper 100 m) of the South Atlantic Ocean (adapted from Stramma and England (1999)). The map illustrates the hypothetical advection of  $+P^*$  (red dashed line) via SEC and SECC towards the Angola Gyre where it fuels  $N_2$  fixation and in turn results in  $+N^*$  (blue dashed line) that is introduced to the NBUS. AC, Agulhas Current; BC, Benguela Current; BrC, Brazil Current; CSEC, Central South Equatorial Current; NBrC; North Brazil Current; SAC, South Atlantic Current; SEC, South Equatorial Current; SECC, South Equatorial Countercurrent; SEUC, South Equatorial Undercurrent.

## CONCLUSION

Our data measured during the cruise in March 2011 show a mean C/N/P/ $-O_2$  ratio that is close to the Redfield stoichiometry. Over the mud belt of the Namibian shelf pore water fluxes lowered the C/N/P/ $-O_2$  ratio to 106/16/1.6/138. N losses further increased C/N and decreased N/P ratios in restricted regions where  $O_2$  concentrations dropped below  $20 \mu\text{mol kg}^{-1}$ . Additional nutrient data measured during 2 cruises in 2008 and 2009 reveal an inter-annual variability of N excess within the SACW that flows from the north into the NBUS with highest  $N^*$  values observed in 2008. The degree to which the N loss on the shelf is

balanced by enhanced inputs of N along with the SACW controls the amount of P\* that is exported from the NBUS into the subtropical South Atlantic. To better understand the role of the northern Benguela upwelling system as P source and N sink, factors controlling the occurrence of N<sub>2</sub> fixation at the Angola Benguela Frontal Zone need to be addressed in future studies.

Acknowledgments: We would like to thank all scientists, technicians, captains and their crews on board the research vessels RV Africana and RV Maria S. Merian. Matthias Birkicht is acknowledged for the nutrient analysis. We sincerely thank Laura Lehnhoff and Claas G. Steigüber for their help during and subsequently to the expeditions. Suzie Christof and Nadine Moroff are thanked for their comprehensive support during the stay in Swakopmund. The comments to this paper offered by 3 reviewers have made valuable contributions to the final version and are gratefully acknowledged. Furthermore, we are grateful to the German Federal Ministry of Education and Research (BMBF) for financial support of the GENUS project (03F0497D-ZMT).

## 4. CHAPTER II

### ALKALINITY PRODUCTION BUFFERS THE CARBONATE SATURATION STATE IN THE BENGUELA CURRENT UPWELLING SYSTEM

Anita Flohr<sup>1</sup>, Tim Rixen<sup>1,2</sup>, Anja van der Plas<sup>3</sup>, Volker Mohrholz<sup>4</sup>, Andreas Neumann<sup>2</sup>, and  
Kay-Christian Emeis<sup>2,5</sup>

[1] Leibniz Centre for Tropical Marine Ecology (ZMT), Fahrenheitstraße 6, 28359 Bremen, Germany

[2] Institute for Biogeochemistry and Marine Chemistry, University of Hamburg, Bundesstraße 55, 20146 Hamburg, Germany

[3] National Marine Information and Research Centre Ministry of Fisheries & Marine Resources, PO Box 912 Swakopmund, Namibia

[4] Leibniz-Institute for Baltic Sea Research (IOW), Seestraße 15, 18119 Rostock, Germany

[5] Helmholtz-Centre for Materials and Coastal Research Geesthacht, Max-Planck-Straße 1, 21502 Geesthacht, Germany

Corresponding author: A. Flohr, Leibniz Centre for Tropical Marine Ecology (ZMT), Fahrenheitstraße 6, 28359 Bremen, Tel.: ++49 421 2380047, Fax: ++49 421 2380030, (anita.flohr@zmt-bremen.de)

To be submitted



## ABSTRACT

The invasion of anthropogenic carbon dioxide ( $\text{CO}_2$ ) into the oceans influences the biological pump as it lowers the saturation states ( $\Omega$ ) of biologically important  $\text{CaCO}_3$  minerals aragonite ( $\Omega_A$ ) and calcite ( $\Omega_C$ ) in the surface water. They directly affect the calcification, growth and survival of many marine calcifying organisms, and  $\text{CO}_2$  invasion raises the carbonate saturation depth in the deep ocean. Among the four major eastern boundary upwelling system (EBUS), the Benguela upwelling system (BUS) off the southwest African coast is the most productive (Carr and Kearns, 2003) but also recognised as the least studied one (Capone and Hutchins, 2013). On the basis of dissolved inorganic carbon (DIC) and total alkalinity (TA) measurements we aimed to investigate the factors that drive the variability of ( $\Omega_A$ ) and calcite ( $\Omega_C$ ) in the northern Benguela upwelling system (NBUS). We show that the NBUS is affected by coastal upwelling of water with  $\Omega$  values minimizing to  $\Omega_A \sim 0.7$  and  $\Omega_C \sim 1.2$ . The results indicate that the strongest reduction of  $\Omega$  is associated with the aerobic decomposition of organic matter in the oxygenated subsurface water column, thereby raising DIC from 2045 to 2200  $\mu\text{mol kg}^{-1}$ . The results further suggest that the increasing contribution of anaerobic remineralisation on the shelf results in a generation of TA, which counterbalances the continuing DIC release maximizing to 2310-2420  $\mu\text{mol kg}^{-1}$ . The results indicate that TA generation in bottom water on the shelf is a mechanism that, apart from elevating  $\Omega$ , reduces the  $\text{pCO}_2$  in upwelling water, thus affects the strength of  $\text{CO}_2$  emissions to the atmosphere. At offshore sites, in oxygenated Antarctic Intermediate Water, the observed TA increase is suggestive of the dissolution of aragonite in the water column. Our data suggest that further invasion of anthropogenic  $\text{CO}_2$  could lower  $\Omega_A$  to  $<1$  within SACW, which would raise the aragonite saturation horizon to depth levels above Antarctic Intermediate Water.

## INTRODUCTION

A reduction of the saturation states ( $\Omega$ ) of the biologically important calcium carbonate ( $\text{CaCO}_3$ ) minerals aragonite ( $\Omega_A$ ) and calcite ( $\Omega_C$ ), e.g. as a consequence of the invasion of anthropogenic carbon dioxide ( $\text{CO}_2$ ) into the surface and subsurface ocean (Feely et al.,

2004; Sabine et al., 2004; Doney et al., 2009), affects the calcification, growth and survival of many marine calcifying organisms (e.g. Doney et al., 2012; Kroeker et al., 2013). Upwelling systems are characterised by intense CO<sub>2</sub> emission and biological CO<sub>2</sub> uptake causing a highly variable inorganic carbonate chemistry of the surface waters. They are naturally characterised by low  $\Omega$  levels in the coastal surface waters (Torres et al., 1999; Leinweber et al., 2009; Santana-Casiano et al., 2009; Rixen et al., 2012). However, it is also suggestive of a higher vulnerability to anthropogenic impacts observed, e.g. off California where the invasion of anthropogenic CO<sub>2</sub> into subsurface waters reduces  $\Omega_A$  to corrosive levels  $<1$  (Feely et al., 2008; Hauri et al., 2009). This emphasises the importance to study impacts of climate change in these systems also with regard to their high economic importance.

Among the four major eastern boundary upwelling systems (EBUS), the Benguela upwelling system (BUS) off the southwest African coast is the most productive (Carr and Kearns, 2003) but also recognised as the least studied one (Capone and Hutchins, 2013). Phytoplankton communities of the BUS are dominated by diatoms and dinoflagellates near the coast in freshly upwelled water (Barlow et al., 2006; Barlow et al., 2009), whereas nanoflagellates and calcite forming coccolithophorids are usually more abundant in mature water, e.g. at the rims of upwelling cells (Mitchell-Innes and Winter, 1987; Pitcher et al., 1992; Giraudeau et al., 1993; Henderiks et al., 2012). High fractions of particulate organic carbon (POC) export, accounting for  $\sim 1.75$  % of surface production to depths below 1000 m (Fischer et al., 2000), are driven by sinking fluxes of carbonate producers. These are mainly coccolithophorids and foraminifera, which dominate the offshore particulate inorganic carbon (PIC) fluxes (Wefer and Fischer, 1993; Giraudeau et al., 2000; Romero et al., 2002) and create the carbonate-rich surface sediments offshore the shelf break (Giraudeau, 1993; Boeckel and Baumann, 2004) (Fig. 4.1.). In contrast, the surface sediment record of the BUS shelf, where highest accumulation of POC occurs (Bremner, 1981; Mollenhauer et al., 2002), shows no significant PIC deposition, but high opal contributions (Bremner and Willis, 1993; Inthorn et al., 2006).

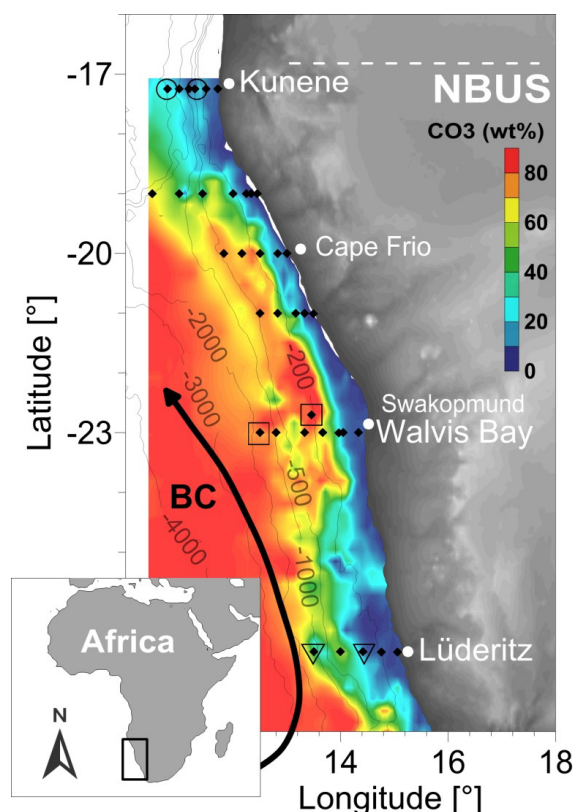


Fig. 4.1.: Schematic map of the northern Benguela upwelling system (NBUS) off southwest Africa. The  $\text{CaCO}_3$  content (wt %) of surface sediments is indicated by colour shading emphasising the low  $\text{CaCO}_3$  content close to the coast. The stations sampled along transects are indicated by black dots. The open circles, squares, and diamonds denote the stations presented in Fig. 4.4..  $\text{CaCO}_3$  data were obtained from Inthorn et al. (2006). Areas of no data were extrapolated (kriging method).

These gradients of  $\text{CaCO}_3$  deposition patterns in coastal and offshore sediments (Fig. 4.1.) (Giraudeau, 1992; Bremner and Willis, 1993; Inthorn et al., 2006) suggests low carbonate production in coastal surface water and/or the dissolution of  $\text{CaCO}_3$  particles in the water column or sediments. Remineralisation ratios suggest that, instead of  $\text{CaCO}_3$  dissolution, the high DIC concentrations in bottom water on the shelf result from (an)aerobic organic matter remineralisation (Flohr et al., 2014) by processes which include denitrification, anammox and sulphate reduction (Brüchert et al., 2003; Kuypers et al., 2005; Nagel et al., 2013). These processes differ with regard to their impact on DIC and TA. The decomposition of organic matter is associated with DIC increase and TA decrease (e.g. aerobic decomposition), whereas other processes increase both DIC and TA (e.g. heterotrophic denitrification, sulphate reduction) or decrease DIC and increase TA (e.g.

autotrophic anammox) (Goldman and Brewer, 1980; Wolf-Gladrow et al., 2007; Koeve and Kähler, 2010). It is probable that diverse processes affect the variability of TA, DIC, and hence  $\Omega$  in the subsurface and upwelling waters of the BUS. However, little is known about the vertical and spatial variability of  $\Omega$  on the shelf. Here we present and discuss carbonate system parameters (DIC, TA,  $\Omega$ ) in the surface layer and in the water column during two sampling campaigns in 2010 and 2011 to investigate the factors that control  $\Omega_A$  and  $\Omega_C$  in the NBUS.

## MATERIAL AND METHODS

### STUDY AREA

The Benguela upwelling regime roughly stretches from  $\sim 16^\circ\text{S}$  to  $\sim 35^\circ\text{S}$  (Fig. 4.1.) and is bordered to the south by the Agulhas Current (AgC) retroflexion and to the north by the Angola Benguela Frontal Zone (ABFZ) that is highly dynamic in shape and position. Persistent southerly winds induce coastal upwelling most pronounced where the shelf narrows at  $17^\circ\text{S}$ ,  $26^\circ\text{S}$  and  $34^\circ\text{S}$  (Nelson and Hutchings, 1983; Shillington et al., 2006; Hutchings et al., 2009). The strong Lüderitz upwelling cell (at  $\sim 26^\circ\text{S}$ ) establishes an environmental barrier that separates the BUS into a northern and southern subsystem (N and SBUS) (Shannon, 1985; Duncombe Rae, 2005). Wind driven upwelling peaks in austral winter and minimises in austral summer in the NBUS although overall the seasonality is less pronounced in the NBUS compared to the SBUS (Shannon, 1985). Upwelling in the southern BUS entrains Eastern South Atlantic Central Water (ESACW) into the offshore Ekman drift (Duncombe Rae, 2005; Mohrholz et al., 2008). Between the ABFZ and the Lüderitz cell, the ESACW mixes with an Angola Gyre subtype of the South Atlantic Central Water (SACW) which is older and thus strongly  $\text{O}_2$  depleted compared to ESACW (Poole and Tomczak, 1999; Mohrholz et al., 2008). The SACW enters the Namibian shelf and continental margin in a poleward undercurrent via the Angola Current (Duncombe Rae, 2005; Mohrholz et al., 2008). Increased inflow of SACW into the NBUS occurs during austral summer and autumn and preconditions the development of an oxygen minimum zone (OMZ) and anoxic events over the Namibian shelf and upper slope (Weeks et al., 2002; Monteiro et al., 2006; Mohrholz et al., 2008). High inshore total organic

carbon (TOC) content forces strong O<sub>2</sub> demand of sediments (van der Plas et al., 2007) reflected in strong O<sub>2</sub> depletion and DIC increase in bottom waters (Flohr et al., 2014). N loss in the sub- and anoxic water column and sediments caused by anammox and denitrification (Kuypers et al., 2005; Nagel et al., 2013) along with P release from sediments, mediated by large sulphur bacteria (Schulz and Schulz, 2005), are reflected in non-standard nutrient ratios (N/P <16) in upwelling water (Dittmar and Birkicht, 2001; Tyrrell and Lucas, 2002).

### SAMPLING AND ANALYSIS OF DIC, TA AND $\Omega$

DIC and TA data comprise surface samples obtained from the jetty in Swakopmund (February – May 2010) and water column samples taken along vertical profiles during RV M.S. Merian 17/3 cruise (January 31<sup>st</sup> – May 8<sup>th</sup> 2011) during austral summer.

The samples of the Swakopmund time series were taken on a non-regular basis from the jetty in Swakopmund using a single 2.5 l Niskin bottle. Sampling was carried out in the morning between 8:00-9:00 a.m.. The sampled water depth ranged between 3 and 5 meter.

During the MSM17/3 cruise samples were collected by CTD casts using a rosette system equipped with 10 l Niskin bottles. The upper water column was sampled at fixed depth levels (5, 10, 15, 20, 30, 50, 100, 200 m). From 200 m downwards the depth levels were extended to 100-300 m intervals depending on the bottom depth and the O<sub>2</sub> profile.

Sampling and analysis of DIC and TA were done following standard procedures (Dickson et al., 2007). The samples were filled in 250 ml borosilicate bottles using silicone tubes (Tygon). The bottles were rinsed twice and filled from the bottom to avoid air bubbles. Periodically duplicate samples were taken. The samples were preserved with half saturated mercury (II) chloride solution (250  $\mu$ l of a 36 g l<sup>-1</sup> HgCl<sub>2</sub>) directly after collection and were stored under cool and dark conditions until measurement. Samples collected from the jetty were measured at the same day in the laboratory of the National Marine Information and Research Center Ministry of Fisheries & Marine Resources, Swakopmund, Namibia. Samples collected during the cruise MSM 17/3 were analysed on board.

All samples were measured using the VINDTA 3C system (Marianda, Kiel, Germany) (Mintrop, 2005). The TA was determined on the basis of the open cell principle. The

samples were titrated with a fixed volume of hydrochloric acid by equal increments of HCl (0.1 N HCl). For the determination of DIC, the CO<sub>2</sub> was extracted out of acidified water samples and quantified by the coulometric method (UIC Inc. Model 5012 in combination with the VINDTA 3C system) with a precision of 0.1%. Certified reference material (CRM, batch #101 and #104, provided by A. Dickson, Scripps Institution of Oceanography, La Jolla, CA, USA) was used to calibrate the VINDTA 3C system before starting the sample measurements and in the course of every 15<sup>th</sup> sample. During calibration with CRM's the DIC and TA measurements agreed to  $<\pm 3 \mu\text{mol kg}^{-1}$  and the reproducibility of parallel measurements was  $\pm 2 \mu\text{mol kg}^{-1}$ .

Based on the measured DIC and TA data, the remaining carbonate species including the saturation state of aragonite ( $\Omega_A$ ) and calcite ( $\Omega_C$ ) were calculated using CO2SYS programme (Lewis and Wallace, 1998; Pierrot et al., 2006). Input parameters were DIC, TA phosphate, silicate concentrations and salinity of in situ conditions whereas the temperature and pressure were chosen as the measurement conditions (25 °C and 1 bar pressure). In situ conditions of temperature and depth were chosen as output conditions and are presented here.

The TA shows a good correlation with salinity which is on average  $35.3 \pm 0.4$  for all the inorganic carbonate data presented here. Therefore the widely used normalisation of TA to a salinity of 35 (TA<sub>35</sub>) is applied for our samples ( $\text{TA}_{35} = \text{TA}_{\text{meas}} \times 35/S_{\text{meas}}$ ). Since the DIC values did not correlate with salinity we did not perform any salinity normalisation.

## RESULTS AND DISCUSSION

The composite of O<sub>2</sub>, TA<sub>35</sub>, DIC concentrations and  $\Omega$  levels measured in the NBUS water column agree well with the ranges documented for the open South Atlantic (SA) (Goyet et al., 2000). The inverse relation of dissolved O<sub>2</sub> and DIC concentrations (Fig. 4.2. a) indicate that the respiration of organic matter lowers dissolved O<sub>2</sub> and increases DIC concentrations. Compared to the open SA, higher DIC concentrations, associated with very low dissolved O<sub>2</sub> concentrations, were observed in the NBUS. The DIC increase is associated with a reduction of  $\Omega_A$  and  $\Omega_C$  to corrosive levels  $\Omega_A < 1$  occurring downward from ~600 m in the SA (Chung et al., 2003) but over the whole depth range in the NBUS

(Fig. 4.2. b, c). Although maximum DIC concentrations of  $>2300 \mu\text{mol kg}^{-1}$  in the NBUS exceed those of the SA, they are not reflected in considerably lower  $\Omega$  values (Fig. 4.2. c). As suggested by Figure 6.2. d, the further acidification is mitigated by an increase of  $\text{TA}_{35}$  at low  $\Omega$  levels, which is discussed in more detail in the following.

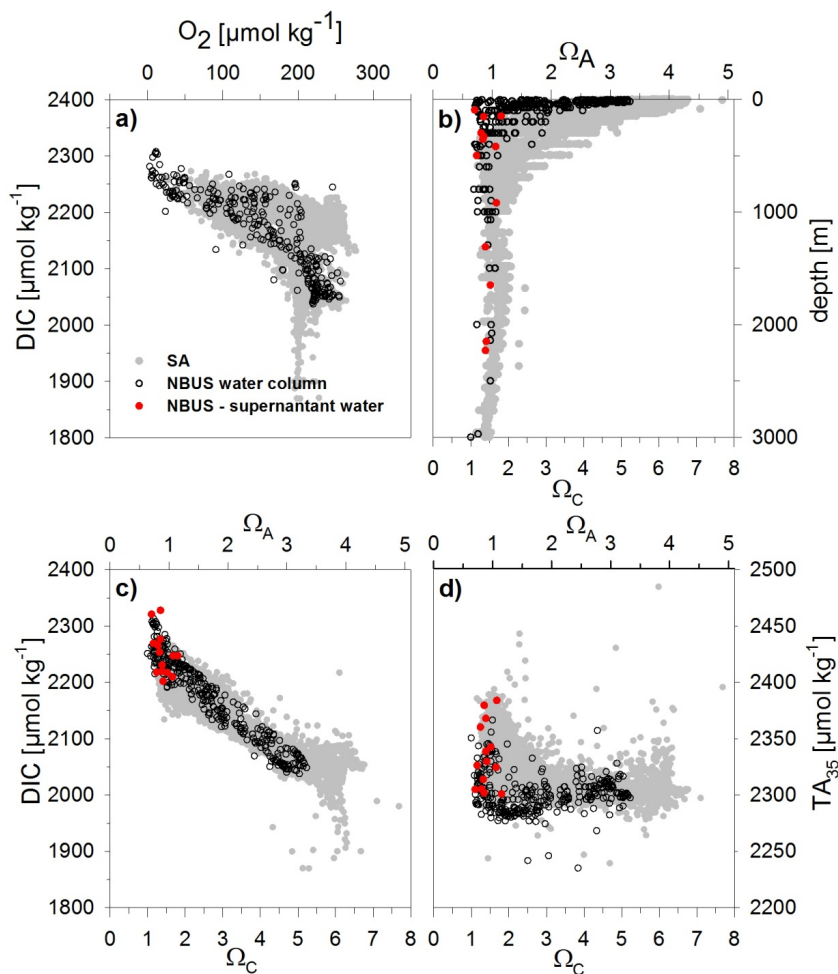


Fig. 4.2.: Comparison of carbonate system parameters measured in the South Atlantic (SA) and the northern Benguela upwelling system (NBUS) between 0-3000 m depth. (a)  $\text{O}_2$  versus DIC (both in  $\mu\text{mol kg}^{-1}$ ), (b)  $\Omega_C$  and  $\Omega_A$  versus depth, (c)  $\Omega_C$  and  $\Omega_A$  versus DIC ( $\mu\text{mol kg}^{-1}$ ), and (d)  $\Omega_C$  and  $\Omega_A$  versus  $\text{TA}_{35}$  ( $\mu\text{mol kg}^{-1}$ ) measured in the South Atlantic (SA) (grey circles), and the NBUS water column (black circles), and supernatant water of sediment cores (red circles). The SA dataset consists of WOCE Atlantic Ocean sections provided by [cdiac.ornl.gov/oceans/atlantic\\_ODV.html](http://cdiac.ornl.gov/oceans/atlantic_ODV.html) and was filtered for a latitudinal range of 0–40 °S and a depth range of 0-3000 m water depth. The  $\Omega_C$  and  $\Omega_A$  were calculated with CO2SYS programme (Pierrot et al., 2006), and are given for in situ salinity, temperature, and pressure conditions.

As illustrated in Fig. 4.3., the increase of DIC in the NBUS samples is primarily associated with both, a decrease of  $TA_{35}$ , expected from aerobic remineralisation of organic matter ( $TA_{35}/DIC=-0.16/1$ ) (Goldman and Brewer, 1980; Broecker and Peng, 1982) but also with a significant generation of  $TA_{35}$ , especially in supernatant water and coastal surface water samples.  $TA_{35}$  and DIC are generated by  $CaCO_3$  dissolution ( $TA_{35}/DIC=2/1$ ) and by anaerobic remineralisation processes, e.g. heterotrophic denitrification ( $TA_{35}/DIC=0.98/1$ ) and sulphate reduction ( $TA_{35}/DIC = 2/1$ ) (Wolf-Gladrow et al., 2007) that considerably contribute to the alkalinity budget above the chemical lysocline in coastal regions (Chen, 2002; Thomas et al., 2009). The generation of  $TA_{35}$  enhances the capacity to buffer high DIC concentrations as reflected in  $\Omega$  values that are much higher than expected for the same DIC levels generated under aerobic decomposition (Fig. 4.3.).

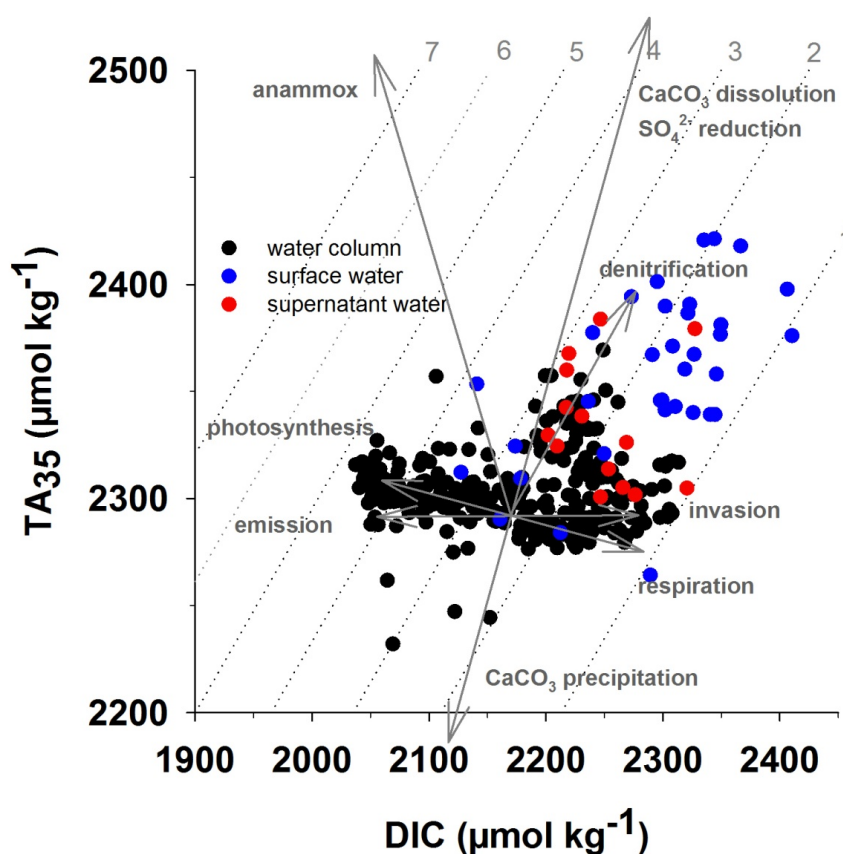


Fig. 4.3.: Composite of DIC versus  $TA_{35}$  (both in  $\mu\text{mol kg}^{-1}$ ) measured in water column samples (black circles, MSM17/3 in 2011), supernatant water of sediment cores (red circles MSM17/3 in 2011) and coastal surface water (Swakopmund time series, blue circles, 2010) of the NBUS. The

black dotted lines show  $\Omega_C$  at constant temperature of 15 °C and salinity of 35. The arrows indicate the impact of biogeochemical processes on DIC and  $TA_{35}$  according to the stoichiometry given in the text.

Since these processes occur under different biogeochemical conditions we compare the vertical profiles of offshore (Fig. 4.4. a-d) and shelf stations (Fig. 4.4. e-h) to better identify the processes that control DIC,  $TA_{35}$  and  $\Omega$  in the water column and supernatant water samples. The decrease in  $TA_{35}$  at increasing DIC ( $\sim 2050$  to  $\sim 2200 \mu\text{mol kg}^{-1}$  DIC) observed in surface and subsurface water samples of offshore and shelf stations indicates that  $TA_{35}/\text{DIC}$  in subsurface water is predominantly driven by aerobic respiration of organic matter (Flohr et al., 2014) that lowers  $\Omega_A$  to  $\sim 1$  and  $\Omega_C$  to  $\sim 2$  (Fig. 4.4. c, g).

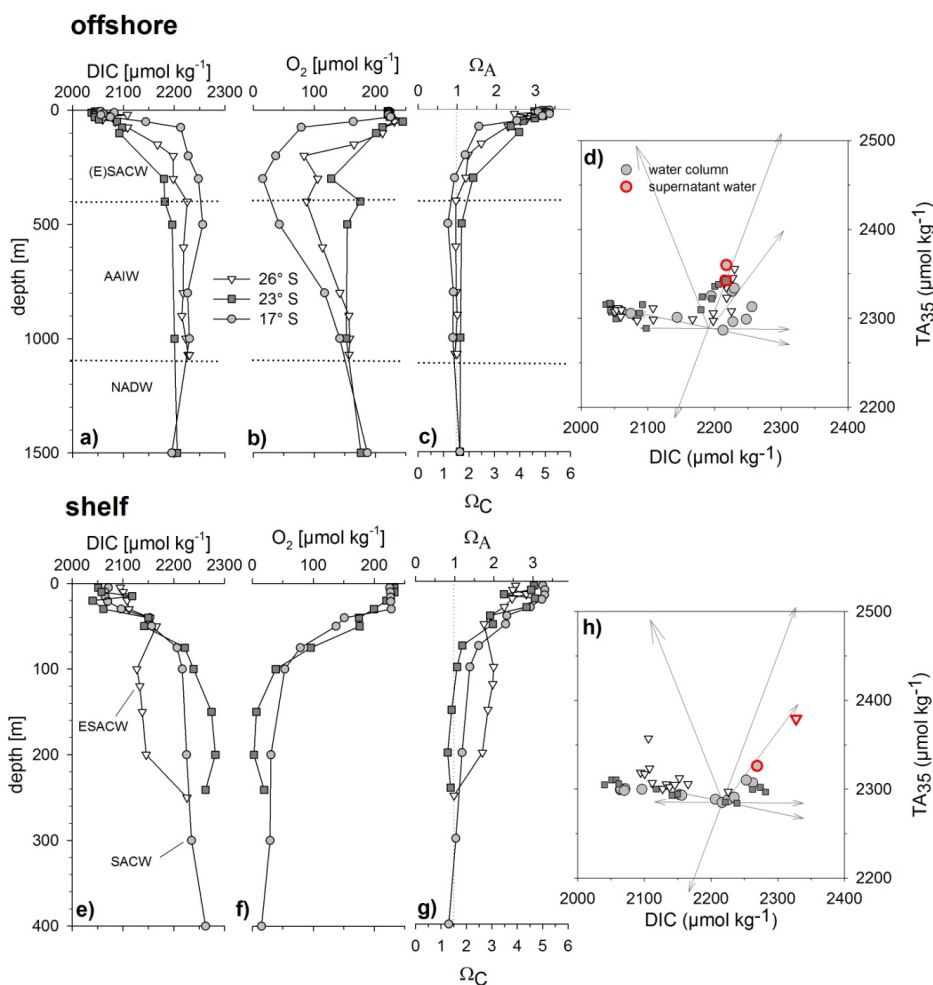


Fig. 4.4.: Differences of  $TA_{35}$  production between offshore (a-d) and shelf sites (e-h). Vertical profiles of DIC,  $O_2$  (both in  $\mu\text{mol kg}^{-1}$ ),  $\Omega_A$  and  $\Omega_C$  are shown. The grey circles, grey squares, and open diamonds denote the location of the stations (refer to Fig. 4.1.). (d, h) The  $TA_{35}/DIC$  plot involves the supernatant water samples of sediment cores obtained at the respective stations (red edged). (f)  $O_2$  profile for the 26 °S station is not available.

Offshore, below ~500 m water depth a minimum in salinity (not shown), associated with high DIC values  $>2200 \mu\text{mol kg}^{-1}$  and low  $\Omega_A$  (Fig. 4.4. a, c), characterises the presence of Antarctic Intermediate Water (AAIW) (Chung et al., 2003; Feely et al., 2004; González-Dávila et al., 2011). It has been shown that the invasion of anthropogenic  $CO_2$  into the SA adds to the high DIC inventory of AAIW and leads to an upward migration of the aragonite saturation horizon (Feely et al., 2004). The steep increase of  $TA_{35}$  and DIC in water samples with  $>50 \mu\text{mol kg}^{-1} O_2$  excludes an anaerobic  $TA_{35}$  source and is suggestive of an impact of  $CaCO_3$  dissolution (Fig. 4.4. d), in line with corrosive  $\Omega_A$  levels of  $\leq 1$  observed off Kunene (17 °S) and Lüderitz (26 °S). It indicates that aragonite particles, e.g. pteropod shields, which contribute to the offshore  $CaCO_3$  flux (Romero et al., 2002), start getting dissolved while descending through AAIW with  $\Omega_A < 1$  levels. It is supported by studies from the Southern Ocean showing that pteropod shells are affected by dissolution in waters where  $\Omega_A < 1$  levels prevail (Roberts et al., 2011; Bednarsek et al., 2012). The absence of a pronounced  $TA_{35}$  and DIC increase in supernatant water samples with respect to the water column (Fig. 4.4. d) suggests that the dissolution of aragonite in the surface sediments is not exceeding the dissolution within AAIW. The results further suggest that  $\Omega_C$  is balanced at the expense of aragonite dissolution reflected in  $\Omega_C > 1$ , in agreement with Boeckel and Baumann (2004), who found high concentrations of well preserved coccolithophores in surface sediment of the South East Atlantic between 1000-2000 m depth. As suggested by the strongly different DIC inventories of SACW and ESACW (Fig. 4.4. a) a further invasion of anthropogenic  $CO_2$ , which currently accounts for  $\sim 30 \mu\text{mol kg}^{-1}$  down to 500 m water depth in the (sub)tropical Atlantic (Gruber, 1998; Feely et al., 2004), could lower  $\Omega_A$  to  $< 1$  within SACW, leading to a further uplift of the aragonite saturation horizon to depth levels above AAIW.

On the shelf, a  $TA_{35}/DIC$  increase of  $\sim 0.64$  ( $r^2=0.7$ ) is observed in samples with  $>2200 \mu\text{mol kg}^{-1}$  DIC,  $< 50 \mu\text{mol kg}^{-1} O_2$  and  $\Omega_A > 0.7 < 2$  implying that a combination of aerobic,

anaerobic decomposition and  $\text{CaCO}_3$  dissolution could be causative. Results on particle fluxes on the shelf off Walvis Bay suggest that the low  $\text{CaCO}_3$  content of the coastal surface sediment (Fig. 4.1.) is predominantly resulting from the overall low annual  $\text{CaCO}_3$  fluxes contributing to <3 % to total fluxes on the shelf (Rixen et al., in prep.). This is in line with studies on phytoplankton community of the BUS which are dominated by diatoms and dinoflagellates near the coast in freshly upwelled water (Barlow et al., 2006; Barlow et al., 2009). It implies that the dissolution of  $\text{CaCO}_3$  cannot be ruled out but is of minor importance for  $\text{TA}_{35}/\text{DIC}$  compared to the impact of anaerobic processes occurring in the sub- and anoxic bottom water and sediments on the shelf. The loss of fixed N by heterotrophic denitrification and autotrophic anammox in sub- and anoxic bottom water (Lavik et al., 2009; Nagel et al., 2013) along with P input from the sediments, which are colonised by sulphur bacteria (Schulz and Schulz, 2005; van der Plas et al., 2007; Goldammer et al., 2010), lead to low N/P ratios in surface and subsurface water (Tyrrell and Lucas, 2002; Flohr et al., 2014). Recent results suggest that N loss by autotrophic anammox dominates over heterotrophic denitrification in the OMZ on the Namibian shelf (Kuypers et al., 2005; Kalvelage et al., 2011; Nagel et al., 2013). Following the C/N stoichiometry given by Koeve and Kähler (2010) anammox is associated with a fractional change of  $\text{TA}_{35}/\text{DIC}$  of 1/-0.05 suggesting that a  $\text{TA}_{35}$  increase of 17-80  $\mu\text{mol kg}^{-1}$  observed in water column and supernatant water samples on the shelf (Fig. 4.4. h) would be associated with a decrease of 0.85-4  $\mu\text{mol kg}^{-1}$  DIC. Thus, the relative changes of DIC would be likely masked by mixing and hardly be detectable, but would nevertheless be visible in  $\text{TA}_{35}$ . This implies that, apart from the contribution of heterotrophic denitrification, the DIC increase could result from aerobic decomposition while  $\text{TA}_{35}$  generation might result from the impact of anammox. However, it has also been suggested that organic bases as part of dissolved organic carbon (DOC) contribute to TA (Hernández-Ayon et al., 2007; Muller and Bleie, 2008). Although we cannot definitely distinguish between the processes and their relative contributions to observed  $\text{TA}_{35}/\text{DIC}$  changes, it is evident from our data that  $\text{TA}_{35}$  is generated on the shelf. The impact of this  $\text{TA}_{35}$  increase is underlined by figure 6.5., which illustrates the theoretical distribution of the aragonite saturation horizon  $\Omega_A = 1$  if all the DIC measured off Walvis Bay (23 °S) would have been produced by aerobic decomposition (Fig. 4.5. b). It shows that  $\Omega_A = 1$  would be much

shallower (Fig. 4.5. b) compared to the observed situation (Fig. 4.5. a). Additionally,  $\Omega_C$  would have reached corrosive levels in bottom water (not shown) likely starting to dissolve calcite in the sediment. Our data revealing  $\Omega_C > 1$  along with well preserved coccolithophores in the water column (Giraudeau and Bailey, 1995; Henderiks et al., 2012) and in coastal surface sediments (Giraudeau, 1992) suggest that calcite dissolution in coastal sediments is not yet occurring. Since the *aerobic-decomposition-scenario* was calculated on the basis of DIC increase observed with depth, it lacks the impact of DIC decrease expectable from anammox, and hence lacks the pronounced  $TA_{35}$  generation suggesting that the drop of  $\Omega$  would even be more pronounced.

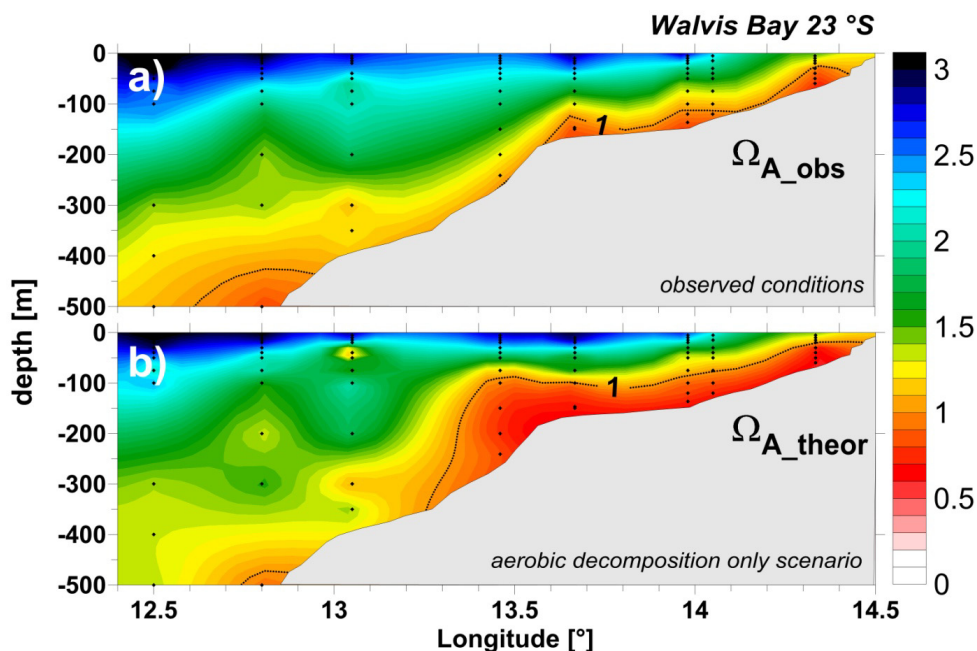


Fig. 4.5.: Vertical distribution of (a)  $\Omega_{A\_obs}$  and (b)  $\Omega_{A\_theor}$  (colour shading) in the water column off Walvis Bay (23 °S); the saturation horizon  $\Omega_A = 1$  is indicated by the black dotted line. The  $\Omega_{A\_obs}$  was calculated for in situ conditions on the basis of observed DIC and  $TA_{35}$  concentrations. The  $\Omega_{A\_theor}$  was calculated for in situ conditions on the basis of observed DIC concentrations. On the basis of the vertical DIC increase the expected rise of nitrate and phosphate, and hence drop of  $TA_{35}$ , was calculated according to Redfield stoichiometry ( $TA/DIC = -17/106$ ).

The immense buffering potential keeping  $\Omega_C > 1$  is further supported by the surface data of the Swakopmund time series, where strongly enhanced DIC concentrations were not reflected in lower but comparable minimum values of  $\Omega_C = 1.20$  and  $\Omega_A = 0.77$  (Fig. 4.6.)

compared to the bottom water on the shelf (Fig. 4.4. e-h). Low  $\Omega$  in coastal surface waters is common in upwelling systems (Mintrop et al., 1999; Fassbender et al., 2011; Loucaides et al., 2012; Rixen et al., 2012). However,  $\Omega_A$  of  $\sim 0.8$  in upwelled surface water has so far only been reported for the California upwelling system where DIC in upwelling waters is  $\sim 100 \mu\text{mol kg}^{-1}$  lower ( $\sim 2300 \mu\text{mol kg}^{-1}$ ) (Feely et al., 2008; Harris et al., 2013), underlining the strong buffering potential of  $\text{TA}_{35}$  production in the NBUS.

The surface data were obtained between February and May, i.e. in austral summer and early autumn when upwelling intensity and hence ventilation of the shelf is low and reflected in prevailing anoxic conditions (Monteiro et al., 2006; Mohrholz et al., 2008). This suggests that anaerobic  $\text{TA}_{35}$  generation in bottom waters on the shallow shelf was likely enhanced with respect to the values measured during the cruise in February (Fig. 4.4. e-h).

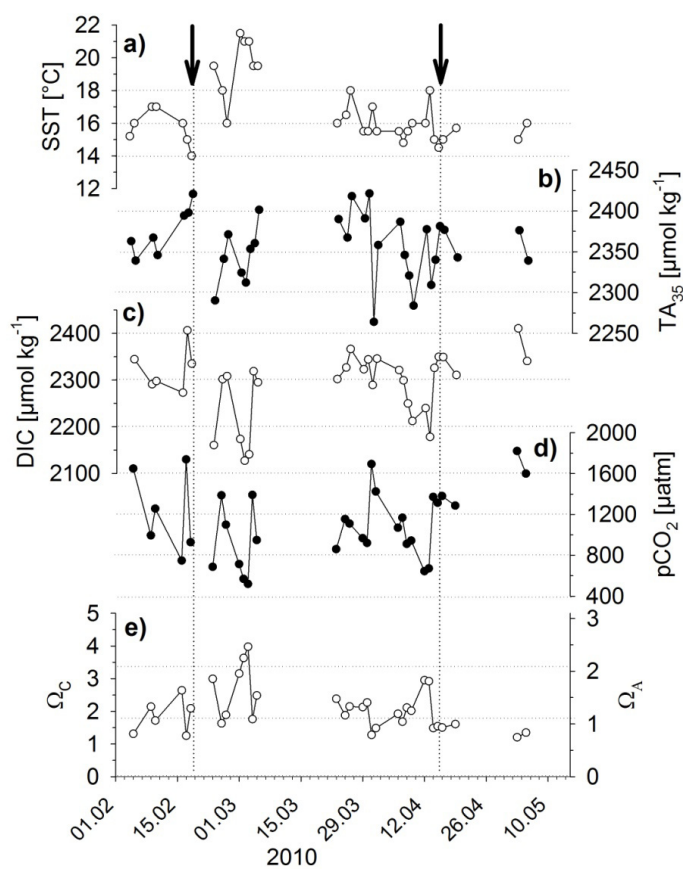


Fig. 4.6.: Swakopmund time series of coastal surface water. (a) SST ( $^{\circ}\text{C}$ ), (b)  $\text{TA}_{35}$ , (c) DIC (both in  $\mu\text{mol kg}^{-1}$ ), (d)  $\text{pCO}_2$  ( $\mu\text{atm}$ ), and (e)  $\Omega_{\text{C}}$  and  $\Omega_{\text{A}}$  in surface water sampled between February and May 2010. The black arrows indicate two main upwelling events with SST  $<15^{\circ}\text{C}$ .

However, nitrate was  $<1 \mu\text{mol l}^{-1}$  throughout the time of sampling, indicating that primary production affected the  $\text{TA}_{35}$ /DIC signature. Primary production along with physical  $\text{CO}_2$  emission reduces DIC values. Nitrate uptake and ammonia release further increase  $\text{TA}_{35}$  (Wolf-Gladrow et al., 2007) which is likely the reason for the elevated  $\text{TA}_{35}$  with respect to the bottom water values. Table 4.1. highlights the impact of  $\text{TA}_{35}$  increase on the  $\text{pCO}_2$  which differs by  $\sim 400 \mu\text{atm}$  despite comparable DIC concentrations.

Table 4.1.: Selection of surface samples of the Swakopmund time series illustrating the impact of increasing  $\text{TA}_{35}$  on  $\text{pCO}_2$ . The reference station is the coastal most station of the  $23^{\circ}\text{S}$  transect sampled in 02/2011 (MSM17/3) and closest to Swakopmund. Given  $\text{pCO}_2$  values refer to surface (1 bar) at  $15^{\circ}\text{C}$ .

	<b>60 m depth reference</b>	<b>surface 31.03.</b>	<b>surface 16.04.</b>	<b>surface 18.02.</b>
Temp [ $^{\circ}\text{C}$ ]	14.7	17	15	14
$\text{O}_2$ [ $\mu\text{mol l}^{-1}$ ]	11.4			259.2
$\text{NO}_3^-$ [ $\mu\text{mol l}^{-1}$ ]	29.2	0	0	0
$\text{NH}_4^+$ [ $\mu\text{mol l}^{-1}$ ]	0.84	3.8	4.4	13.8
$\text{PO}_4^{3-}$ [ $\mu\text{mol l}^{-1}$ ]	4.7	2.16	1.9	1.96
$\text{TA}_{35}$ [ $\mu\text{mol kg}^{-1}$ ]	<b>2293</b>	<b>2264</b>	<b>2376</b>	<b>2420</b>
DIC [ $\mu\text{mol kg}^{-1}$ ]	<b>2308</b>	<b>2289</b>	<b>2349</b>	<b>2335</b>
$\text{pCO}_2$ [ $\mu\text{atm}$ ] <sub>1 bar, 15 <math>^{\circ}\text{C}</math></sub>	<b>1781</b>	<b>1601</b>	<b>1398</b>	<b>980</b>

This indicates that  $\text{TA}_{35}$  generation in coastal bottom water, its upwelling to the surface, followed by strong nutrient uptake, is a powerful mechanism that increases  $\text{TA}_{35}$ . Apart from elevating  $\Omega$ , it reduces the  $\text{pCO}_2$  in upwelling systems, thereby affecting the strength of  $\text{CO}_2$  emissions to the atmosphere. However, the net effect of reduced  $\text{CO}_2$  emission might be balanced by lower potential nitrate driven biological  $\text{CO}_2$  drawdown due to N loss in the subsurface waters and remains to be studied.

## CONCLUSION

The invasion of anthropogenic CO<sub>2</sub> currently accounts for ~30 μmol kg<sup>-1</sup> down to 500 m water depth in the (sub)tropical Atlantic (Gruber, 1998; Feely et al., 2004) suggesting that the central water masses SACW and ESACW which flow onto the Namibian shelf (Duncombe Rae, 2005; Mohrholz et al., 2008) are already carrying ~30 μmol kg<sup>-1</sup> of anthropogenic CO<sub>2</sub> accounting for a mean drop of Ω<sub>A</sub> by -0.36 and Ω<sub>C</sub> by -0.23 between 200 – 400 m depth at offshore most sites off Walvis Bay. The results show, that strongest Ω decrease to Ω<sub>A</sub> ~1 and Ω<sub>C</sub> ~1.5 occurs in the oxygenated water column where aerobic decomposition of organic matter causes an increase of DIC to ~2200 μmol kg<sup>-1</sup> associated with a decrease in TA<sub>35</sub>. Hence a further invasion of anthropogenic CO<sub>2</sub> could lower Ω<sub>A</sub> to <1 particularly in SACW which is characterised by a higher DIC inventory than ESACW. This in turn would lead to a further uplift of the aragonite saturation horizon to depth levels above AAIW where high SACW fractions occur, i.e. in the NBUS and Angola Gyre region. However, the results indicate that TA<sub>35</sub> generation in bottom water on the shelf followed by upwelling to the surface, where strong nutrient uptake further increases TA<sub>35</sub>. This might be a powerful mechanism that, apart from elevating Ω, reduces the pCO<sub>2</sub> in upwelled surface water, thereby affecting the strength of CO<sub>2</sub> emissions to the atmosphere.

Acknowledgements: We would like to thank all scientists, technicians, the captain and the crew on board the research vessel RV Maria S. Merian. Suzie Christof is thanked for her support during the sampling in Swakopmund. Furthermore, we are grateful to the German Federal Ministry of Education and Research (BMBF) for financial support of the GENUS project (03F0497D-ZMT).



## 5. CHAPTER III

UPWELLING LOWERS CARBON EXPORT IN THE BENGUELA  
UPWELLING SYSTEM OFF NAMIBIA

Tim Rixen<sup>1,2\*</sup>, Anita Flohr<sup>1\*</sup>, Niko Lahajnar<sup>2</sup>, Martin Schmidt<sup>3</sup>, Volker Mohrholz<sup>3</sup>, Anja van der Plas<sup>4</sup>, Birgit Gaye<sup>2</sup>, Anja Eggert<sup>3</sup>, and Kay-Christian Emeis<sup>2,5</sup>

[1] Leibniz Centre for Tropical Marine Ecology (ZMT), Fahrenheitstraße 6, 28359 Bremen, Germany

[2] Institute for Biogeochemistry and Marine Chemistry, University of Hamburg, Bundesstraße 55, 20146 Hamburg, Germany

[3] Leibniz-Institute for Baltic Sea Research (IOW), Seestraße 15, 18119 Rostock, Germany

[4] National Marine Information and Research Centre Ministry of Fisheries & Marine Resources, PO Box 912 Swakopmund, Namibia

[5] Helmholtz-Centre for Materials and Coastal Research Geesthacht, Max-Planck-Straße 1, 21502 Geesthacht, Germany

\*Authors contributed equally to this work

Corresponding author: T. Rixen, Leibniz Centre for Tropical Marine Ecology (ZMT), Fahrenheitstraße 6, 28359 Bremen, (tim.rixen@zmt-bremen.de); Institute for Biogeochemistry and Marine Chemistry, University of Hamburg, Bundesstraße 55, 20146 Hamburg

To be submitted



The Benguela upwelling system (BUS) is the most productive eastern boundary upwelling system (EBUS) (Carr, 2002) and so far the only one suffering from the periodic occurrence of anoxic events and the associated loss of economically important marine resources (Weeks et al., 2002). Although climate models provide inconsistent results on the future of upwelling systems (Wang et al., 2010; Zuidema et al., 2011), an increasing atmospheric pressure gradient between land and ocean under continued global warming is suggested to intensify upwelling favourable trade winds (Bakun et al., 2010). Here we show that increasing upwelling favourable winds enhance the Benguela upwelling but lower the export of primary produced organic matter, indicative for the productivity of the system, as it also strengthens the Benguela Current (BC) carrying nutrient-poor and oxygen-enriched subsurface waters from the south into the BUS. Favoured by weaker upwelling favourable winds, pulses of enhanced inflow of nutrient-enriched and oxygen-depleted waters, in the poleward undercurrent from the north, enhances organic carbon export. The ensuing enhanced respiration of organic matter depletes the inherited small stock of dissolved oxygen and promotes the development of anoxia in sub-thermocline waters. Our results suggest that intensified wind forcing will increase upwelling and decrease nutrient concentrations in the feed waters, which will make the BUS less prone to anoxia in future.

The Benguela upwelling system is situated along the southwest African coast from Cape Agulhas at ~34 °S to the Angola Benguela Frontal Zone (ABFZ) at 14 to 16 °S (Fig. 5.1.). Driven by the southeast trade winds the Benguela Current carries Eastern South Atlantic Central Water (ESACW) northwards that originates from mode-water formation at the Brazil/Falkland confluence off South America and mixes with the Indian Ocean Central Water at the Agulhas retroflection in the Cape Basin (Gordon, 1981; Gordon et al., 1987). From the north an Angola Gyre subtype of the South Atlantic Central Water (SACW) (Duncombe Rae, 2005; Mohrholz et al., 2008) is introduced into the BUS by feeding a poleward undercurrent that develops south of the ABFZ. The SACW is in principle of the same origin as the ESACW but older and thus more enriched in nutrients and depleted in oxygen (Mohrholz et al., 2008).

Continuous measurements of temperature, salinity, and dissolved oxygen ( $O_2$ ) concentrations off Walvis Bay in the BUS between January 2004 and September 2005 showed that ESACW dominated the subsurface water mass composition during the peak upwelling season approximately between June and October. In austral summer, between January and March, when the poleward undercurrent gained strength, the enhanced inflow of SACW suppressed the inflow of ESACW, which led to the development of persistent anoxia between January and July 2005 (Mohrholz et al., 2008).

We operated an oceanographic and a sediment trap mooring off Walvis Bay between 2009 and 2011 in order to investigate the interplay of oxygen inputs through the inflow of SACW and ESACW as well as the oxygen consumption caused by the respiration of organic matter produced and exported from the mixed layer during upwelling-driven plankton blooms. The collected sediment trap material revealed a similar bulk composition as the underlying sediments (Bremner, 1981) with highest contribution of biogenic opal (~38 %) and lithogenic matter (~27%) (Fig. 5.1., Tab. 7.1). Biogenic opal originates mainly from diatoms which often dominate the coastal phytoplankton communities in freshly upwelled water over the shelf and generate high biomass blooms (Barlow et al., 2006; Barlow et al., 2009). The annual mean flux of lithogenic matter ( $96 \text{ g m}^{-2} \text{ yr}^{-1}$ ) exceeds that measured by previous sediment trap experiments over the Namibian continental margin and the Walvis Ridge ( $3.8\text{-}9 \text{ g m}^{-2} \text{ yr}^{-1}$ ) (Wefer and Fischer, 1993; Giraudeau et al., 2000). Offshore decreasing fluxes and concentrations of lithogenic matter in sediments (Fig. 5.1.) reflect the distance to the estuaries of the intermittent rivers at the Namibian coast through which the majority of dust is introduced into the ocean (Eckardt and Kuring, 2005).

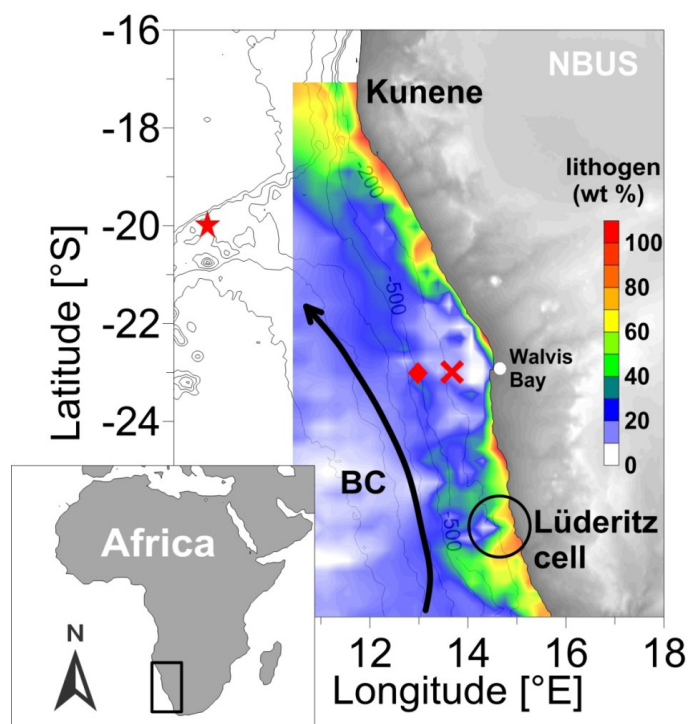


Fig. 5.1.: Study area. The Benguela Current (BC, black line) and locations of our oceanographic ( $23.0^{\circ}\text{S}$ ,  $14.04^{\circ}\text{E}$ ) and the sediment trap mooring ( $23.0^{\circ}\text{S}$ ,  $14.05^{\circ}\text{E}$ ) our study site (red cross) at a water depth of 140 m. The sediment trap mooring was equipped cylindrical Hydro-Bios sediment trap (MST 12) at a water depth of 70 m. Sampling interval was 21 days during first (December 2009-September 2010) and 12 days during the second deployment period (October 2010-February 2011). The deployed Seabird MircoCat recorded seawater temperature and salinity with a sampling interval of ten minutes at a water depth of 128 m. The oceanographic and the meteorological data presented in Fig. 5.2. were converted into three-weekly means in order to link it to the sediment trap data. Sample and data processing is described in Haake et al. (1993) and Mohrholz et al. (2008). The contribution of lithogenic matter (wt %) in surface sediments (Inthorn et al., 2006) is indicated by colour shading. The position of previous sediment traps sites in the BUS region is marked by filled asterisk (Wefer and Fischer, 1993) and filled diamond (Giraudeau et al., 2000).

Due to the preferential decomposition of nitrogen (N) containing organic compounds, C/N ratios of organic matter buried in sediments often exceed those measured in plankton (Lee and Cronin, 1982). The C/N ratios in the organic-rich surface sediments off Walvis Bay range between 7-10.4 (van der Plas et al., 2007) and the C/N ratios measured in the trap samples range between 7.7-9.5 during the first and between 6-8 in the second deployment period (Fig. 5.2. a). The C/N ratios of the second deployment period are similar to that of organic matter (C/N = 6.6) freshly produced by plankton (Redfield et al., 1963; Flohr et al., 2014).

Table 5.1.: Sampling periods and results of particle fluxes ( $\text{mg m}^{-2} \text{d}^{-1}$ ) are listed. The flux calculations refer to the  $<1$  mm size fraction. Columns marked with \* indicate that the amount of sample was insufficient for further analysis. Cup no. 3 was lost during operation and n.d. means non-detectable. Trap position:  $23.0^\circ\text{S}$ ,  $14.05^\circ\text{E}$ , trap depth: 70 m, bottom depth: 140 m.

Sample no	Trap cup		Fluxes ( $\text{mg m}^{-2} \text{d}^{-1}$ )						
	Open	close	Total	$C_{\text{total}}$	$N_{\text{total}}$	$C_{\text{org}}$	$C_{\text{CaCO}_3}$	Opal	Lithog.
1	15/12/2009	05/01/2010	811.87	144.43	20.19	141.72	22.60	533.72	0.09
2	05/01/2010	26/01/2010	50.80	*	*	*	*	*	*
3	26/01/2010	16/02/2010	no data	-	-	-	-	-	-
4	16/02/2010	09/03/2010	693.19	116.86	17.72	116.00	7.16	117.21	348.43
5	09/03/2010	30/03/2010	860.91	202.81	30.39	202.84	n.d.	268.71	196.74
6	30/03/2010	21/04/2010	1705.33	276.86	35.85	276.04	6.82	1015.80	156.41
7	21/04/2010	11/05/2010	917.85	137.46	18.10	136.26	9.94	526.78	126.61
8	11/05/2010	01/06/2010	407.45	79.19	10.56	78.53	5.50	135.70	118.49
9	01/06/2010	22/06/2010	237.79	35.02	4.86	34.60	3.51	146.80	22.37
10	13/07/2010	13/07/2010	2847.57	330.57	43.45	332.74	n.d.	1834.40	371.42
11	03/08/2010	03/08/2010	1088.29	132.80	16.79	132.64	1.36	736.15	96.47
12	24/08/2010	24/08/2010	1475.75	114.92	16.23	113.37	12.91	1024.38	230.19
Break									
13	10/10/2010	22/10/2010	802.56	162.98	29.52	157.23	47.90	219.34	252.31
14	22/10/2010	03/11/2010	2510.33	370.03	58.71	353.10	141.06	1111.83	621.87
15	03/11/2010	15/11/2010	1659.89	287.68	45.89	283.13	37.88	546.44	565.94
16	15/11/2010	27/11/2010	2375.78	398.89	55.16	390.87	66.85	977.63	627.73
17	27/11/2010	09/12/2010	658.44	148.50	24.39	143.35	42.96	112.13	245.33
18	09/12/2010	21/12/210	532.50	110.32	18.08	106.56	31.36	69.17	240.16
19	21/12/210	02/01/2011	777.67	182.27	32.15	176.49	48.13	38.42	373.44
20	02/01/2011	14/01/2011	447.61	112.58	20.32	105.46	59.30	39.84	158.64
21	14/01/2011	26/01/2011	609.83	153.60	26.86	148.82	39.88	29.64	272.44
average			<b>1073.57</b>	<b>184.1</b>	<b>27.64</b>	<b>180.5</b>	<b>30.86</b>	<b>499.16</b>	<b>264.48</b>
			$\pm 778.5$	$\pm 101.1$	$\pm 14.65$	$\pm 99.31$	$\pm 34.3$	$\pm 500.12$	$\pm 183.75$

These low C/N ratios associated with high fluxes of lithogenic matter as seen during the second deployment period (Fig. 5.2. a) imply that resuspended sediments are minor contributors to the trapped material and that the collected organic matter was mainly produced by plankton and exported from the mixed layer.

A previous sediment trap study carried out close to our trap position between October 2002 and December 2003 reported organic carbon flux of  $20\text{-}100 \text{ mg m}^{-2} \text{d}^{-1}$  (Monteiro et al., 2006). During this experiment only the fraction  $<200 \mu\text{m}$  was considered whereas in our and other sediments tap studies (Wefer and Fischer, 1993; Giraudeau et al., 2000) the

collected material was wet-sieved through 1 mm net, basically to separate swimmers from passive sinking particles. Such a different sample procedure complicates a quantitative comparison and explains the low organic carbon fluxes in 2002/3 falling even below our mean of  $180 \text{ mg m}^{-2} \text{ d}^{-1}$ .

Organic carbon fluxes measured over the Namibian continental margin and the Walvis Ridge during a period of approximately 5 and 12 months at water depths of 545 and 599 m (Wefer and Fischer, 1993; Giraudeau et al., 2000) were  $7.1$  and  $13.97 \text{ mg C m}^{-2} \text{ d}^{-1}$ . Considering the organic carbon respiration below the mixed layer (Martin et al., 1987; van Mooy et al., 2002) these fluxes correspond to an organic carbon export of  $<40 \text{ mg C m}^{-2} \text{ d}^{-1}$  at a water depth of 70 m. These export rates are well below the  $180 \text{ mg m}^{-2} \text{ d}^{-1}$  (Fig. 5.2.c; Tab. 5.1.) measured over the shelf reflecting the onshore-offshore gradient in productivity (Carr, 2002).

Global estimates of organic carbon export rates reveal a wide range whereas estimates based on sediment trap data are with  $1.9\text{-}5.3 \text{ Pg C yr}^{-1}$  (Lutz et al., 2002; Honjo et al., 2008) within the lower range and those based on organic carbon respiration rates are with up to  $27.5 \text{ Pg C yr}^{-1}$  (del Giorgio and Duarte, 2002) within the upper range. The resulting area normalised global average organic carbon export rate of  $110 \text{ mg C m}^{-2} \text{ d}^{-1}$  (area normalised mean) is below that measured on the Namibian shelf showing in line with satellite-derived primary production rates (Carr, 2002) that the BUS is a highly productive system. Furthermore, the mean organic carbon burial rate on the Namibian shelf of  $68 \text{ mg C m}^{-2} \text{ d}^{-1}$  (Meisel et al., 2011b) suggests that 62 % ( $180-68 = 112 \text{ mg C m}^{-2} \text{ d}^{-1}$ ) of the exported organic carbon is decomposed in the water column below the mixed layer.

During the period of our observation the export of sinking organic carbon showed pronounced temporal variations with enhanced fluxes in March, July, and October/November 2010 (Fig. 5.2. b). Previous studies covering a full annual cycle over the shelf (Monteiro et al., 2006) and the Walvis Ridge (Wefer and Fischer, 1993) show a similar seasonality with peak fluxes between October and November as well as in July. Thus, a consistent organic carbon flux pattern emerges with high fluxes in late austral autumn (July) and early spring (October-November).

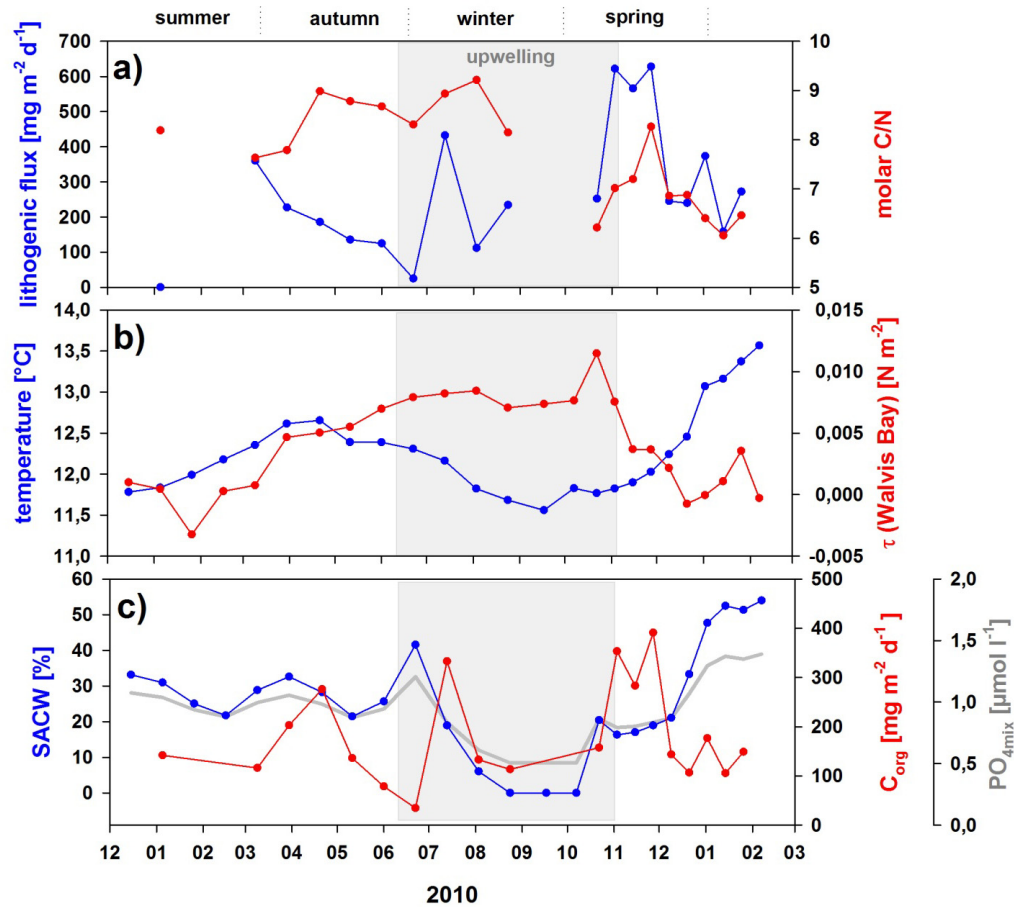


Fig. 5.2.: Mooring data. Lithogenic matter fluxes and the C/N ratio measured in the trapped material during the period of observation (a). Sea water temperatures measured by the CTD and the alongshore wind stress ( $\tau$ ). The wind speeds and wind directions used to calculate  $\tau$  were measured at the weather station at the National Marine Information and Research Center (NatMIRC) in Swakopmund that is roughly 62 km away from the mooring site. (b) The fraction of SACW (%) calculated from sea water temperature and the salinity measured at 128 m water depth (Mohrholz et al., 2008),  $\text{PO}_4$  concentration inferred from mixing of SACW and ESACW and the  $C_{\text{org}}$  flux ( $\text{mg m}^{-2} \text{d}^{-1}$ ) as measured with the sediment trap.

In winter between June and September when low subsurface water temperature indicate strong upwelling in response to upwelling favourable winds (Fig. 5.2. b), organic carbon fluxes show their minimum over the Walvis Ridge (Wefer and Fischer, 1993) and the shelf (Fig. 5.2. c). This result is furthermore supported by the five month sediment trap experiment over the Namibian continental margin which could also show no link between upwelling of organic carbon exports (Giraudeau et al., 2000). A decoupling between upwelling and organic carbon export and a consistent organic carbon flux pattern near the coast and far offshore suggest that factors other than upwelling and/or time lags associated

with the development of the massive upwelling-driven plankton blooms affect export of organic carbon from the surface mixed layer in the BUS.

Data recorded by our oceanographic mooring in 2010/11 showed similar to the situation in 2004/5 a dominance of ESACW between June and October and a higher fraction of SACW in April, June, October and January/February (Fig. 5.2. c). These pulses of enhanced inflow of SACW showed highest SACW fraction in January/February 2011 as upwelling was weakest or even absent. The lowest SACW fraction coincided with the strongest upwelling event in October 2010 suggesting that an intensification of upwelling favourable wind lowers the inflow of SACW during the pulses.

Subsurface nutrient concentrations can increase by >100 % in response to these pulses of enhanced inflow of the nutrient-enriched SACW, which becomes obvious when the SACW/ESACW mixing ratio and the initial phosphate ( $\text{PO}_4$ ) concentrations of these water masses (SACW= $2.8 \mu\text{mol l}^{-1}$ , ESACW =  $1.3 \mu\text{mol l}^{-1}$ ) (Mohrholz et al., 2008) are taken into account (Fig. 5.2.). Maxima in organic carbon exports follow these pulses of enhanced SACW inputs with a delay of ~3.5 weeks. Since such a time lag is required for the development of a diatom bloom it can be assumed that nutrient inputs due to the inflow of SACW along with the poleward undercurrent is a factor that could increase organic carbon exports in times of weak to moderate upwelling.

The highest peak of organic carbon flux was measured in October as the pulse of enhanced inflow of SACW was relatively weak and upwelling was extremely strong. This suggests that strong upwelling in combination with the enhanced inflow of SACW lead to the high organic carbon fluxes in late spring and that on the other hand upwelling reduces its impact on the organic carbon export by weakening the poleward undercurrent and the associated inflow of SACW (Mohrholz et al., 2008).

The organic carbon flux minima paired with low sea water temperatures in winter between June and October, observed over the Walvis Ridge (Wefer and Fischer, 1993) and the shelf sites, mark the upwelling of nutrient-poor and cooler ESACW that is carried along the BC into the BUS. The BC as well as upwelling are assumed to strengthen with an intensification of the southeast trade winds which in turn weakens the poleward undercurrent (Mohrholz et al., 2008). Stronger upwelling coinciding within lower

subsurface nutrient concentrations implies a reduced impact of changes in the southeast trade winds on the productivity in the BUS.

An increase of the SACW fraction from 20 to 40 % is accompanied by an increase in organic carbon flux from approximately 50 to 330 mg C m<sup>-2</sup> d<sup>-1</sup>, as seen in May/June 2010 (Fig. 5.2. c). Assuming that 62 % of the organic carbon flux is decomposed in the water column, such an increase in the SACW fraction could enhance the organic carbon respiration from 31 (= 50 · 0.62) to 204.6 (330 · 0.62) mg C m<sup>-2</sup> d<sup>-1</sup>. Assuming remineralisation according to Redfield (C/O<sub>2</sub> = 0.768) and a mean water depth of 100 m, an increase in the SACW fraction from 20 to 40 % raises oxygen consumption rates from 0.033 μmol l<sup>-1</sup> d<sup>-1</sup> to 0.222 μmol l<sup>-1</sup> O<sub>2</sub> d<sup>-1</sup>. Accordingly, an increase of the SACW fraction by 1 % raised the oxygen consumption by 0.0094 μmol l<sup>-1</sup> O<sub>2</sub> d<sup>-1</sup> %<sup>-1</sup> ((0.033 – 0.222)/20%) in May/June 2010.

In 2004/2005 an increase of the SACW fraction from 0 to 55 % between November and February (ca. 122 days) led to anoxia (Mohrholz et al., 2008). Associated with this development was an increasing difference between calculated oxygen concentrations expected from mixing of SACW with ESACW and direct oxygen measurements; the difference is here referred to as the biological oxygen consumption (BOC). The calculated decrease of 65 μmol l<sup>-1</sup> due to BOC corresponds approximately to an oxygen consumption rate of 0.0094 μmol l<sup>-1</sup> O<sub>2</sub> d<sup>-1</sup> %<sup>-1</sup> as derived from our study if one considers an increase of the SACW fraction from zero to 55 % during a period of 122 days (63 μmol l<sup>-1</sup> = 0.0094 μmol l<sup>-1</sup> O<sub>2</sub> d<sup>-1</sup> %<sup>-1</sup> · 55 % · 122 days). The consensus between sediment trap results and data on respiration emphasises furthermore the reliability of our data and shows that an increasing inflow of SACW can lead to anoxia by lowering oxygen inputs and enhancing the export of organic matter during times of weak upwelling. This implies that an intensification of upwelling could counteract the development of anoxia as it is associated with the enhanced inflow of nutrient-poor and oxygen-enriched ESACW.

**Acknowledgments:** We thank Toralf Heene and the NatMIRC for technical assistance and logistic support during the mooring operation. We also gratefully acknowledge the excellent support from the captains and crews of the research vessels *Africana*, *Discovery*, *M. S. Merian*, and *Welwitschia* and for the financial support from the German Federal

Ministry of Education and Research (BMBF, Bonn) of the GENUS programme (03F0497D-ZMT).



## 6. CHAPTER IV

CARBON AND NUTRIENT BALANCES OF THE  
BENGUELA UPWELLING SYSTEM

Tim Rixen<sup>1,2</sup>, Anita Flohr<sup>1</sup>, Niko Lahajnar<sup>2</sup>, Anja van der Plas<sup>3</sup>, Kay-Christian Emeis<sup>2,4</sup>

[1] Leibniz Centre for Tropical Marine Ecology (ZMT), Fahrenheitstraße 6, 28359 Bremen, Germany

[2] Institute for Biogeochemistry and Marine Chemistry, University of Hamburg, Bundesstraße 55, 20146 Hamburg, Germany

[3] National Marine Information and Research Centre Ministry of Fisheries & Marine Resources, PO Box 912 Swakopmund, Namibia

[4] Helmholtz-Centre for Materials and Coastal Research Geesthacht, Max-Planck-Straße 1, 21502 Geesthacht, Germany

Corresponding author: T. Rixen, Leibniz Centre for Tropical Marine Ecology (ZMT), Fahrenheitstraße 6, 28359 Bremen, (tim.rixen@zmt-bremen.de); Institute for Biogeochemistry and Marine Chemistry, University of Hamburg, Bundesstraße 55, 20146 Hamburg

To be submitted



The Benguela upwelling system (BUS) in the Atlantic Ocean is one of the four major eastern boundary upwelling systems (EBUS) in the world's ocean that link the enormous deep sea carbon and nutrient reservoir to the surface ocean, and the atmosphere. The leakage of CO<sub>2</sub> and nutrient laden waters from the sub-thermocline into the mixed layer sustain a high emission of CO<sub>2</sub> into the atmosphere and a high biological productivity capturing and returning CO<sub>2</sub> as organic matter back into the ocean's interior. High fluxes of CO<sub>2</sub> into the atmosphere and back into the deep sea carbon reservoirs lead to the often raised and still unanswered question whether upwelling systems are CO<sub>2</sub> sinks or sources in the BUS. Here we present data demonstrating that the surfacing and utilisation of biologically unused phosphate (preformed PO<sub>4</sub><sup>0</sup>) formed at high latitudes is a key factor influencing the regional distribution of CO<sub>2</sub> sinks and sources. Fuelled by a substantial supply and assimilation of PO<sub>4</sub><sup>0</sup>, the southern sector of the BUS is a CO<sub>2</sub> sink. The northern sector is an immediate source of CO<sub>2</sub> due the dominance of regenerated nutrients in upwelling subsurface waters, which are stoichiometrically balanced by metabolic CO<sub>2</sub>.

The amount and history of nutrients, available for biological assimilation of CO<sub>2</sub> in the ocean's surface mixed layer, are a key factor for the sequestration of CO<sub>2</sub> as organic carbon (OC) in subsurface waters (Ito and Follows, 2005; Sigman et al., 2010). Nutrients in the ocean are either new (introduced from land or atmosphere), regenerated, or preformed (Eppley and Peterson, 1979; Broecker et al., 1985). Regenerated nutrients are those released during the mineralisation of sinking organic matter (OM) that also liberates metabolic CO<sub>2</sub> at the expense of dissolved oxygen (O<sub>2</sub>) according to the Redfield stoichiometry (Redfield et al., 1963; Anderson and Sarmiento, 1994). Preformed nutrients lose their metabolic CO<sub>2</sub> in high latitude zones when after their introduction into the surface layer, light or other factors limit their complete assimilation by phytoplankton. They are exported from the surface ocean during mode water formation in the course of which they are introduced into the thermocline of the subtropical and tropical oceans (Fig. 6.1.. a) Dissolved oxygen budgets indicate that PO<sub>4</sub><sup>0</sup> contributes 60-64 % to the total phosphate (PO<sub>4</sub>) dissolved in the ocean today (Broecker et al., 1985; Ito and Follows, 2005). The more of PO<sub>4</sub><sup>0</sup> can be assimilated and exported as OM the more CO<sub>2</sub> can be

stored in the deep sea by the so called organic carbon pump (Ito and Follows, 2005; Sigman et al., 2010).

Surface water, loaded with unused nutrients, which is subducted below the warm subtropical and tropical mixed layer north of the Antarctic Polar Front is forced to the ocean's surface in the Benguela upwelling system (BUS). Upwelling is driven by the southeast trade winds and occurs along the southwest African coast from Cape Agulhas (~34 °S) to the Angola Benguela Frontal Zone (ABFZ) (14 to 16 °S). At 26.6 °S the strong Lüderitz upwelling cell acts as perennial barrier, separating the BUS into a northern and a southern subsystem (N- and SBUS) (Duncombe Rae, 2005). At the ABFZ the cold northward flowing Benguela Current converges with the warm southward flowing Angola Current feeding into a poleward flowing undercurrent that develops south of the ABFZ. It carries the Angola Gyre subtype of South Atlantic Central Water (SACW) to the NBUS shelf where it mixes with Eastern South Atlantic Central Water (ESACW), which dominates the subsurface water mass composition in the SBUS (Duncombe Rae, 2005; Mohrholz et al., 2008).

To elucidate the role of  $\text{PO}_4^0$  as factor controlling the  $\text{CO}_2$  sink and source function of the BUS we measured the  $\text{CO}_2$  partial pressure ( $\text{pCO}_2$ ) along the continental margin off South Africa, Namibia and Angola during six cruises between 2008 and 2011 (see supplementary information for detailed descriptions of methods). The  $\text{pCO}_2$  measured in surface waters of the NBUS is high ( $>750 \mu\text{atm}$  reaching up to  $1200 \mu\text{atm}$ ) in a narrow belt along the coast and above the atmospheric  $\text{pCO}_2$  in a large halo seaward of the immediate upwelling area (Fig. 6.2. a, b). In the NBUS, the time- and area-integrated  $\text{CO}_2$  flux into the atmosphere exceed those of other coastal upwelling systems (Tab. 8.1.) and marks the NBUS as a significant oceanic  $\text{CO}_2$  source (Fig. 6.2. c).

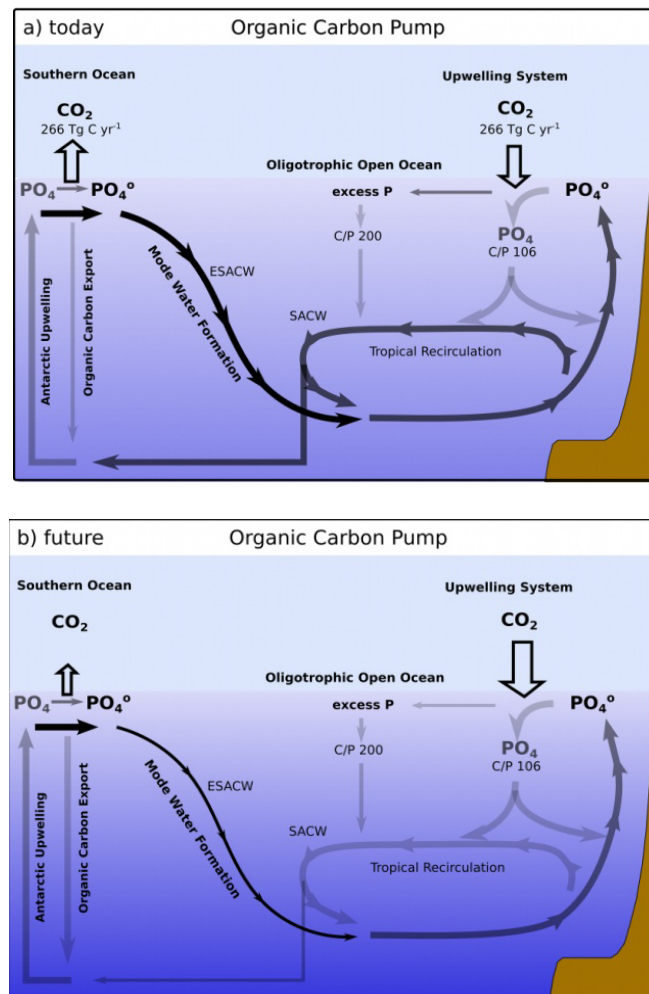


Fig. 6.1.: Organic carbon pump. (a) Schematic view of  $PO_4^0$  formation by the combination of upwelling at the Antarctic Divergence and subduction of Antarctic Surface Water north of the Antarctic Polar Front (Sarmiento et al., 2004). On its way into the BUS it mixes with SACW that was enriched with regenerated phosphate (indicated by the lighter grey) during its passage through the tropics and subtropics. Excess P that remained unused in the upwelling system is carried into the oligotrophic open ocean where it favours  $N_2$ -fixation and its export by diazotrophic organisms revealing C/P ratios  $>200$ . (b) An increased productivity and a reduced mode water formation lower the  $PO_4^0$  formation and the associated  $CO_2$  release at higher latitudes. Upwelling on the other hand continues to take up  $CO_2$  by converting  $PO_4^0$  into  $PO_4$  in the course of which its reservoir size in the sub-thermocline water shrinks at the expense of expanding OMZs. The declining reservoir size is indicated by the lighter grey and the expanding OMZ by the darker blue.

In contrast, the ocean surface  $pCO_2$  south of the Lüderitz divide is below the atmospheric  $pCO_2$  showing that the SBUS is a sink for atmospheric  $CO_2$  in line with other observations (Santana-Casiano et al., 2009; González-Dávila et al., 2011).

The difference in  $p\text{CO}_2$  of the S- and NBUS is independent of temperature and caused by different  $\text{CO}_2$  concentrations in the sub-thermocline waters that well up along the coast (Fig. 6.2. c). The upwelling feed water in the NBUS is dominated by the  $\text{O}_2$ -depleted SACW, which is enriched in regenerated nutrients and  $\text{CO}_2$  (Tab. 8.3.- see supplementary information) as a consequence of the remineralisation of sinking OM. By contrast, a substantial part of the nutrient inventory in ESACW, which is the predominant feed water of upwelling in the SBUS, is preformed ( $\text{PO}_4^0$  contributes 67 % to total phosphate, Tab. 8.1.). Thus, concentrations of regenerated  $\text{CO}_2$  in upwelling ESACW are low and phytoplankton which assimilates  $\text{PO}_4^0$  causes a  $\text{CO}_2$  flux from the atmosphere into the sea surface even in the upwelling centres along the coast (Fig. 6.2.).

On a global scale, the domain where  $\text{PO}_4^0$  dominates over regenerated  $\text{PO}_4$  in the ocean's thermocline coincides with tropical/subtropical transition zones (Fig. 6.2. d). The latitudinal gradient reflects higher ages of tropical water masses that are loaded with respiration products rather than with  $\text{PO}_4^0$  (Brea et al., 2004). All major upwelling systems (Körtzinger et al., 1997; Friederich et al., 2008; Steinhoff et al., 2012) except the SBUS and the California/Oregon upwelling system (Friederich et al., 2002; Hales et al., 2005) are located within the tropical domain where  $\text{PO}_4^0 < 50\%$ , and are  $\text{CO}_2$  sources (Fig. 6.1.).

Table 6.1.: Characteristics of major upwelling systems: Area and duration of upwelling, N/P ratios and the contribution of  $\text{PO}_4^0$  to the total  $\text{PO}_4$  from subsurface water, Ekman transport and pumping as well as nutrient concentrations within the subsurface water that is injected by Ekman transport and pumping into the surface layer. The Redfield C/N/P ratio of 106/16/1 was used to convert nutrient into carbon fluxes. The area of the upwelling regions was derived from the ETOP1 data set, the width, the transport rates, and the nitrate concentration were obtained from (Messié et al., 2009). Data from the Arabian Sea were taken from (Rixen et al., 2000; Rixen et al., 2006). The Arabian Sea upwelling occurs only for four month during the SW monsoon season. The  $\text{CO}_2$  flux from the California and the Peruvian upwelling system were obtained from (Friederich et al., 2002; Friederich et al., 2008) whereas the fluxes from the non El Niño years were chosen for the California upwelling system. The  $\text{CO}_2$  fluxes from off Mauretania were estimated based on the data presented in (Steinhoff et al., 2012). The contribution of  $\text{PO}_4^0$  to the total  $\text{PO}_4$  and the N/P ratio were obtained from the (Garcia et al., 2010) at water depths between 75 and 200 m. CUS, California upwelling system; PUS, Peruvian upwelling system; MUS, Mauretania upwelling system; SBUS, Southern Benguela upwelling system; NBUS, Northern Benguela upwelling system; ASUS, Arabian Sea upwelling system.

		Eastern boundary upwelling systems						
		CUS	PUS	MUS	SBUS	NBUS	ASUS	Sum
Area	$10^{12} \text{ m}^2$	0.16	0.17	0.15	<b>0.14</b>	<b>0.19</b>	0.36	
Duration	year	1	1	1	<b>1</b>	<b>1</b>	0.3	
<b>Nutrient ratios:</b>								
N/P ratio		10.39	8.90	15.17	<b>11.49</b>	<b>12.73</b>	11.15	
$\text{PO}_4^0$	%	50.17	43.12	35.72	<b>67.09</b>	<b>44.82</b>	41.72	
<b>Transport</b>								
<i>Ekman pumping</i>	$10^6 \text{ m}^3 \text{ s}^{-1}$	0.27	0.72	0.44	<b>0.20</b>	<b>0.51</b>	1.07	
Nitrate concentration	$\text{mmol m}^{-3}$	14.90	16.80	19.00	<b>16.90</b>	<b>16.90</b>	16.20	
Phosphate = Nitrate / (N/P)	$\text{mmol m}^{-3}$	1.43	1.89	1.25	<b>1.47</b>	<b>1.33</b>	1.45	
<i>Ekman transport</i>	$10^6 \text{ m}^3 \text{ s}^{-1}$	0.90	1.58	1.30	<b>0.61</b>	<b>1.69</b>	3.00	
Nitrate	$\text{mmol m}^{-3}$	17.20	17.00	19.20	<b>18.10</b>	<b>18.10</b>	16.20	
Phosphate = Nitrate / (N/P)	$\text{mmol m}^{-3}$	1.66	1.91	1.27	<b>1.58</b>	<b>1.42</b>	1.45	
<b>OM flux based on:</b>								
1. $\text{PO}_4$ (C/P = 106)	Tg C $\text{yr}^{-1}$	11.1	21.9	51.9	<b>2.4</b>	<b>43.0</b>	21.8	152.20
2. $\text{PO}_4^0$ (C/P = 106)	Tg C $\text{yr}^{-1}$	37.8	75.6	31.4	<b>34.0</b>	<b>55.5</b>	32.6	266.86
								419.06
3. Excess P (C/P = 106)	Tg C $\text{yr}^{-1}$	26.4	77.8	4.6	<b>14.3</b>	<b>25.3</b>	23.7	172.04
Net OC flux (2-3)	Tg C $\text{yr}^{-1}$	11.4	-2.2	26.8	<b>19.7</b>	<b>30.2</b>	8.9	
4. Excess P (N fix: C/P = 200)	Tg C $\text{yr}^{-1}$	49.9	146.8	8.6	<b>27.0</b>	<b>47.7</b>	44.6	324.61
								743.67
<b>OC Export (upwelling + open ocean: 1+2+3)</b>								
<b>CO<sub>2</sub>-emission</b>								
CO <sub>2</sub> -flux	$\text{mol C m}^{-2} \text{ yr}^{-1}$	1.85	5.10	4.79	<b>-1.75</b>	<b>6.46</b>	8.87	
CO <sub>2</sub> -flux = CO <sub>2</sub> -flux * area	Tg C $\text{yr}^{-1}$	3.58	10.60	8.80	<b>-2.92</b>	<b>14.90</b>	38.03	72.98
Period of measurement		1998-1999	2004-2006	2005	<b>2009-2010</b>	<b>2008-2011</b>	1995	

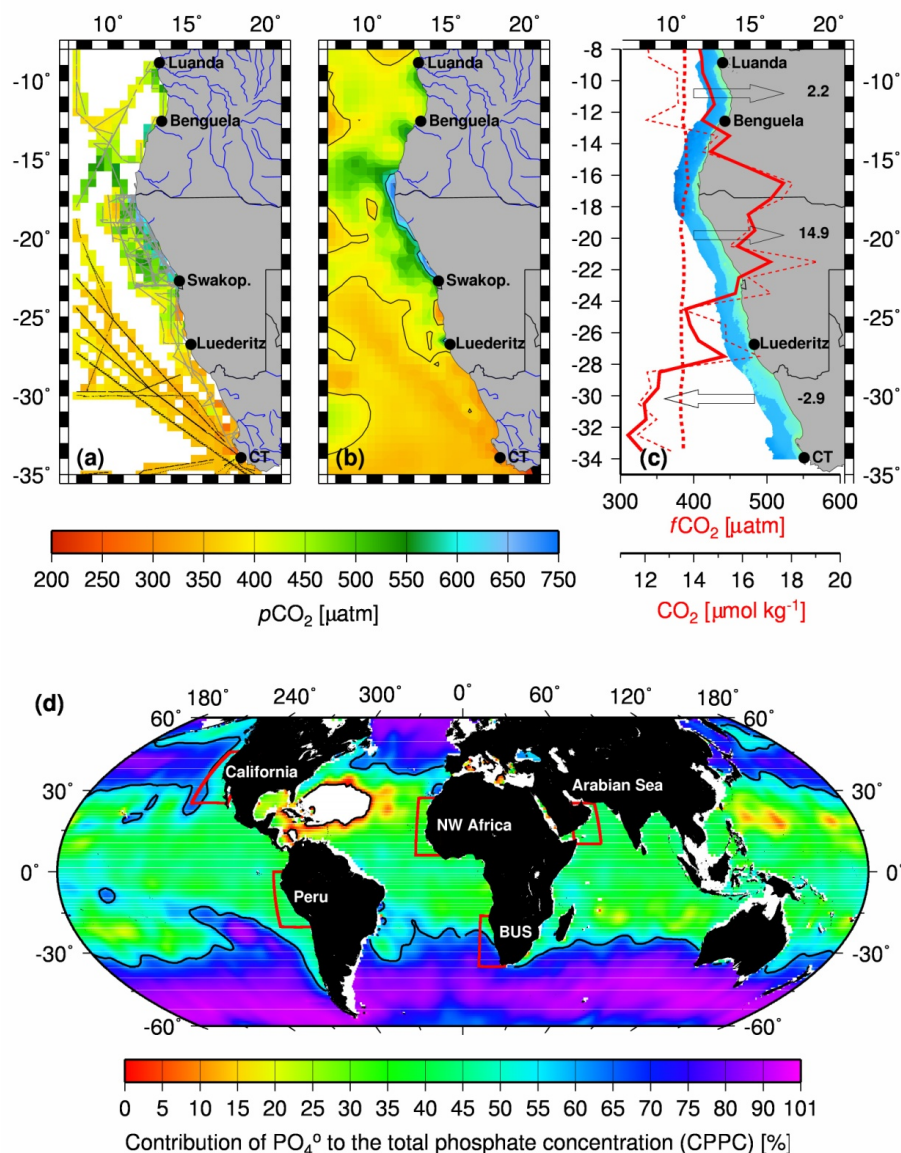


Fig. 6.2.: pCO<sub>2</sub> along the southwest African continental margin and the global distribution of the PO<sub>4</sub><sup>0</sup>. (a) pCO<sub>2</sub> measured and gridded on 0.25° grid along the cruise tracks (grey lines) and the volunteer observing ship (VOS) lines obtained from Takahashi et al. (2009) (black lines). The VOS data were normalised to the year 2010 by assuming a mean annual increase of 1.84 ppm yr<sup>-1</sup> as seen in the Mauna Loa pCO<sub>2</sub> data between 1990 and 2013. The Mauna Loa data were obtained from: <http://www.esrl.noaa.gov/gmd/ccgg/trends/mlo.html>. (b) The map shows the interpolated mean pCO<sub>2</sub> of the entire region. The black line represents a pCO<sub>2</sub> of 389 and 600 μatm. (c) The mean fugacity of CO<sub>2</sub> (fCO<sub>2</sub>) measured during all cruises in the ocean (bold red line) and the atmosphere (bold red broken line). The red thin broken line shows the CO<sub>2</sub> concentrations. All data were averaged by 1° x 1° for each cruise and subsequently within latitudinal bands. The arrows show the air-sea CO<sub>2</sub> flux estimates from the Angolan margin (8-16°S), the NBUS (16-26.6°S) and the SBUS (26.6-34°S) whereby the negative values indicate a CO<sub>2</sub> flux from the atmosphere into the ocean (Tab. 8.1). The water depth was obtained from the ETOPO1 data

(<http://www.ngdc.noaa.gov/mgg/global/global.html>). (CT = Cape Town). (d) The fraction of  $\text{PO}_4^0$  derived from the World Ocean Atlas 2009 (Garcia et al., 2010) at a water depth of 200 m. The bold line indicates a  $\text{PO}_4^0$  of 60 %. The white area in the Sargasso Sea (western Atlantic Ocean) is caused by the fact that the calculated regenerated  $\text{PO}_4$  exceeds the total phosphate concentrations. This suggests that the  $\text{O}_2/\text{P}$  ratio of 175 is too low which might be caused by the high C/P ratio of  $\text{N}_2$  fixing bacteria.

Available estimates of air-sea  $\text{CO}_2$  fluxes from all the EBUS and the Arabian Sea upwelling (ASUS) correlate with the contribution of  $\text{PO}_4^0$  to the  $\text{PO}_4$  concentrations in the sub-thermocline waters. The fraction of  $\text{PO}_4^0$  in upwelling feed waters thus determines the magnitude and the direction of  $\text{CO}_2$  fluxes between ocean surface and atmosphere in all major coastal upwelling systems.

The main factors raising  $\text{CO}_2$  levels in upwelled waters are increasing temperatures, the formation of carbonate shells shifting the carbonate system towards higher  $\text{CO}_2$  concentrations, and the incomplete uptake of regenerated  $\text{PO}_4$ . The latter is caused by nitrate reduction that occurs in the mid-water oxygen minimum zones (OMZ) when due to the lack of  $\text{O}_2$  bio-available nitrate is reduced to di-nitrogen gas during the decomposition of sinking OM. When such N deficits are introduced into the surface layer via upwelling,  $\text{PO}_4$  (Deutsch et al., 2007) remains unused after nitrate has been consumed and is referred to as excess P in the BUS (Flohr et al., 2014) and other upwelling systems (Rixen et al., 2005).

Carbon export rates derived from upwelling velocities, nitrate concentrations (Messié et al., 2009), and subsurface N/P ratios of all major upwelling systems suggest that the excess P could support an export of 172 Tg organic carbon  $\text{yr}^{-1}$  provided that nitrate is not limited (Tab. 8.1.).  $\text{N}_2$  fixing cyanobacteria such as *Trichodesmium*, which are independent of nitrate supply, assimilate excess P in the oligotrophic subtropical gyres. Their C/P ratios of  $\sim 200$  (Hutchins et al., 2007) exceed the common Redfield ratio of phytoplankton (106), so that diazotrophic utilisation of excess P at the fringe of the upwelling systems theoretically may overcompensate the  $\text{CO}_2$  loss caused the incomplete  $\text{PO}_4$  utilisation in the nitrate-driven upwelling systems (Tab. 8.1.). The utilisation of excess P by  $\text{N}_2$  fixing cyanobacteria may become more efficient in the future because diazotrophic  $\text{N}_2$  fixers tend to increase their C/P ratios under rising  $\text{CO}_2$  concentrations (Hutchins et al., 2007). However, within the N-driven upwelling systems, the reduced carbon export caused by the

incomplete utilisation of  $\text{PO}_4$  declines, except for the Peruvian upwelling system, below the carbon export driven by the assimilation of  $\text{PO}_4^0$  (Tab. 8.1.). The uptake of new  $\text{CO}_2$  by the assimilation of  $\text{PO}_4^0$  exceeds the losses of metabolic  $\text{CO}_2$  and indicates that the organic carbon pump acts in all major upwelling systems, except the Peruvian, as  $\text{CO}_2$  sinks.

Considering a balanced marine N cycle (Großkopf et al., 2012), i.e. N reduction within the OMZ is compensated by  $\text{N}_2$  fixation in the oligotrophic ocean, the uptake of new  $\text{CO}_2$  by the assimilation of  $\text{PO}_4^0$  in the major upwelling systems amounts to  $266 \text{ Tg C yr}^{-1}$ . This represents 63 % of the mean carbon export of  $419 \text{ Tg C yr}^{-1}$  of the major upwelling systems (Tab. 8.1.) and accounts for approximately 10 % of the global mean carbon export into the deep ocean (Chavez and Toggweiler, 1995). To what extent this  $\text{CO}_2$  uptake potential is realised depends on the  $\text{CO}_2$  release during the formation of  $\text{PO}_4^0$ . Global warming lowers the formation and export of  $\text{PO}_4^0$  into the subtropical thermocline water by favouring the productivity and reducing the mode-water formation at higher latitudes (Manabe and Stouffer, 1993; Bopp et al., 2001). At the same time it is likely that global warming strengthens upwelling in all EBUS's (Bakun, 1990; Bakun et al., 2010) and thus enhances the export of upwelled  $\text{PO}_4^0$  in the form of OM. A reduced formation and supply of  $\text{PO}_4^0$  from the high latitudes and an accelerated utilisation of  $\text{PO}_4^0$ , stored currently in subtropical and tropical waters, will decrease the  $\text{PO}_4^0$  concentrations and therewith increase the amount of nutrients used for binding  $\text{CO}_2$  in the ocean's interior. The associated increased  $\text{O}_2$  consumption is in line with the currently expanding OMZ's which cannot solely be explained by physical processes (Oschlies et al., 2008). This implies that the marine biosphere is responding already with an increasing  $\text{CO}_2$  uptake to global warming at the expense of expanding OMZ's.

Acknowledgements: We would like to thank the German Federal Ministry of Education and Research (BMBF) for the financial support of project 03F0497D. We are extremely thankful to Ludger Mintrop, for helpful discussion. We are also grateful to P. Wessels and W. H. F. Smith for providing the generic mapping tools (GMT).

#### SUPPLEMENTARY INFORMATION - METHODS

*From  $x\text{CO}_2$  to  $f\text{CO}_2$* 

During six cruises (Tab. 8.2., 8.3.) the mole fraction of  $\text{CO}_2$  ( $x\text{CO}_2$ ) in the surface waters and the atmosphere was measured by an underway  $\text{pCO}_2$  system (SUNDANS). The SUNDANS was developed by “marine analytics and data” (MARIANDA, Germany, [www.marianda.com](http://www.marianda.com)) according to the recommendations of the 2002 underway  $\text{pCO}_2$  system workshop in Miami (<https://www.aoml.noaa.gov/ocd/gcc/uwpc2/workshps/>). It was equipped with a shower type equilibrator, an open pre-equilibrator and a non-dispersive dual cell infrared gas analyser (LI-7000). The LI-7000 was calibrated by using  $\text{N}_2$  gas (zero  $\text{CO}_2$ ) and a standard gas for  $\text{CO}_2$ . During the cruises with RV Africana and RV Discovery a 802.2 ppm and during the RV M. S. Merian cruise a 450.2 ppm standard gas was used. The resulting linear calibration curve was controlled by a third standard gas for  $\text{CO}_2$  (340.2 ppm). The  $\text{CO}_2$  standard gases were checked against the standard gases provided by NOAA (CA07600 and CC311968) at the Institute for Baltic Sea Research in Warnemünde, Germany. The  $x\text{CO}_2$  data were recorded each 6 seconds and subsequently averaged minute by minute. Minute by minute data on atmospheric pressure, wind speed, surface water temperature (5 m water depth) and salinity were obtained by the research vessels. The  $x\text{CO}_2$  was converted into the partial pressure ( $\text{pCO}_2$ ) and into the fugacity of  $\text{CO}_2$  ( $f\text{CO}_2$ ) according to the equations given by Zeebe and Wolf-Gladrow (2001; page 281 and 65). Sea surface temperatures, measured by the thermosalinograph installed on board the research vessels, and the temperature measured in the equilibrator were correlated ( $r^2=0.953$ ;  $n=29291$ ) to each other. The resulting regression equation was used to calculate the equilibrator temperature during the cruise D356 because the temperature sensor within the equilibrator failed due to technical problems during this cruise. The difference between the equilibrator and the sea surface temperature was taken into account as suggested by Dickson et al. (2007; SOP 5, page 8). During the RV Africana cruise in December 2009, the  $\text{pCO}_2$  was additionally measured by an underwater carbon dioxide sensor ( $\text{CO}_2$ -Pro, Pro Oceanus Systems Inc.). The determined  $\text{pCO}_2$  is highly correlated to the  $\text{pCO}_2$  data measured by the SUNDANS (Fig. 6.4.). The resulting regression equation was used to calibrate the  $\text{pCO}_2$  measured by the PSI  $\text{CO}_2$ -Pro during the RV Meteor cruise

in May 2008. The mean atmospheric pressure of 1.01357 atm derived from the other three cruises was used to convert  $p\text{CO}_2$  into  $f\text{CO}_2$ .

### *CO<sub>2</sub> FLUXES*

In order to calculate the annual mean air-sea  $\text{CO}_2$  fluxes we first gridded the measured data on  $1^\circ \times 1^\circ$  grid for each cruise. These fields were averaged and the mean  $f\text{CO}_2$ , wind speeds, SST's und salinity were calculated for the Angolan coast, the N- and the SBUS. Since the mean  $x\text{CO}_2$  measured in the atmosphere during the other three cruises was similar to those measured at the Mauna Loa Observatory, Hawaii (Fig. 6.5.) (Keeling and Whorf, 2005) the Mauna Loa value determined in May/June 2008 (388.2 ppm) was used to calculate the  $\Delta f\text{CO}_2$  during the RV Meteor M67/2 cruise. The piston velocity ( $k$ ) was calculated according to Wanninkhof (1992). This equation was also used to calculate the  $\text{CO}_2$  fluxes presented in Table 6.1. (main text) except for the California upwelling system where the equation derived from Wanninkhof and McGillis (1999) was used (Friederich et al., 2002). The area of the continental shelf and slope was defined by a water depth of  $<2000$  m and calculated based on the ETOPO1 data set (<http://www.ngdc.noaa.gov/mgg/global/global.html>).

### *PREFORMED PHOSPHATE ( $\text{PO}_4^0$ )*

To calculate the contribution of the preformed phosphate ( $\text{PO}_4^0$ ) to the total phosphate ( $\text{PO}_4$ ) the equation (1) derived from Broecker and Takahashi (1985) and the data obtained from the World Ocean Atlas 2009 were used.

$$PO_4^0 = PO_4 - \frac{O_{2sat} - O_2}{175} = PO_4 - \frac{AOU}{175} \quad (1)$$

*WATER MASS CHARACTERISTICS*

The SACW and ESACW are defined as mixtures of deeper and shallower subsurface waters whose potential temperatures ( $T_{\text{pot}}$ ) and salinities (S) fall on straight lines within the  $T_{\text{pot}}$ -S space (Mohrholz et al., 2008). See Table 6.4. for more details.

Table 6.2.: Cruise details; WB-Walvis Bay, CT-Cape Town.

Research vessel	Cruise ID	Period	Harbours
RV M.S. Merian	MSM07/2	Mar. 10-20, 2008	WB-WB
RV Meteor	M67/2	May 15-June 05, 2008	WB-WB
RV Africana	A258	Dec. 02-16, 2009	CT-CT
RV Discovery	D356	Sep. 10-Oct 19, 2010	WB-CT
RV M.S. Merian	MSM17/3	Jan. 20-March 07, 2011	WB-Dakar
RV M.S. Merian	MSM18/4	July 24-Aug. 20, 2011	Libreville-WB
RV M.S. Merian	MSM19/1b	Oct. 02-Oct.11, 2011	WB-WB

Table 6.3.: Cruise summary, cruise I.D. and period as well as the mean  $p\text{CO}_2$ , SST's, wind speed and direction within the coastal region off Angola, the N- and SBUS. (n.d. - not determined).

Cruise	Period	$p\text{CO}_2$		SST [°C]	Wind speed [m s <sup>-1</sup> ]	Wind direction [°]
		Atm. [µatm]	Water			
<b>Angola</b>						
MSM17/3	Jan./March 2011	374.4	428.6	28.2	n.d	n.d.
MSM18/4	July/Aug. 2011	390.7	439.5	20.4	4.8	178.5
<b>NBUS</b>						
MSM07/2	March 2008	383.6	395.5	20.4	4.9	203.5
M76/2	May/June 2008	386.5	656.4	16.3	n.d	n.d.
Afr258	December 2009	384.6	434.6	17.9	7.6	181.9
D356	Sep./Oct. 2010	386.8	518.0	15.7	6.9	178.1
MSM17/3	Jan./March 2011	382.7	452.8	20.3	10.9	218.5
MSM18/4	July/Aug. 2011	395.5	536.4	15.9	7.6	162.0
MSM19/1	October 2011	388.7	593.1	14.9	7.6	141.9
<b>SBUS</b>						
Afr258	December 2009	385.4	356.2	18.1	7.4	191.0
D356	Sep./Oct. 2010	386.1	376.3	16.1	3.7	196.7

Table 6.4.: Subsurface water masses. Properties of the SACW and ESACW (Mohrholz et al., 2008) as well as the  $\text{PO}_4^0$  concentration derived from the equation (1) and the contribution of  $\text{PO}_4^0$  to the total  $\text{PO}_4$  concentration.

	Temp. [°C]	Salinity	$\text{O}_2$ [ $\mu\text{mol l}^{-1}$ ]	$\text{O}_2\text{sat}$	$\text{PO}_4$	$\text{PO}_4^0$	$\text{PO}_4^0$ [%]
SACW	8.00	34.72	22.43	295.26	2.71	1.15	42.38
	16.00	35.64	68.48	248.29	1.50	0.48	31.63
ESACW	5.96	34.41	300.06	310.06	1.31	1.25	95.63
	14.41	35.30	249.34	256.76	0.24	0.19	82.02

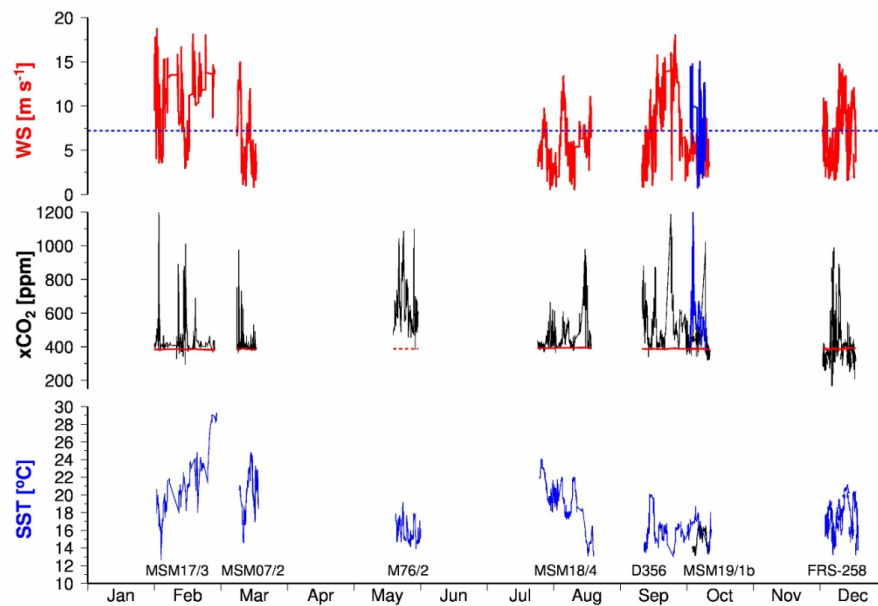


Fig. 6.3.: (a) Wind speeds measured on board the research vessels smoothed with a 30 minute moving average (red) versus Julian days. The broken blue line indicates the mean wind speed (WS) of  $7.2 \text{ m s}^{-1}$  obtained from QuickSCAT between 1999 and 2008 along the Namibian and South African coast (Chavez and Messié, 2009). (b)  $x\text{CO}_2$  and  $p\text{CO}_2$  (only during the RV Meteor cruise) measured in the surface water (black) and the atmosphere (red) averaged minute by minute. Data gaps between the atmospheric data were filled by interpolating linearly between the measured data (red line). The broken red line indicates the mean atmospheric  $x\text{CO}_2$  at Mauna Loa in May/June 2008 (388.2 ppm, compare Fig. 6.5.). (c) Sea surface temperatures (SST) measured by the thermosalinograph and the Ferrybox system in May 2008. The black line in the SST plot and the blue line in the WS and  $x\text{CO}_2$  plot indicate data obtained from the cruise MSM19/1b.

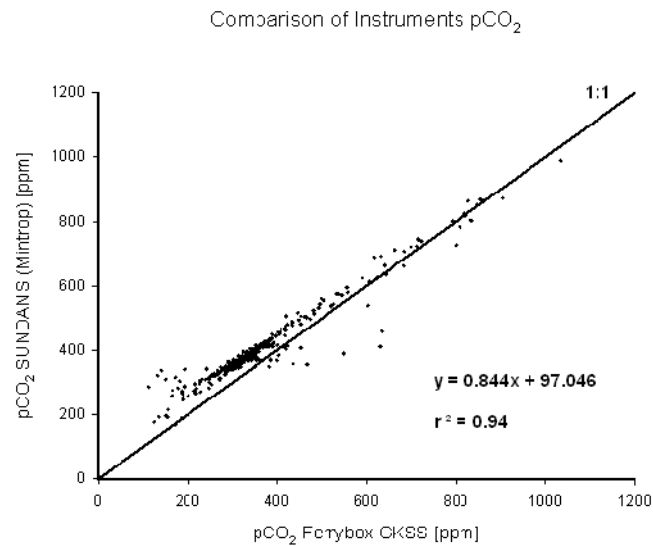


Fig. 6.4.: pCO<sub>2</sub> measured by the underwater carbon dioxide sensor (PSI CO<sub>2</sub>-Pro) which was integrated into a Ferrybox system (developed at GKSS, Geesthacht, Germany) versus the pCO<sub>2</sub> measured with SUNDANS (developed by Ludger Mintrop; MARIANDA, Germany, [www.marianda.com](http://www.marianda.com)) during the RV Africana cruise. The resulting regression equation was used to calibrate the pCO<sub>2</sub> data measured of the RV Meteor M67/2 cruise during which only the Ferrybox was on board.

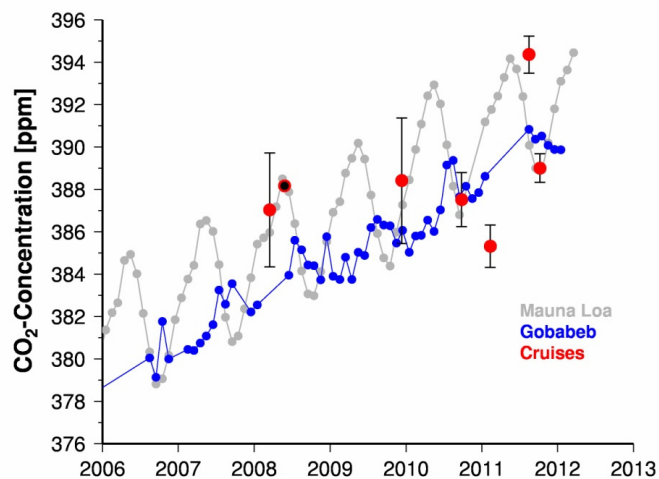


Fig. 6.5.: CO<sub>2</sub> concentrations measured at the Mauna Loa Observatory, Hawaii (grey line) at the Namibian Training and Research Center Gobabeb (blue line) and during the cruises with RV M.S. Merian, RV Meteor, RV Africana, RV Discovery in 2008, 2009, 2010 and 2011 (red circles). The standard deviations are indicated by the error bars and the black circle indicates an xCO<sub>2</sub> of 388.2 ppm which was used to calculate the  $\Delta f\text{CO}_2$  during the RV Meteor cruise in May 2008. The data from the Namibian Training and Research Center in Gobabeb and from the Mauna Loa Observatory were obtained from the NOAA CMDL Carbon Cycle Cooperative Global Air Sampling Network. The low pCO<sub>2</sub> measured during the cruise MSM17/3 seem to indicate the

influence of the CO<sub>2</sub>-poor air mass which often develops during this time of the year over the southern part of tropical Africa (Buchwitz et al., 2005; Warneke et al., 2005).

## 7. SYNOPTIC DISCUSSION AND CONCLUSION

The overall aim of this thesis is to investigate the functioning of the biological carbon pump in the northern Benguela upwelling system (NBUS). A main focus is given on parameters indicative of the strength and efficiency of carbon cycling; more specifically the variability of nutrient supply, the dynamics of carbonate saturation and their effects on the magnitude and composition of particle export to the shelf. Along with patterns of air-sea CO<sub>2</sub> fluxes, they provide a basis to assess the net C source-sink function of the NBUS.

In the following, the main findings of the previous chapters are summarised and discussed to answer the thesis objectives (Chapter 7.1) and to briefly evaluate the findings in the light of climate change (Chapter 7.2).

### 7.1. ASPECTS OF CARBON PUMPING IN THE BENGUELA CURRENT UPWELLING SYSTEM

The ratios of remineralised C, N, P and consumed oxygen (-O<sub>2</sub>) (C/N/P/-O<sub>2</sub>) are poorly constrained in the subsurface waters of the NBUS. My findings on the remineralisation patterns (Chapter I) indicate that the release of N and P by organic matter remineralisation follows the Redfield stoichiometry of C/N/P/-O<sub>2</sub> of 106/16/1/-138 in the oxygenated water column. The results further indicate that the N/P ratio on the shelf is altered by P efflux from sediments resulting in a C/N/P/-O<sub>2</sub> ratio of 106/16/1.6/-138. N reduction further increases C/N and reduces N/P ratios in those regions where O<sub>2</sub> concentrations in bottom waters are <20 μmol O<sub>2</sub> kg<sup>-1</sup>, in line with earlier studies (Tyrrell and Lucas, 2002; Nagel et al., 2013). This N deficiency (N/P <16) in subsurface water is expressed in a P excess (+P\*), which surfaces in the course of upwelling, and is exported within the offshore moving surface water. Approximately 300 km offshore, the mean P\* in surface water varied between P\* ~0.007 μmol kg<sup>-1</sup> in 2008 and P\* ~0.3 μmol kg<sup>-1</sup> in 2010/2011. The role of the Benguela upwelling system (BUS) as a P\* source for the South Atlantic has been stated earlier (Moore et al., 2009). However, my findings show that the magnitude of P\*

varies with time and the results provide evidence on the controlling mechanism behind the varying amount of  $P^*$ . The key finding with regard to the controlling mechanism is the existence of an inter-annual variability of high  $N/P > 16$  ratios ( $+N^*$ ) observed within the South Atlantic Central Water (SACW). Elevated  $N/P > 16$  indicates the decomposition of organic matter which was produced by  $N_2$  fixation (Gruber and Sarmiento, 1997) and is supported by studies on  $N_2$  fixation activity in the Angola Gyre and the ABFZ region (Foster et al., 2009; Sohm et al., 2011). The SACW prevails in the Angola Gyre region and enters the Namibian shelf from the north. Off Kunene, where high fractions of SACW prevail,  $N^*$  was increased 3 fold within the SACW in 2008 ( $N^* = \sim 12 \mu\text{mol kg}^{-1}$ ) compared to 2009/2011 ( $N^* = \sim 3-4 \mu\text{mol kg}^{-1}$ ). This positive  $N^*$  anomaly is imported to the NBUS along with SACW and was reflected in less  $N^*$ -deficient water masses on the shelf in 2008 compared to 2009/2011 despite similarly low  $O_2$  concentrations. This, in turn was reflected in a lower  $P^*$  export in 2008 compared to 2009/2011. Summarised, my findings suggest that advected  $+P^*$  fuels  $N_2$  fixation in the (sub)tropical eastern South Atlantic where the decomposition of this organic matter leads to  $N/P > 16$  in SACW which flushes the Namibian shelf from the north, partly compensates the N deficit on the NBUS shelf, and thus controls the varying amount of  $+P^*$  that is exported from the NBUS to the tropical South Atlantic. It points to a negative feedback mechanism within the South East Atlantic by which the N loss on the central Namibian shelf is replenished on relatively short time and spatial scales by the intrusion of N-enriched SACW from the Angola Gyre region (Fig. 7.1.) and thus represents a mechanism which counteracts the N limitation that hampers the N-driven  $CO_2$  drawdown of the biological carbon pump in the NBUS.

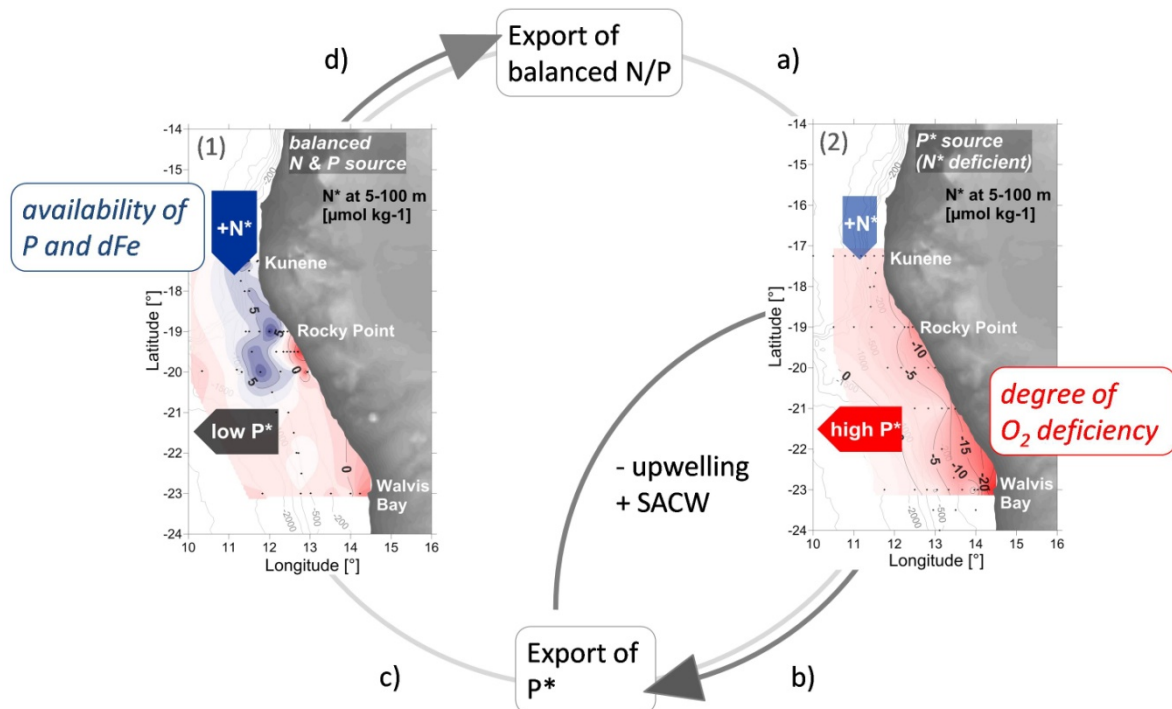


Fig. 7.1.: The composite illustrates the NBUS shifting between two states in regional scale nutrient cycling acting as (1) *balanced N & P source* and as (2) *P\* source* mediated by a negative feedback mechanism that is driven by the extent of N\* deficiency exported to the South Atlantic. (a) High contribution of SACW favours O<sub>2</sub> depletion down to anoxic conditions in bottom water on the shelf. This results in elevated P\* excess (red arrow) which is exported offshore to the South Atlantic and Angola Gyre where it fuels N<sub>2</sub> fixation (b) if dissolved iron (dFe) is available in the surface water. The sinking and subsequent remineralisation of this N<sub>2</sub>-fixed organic matter is reflected in N\* excess of subsurface waters (blue arrow) that (c) is transported to the NBUS (blue shaded area) where it replenishes the N\* deficiency on the shelf. Thereby the system is shifted towards a more balanced N & P export (black arrow). (d) This is reflected in less N\* excess import from the Angola Gyre (blue arrow).

Quantitative along with qualitative estimates on particle fluxes on the shelf are lacking but are crucial to characterise the functioning of the biological pump. Another aspect of my thesis deals with the factors that control the magnitude and composition of particle fluxes on the NBUS shelf. The particulate organic carbon (POC) export to 70 m water depth varied strongly between 13-143 g POC m<sup>-2</sup> yr<sup>-1</sup>. Results of the meteorological and hydrographical data, obtained during the time of particle flux measurements (12/2009-02/2011), show that an intensification of upwelling was associated with enhanced inflow of oxygenated ESACW from the south. In contrast, quiescent periods were associated with an enhanced inflow of oxygen-depleted SACW from the north. This change in subsurface water mass composition as a response of changes in the upwelling intensity had been

described earlier (Monteiro et al., 2006; Mohrholz et al., 2008). However, the significance of the results presented in chapter III arises from the linkage of the subsurface water mass composition and the magnitude of POC fluxes: the combined results suggest that weak upwelling of enhanced SACW fractions fuel higher POC fluxes on the shelf ( $>91 \text{ g POC m}^{-2} \text{ yr}^{-1}$ ) than intense upwelling of high ESACW fractions. This reflects the higher nutrient inventory of SACW compared to ESACW, among other factors. Overall, it points to a close link between changes in upwelling intensity, which are accompanied by changes in the subsurface water mass and in turn affect the variability of POC export on the shelf. A key implication arising from these findings refers to the response of the NBUS to climate change (Chapter 3.2.). The annual mean POC flux on the shelf is  $66 \text{ g POC m}^{-2} \text{ yr}^{-1}$  (Chapter III). Organic carbon fluxes measured on the Namibian continental margin and the Walvis Ridge at water depths of 545 and 599 m accounted for  $2.6$  and  $5.1 \text{ g POC m}^{-2} \text{ yr}^{-1}$ , respectively (Wefer and Fischer, 1993; Giraudeau et al., 2000). Considering the organic carbon respiration below the mixed layer (Martin et al., 1987; van Mooy et al., 2002), these fluxes correspond to a POC export of  $<15 \text{ g C m}^{-2} \text{ yr}^{-1}$  at 70 m depth. These export rates are well below the mean of  $66 \text{ g POC m}^{-2} \text{ yr}^{-1}$  measured on the shelf and reflect the onshore-offshore gradient in productivity (Carr, 2002).

The qualitative composition of the particles fluxes show that the majority of the trapped material consists of biogenic opal ( $\sim 38 \%$ ). Biogenic opal originates from diatoms that in conjunction with dinoflagellates dominate phytoplankton communities of the BUS near the coast in freshly upwelled water (Barlow et al., 2006; Barlow et al., 2009; Hansen et al., 2014). This indicates that biogenic opal is the main carrier phase of POC to the shelf sediments and agrees with the high contribution of opal in the POC-enriched mud belt sediment on the shelf (Bremner and Willis, 1993; Inthorn et al., 2006). My combined results of the remineralisation patterns and particle fluxes (Chapter I, III) suggest that the decomposition of the basically diatomaceous organic matter causes low minimum carbonate saturation states of  $\Omega_A = 0.7$  and  $\Omega_C = 1.2$  (Chapter II) in freshly upwelled surface water. These values rank among the lowest values reported in surface water of upwelling systems (Loucaides et al., 2012; Rixen et al., 2012; Harris et al., 2013). In the summer of 2010, the mean  $\Omega_C$  in surface waters off Swakopmund was  $\sim 2$  (Chapter II). An

average  $\Omega_C$  value of  $\sim 2$  refers to  $[\text{CO}_3^{2-}]$  of  $\sim 90 \mu\text{mol kg}^{-1}$ , pH of  $\sim 7.7$  and  $\text{pCO}_2$  of  $\sim 1000 \mu\text{atm}$  and falls below the “thresholds” that were found to affect the calcification in coccolithophorids and foraminifera under in situ (e.g. Moy et al., 2009; Beaufort et al., 2011) and experimental conditions (Riebesell et al., 2000; Bijma et al., 2002). However, the responses may differ considerable among strains and species and reduced calcification does not necessarily alter growth or photosynthesis (Trimborn et al., 2007; Langer et al., 2009). Nevertheless, I assume that in addition to the low  $\Omega$  in ascending thermocline waters, the high silicate ( $\text{Si(OH)}_4$ ) concentrations favour the onset of diatom blooms and is disadvantageous for calcifying coccolithophorids. This leads to the reduction of PIC production relative to the high formation and export of POC on the Namibian shelf (Fig. 7.2.) and is reflected in a mean POC/PIC ratio of  $\sim 6$  in sinking matter exported from the euphotic zone (Chapter III). This suggests a dominance of the soft tissue pump near the coast indicating a highly efficient biological  $\text{CO}_2$  uptake.

Towards the slope and open ocean an increasing contribution of the carbonate counter pump is indicated by rising carbonate saturation states in the surface water (Chapter II), by high PIC contribution to total particle fluxes on the slope (Giraudeau et al., 2000) and by high carbonate contribution in surface sediments (Bremner, 1981) (Fig. 7.2.). In contrast to the coastal soft tissue pump, the offshore part of the biological pump is likely limited by the availability of fixed N which is in deficiency relative to P, hence lowering the N driven  $\text{CO}_2$  drawdown of the biological pump (Chapter I). We estimated that the potential carbon export fuelled by the excess P accounts for  $\sim 25\%$  of the N based carbon export fluxes of  $\sim 98 \text{ Tg C yr}^{-1}$  (Chapter IV). That shows that the NBUS productivity suffers from the impact of N reduction on the shelf. However, as mentioned earlier this might be partly compensated by intrusion of N-enriched SACW supplying  $+\text{N}^*$  (Chapter I) to the offshore surface water. The supply of this N-enriched subsurface water to the surface could be established, e.g. by shelf break upwelling, which has been assumed to be a likely mechanism by which the N deficit in offshore surface water is replenished (Nagel et al., 2013).

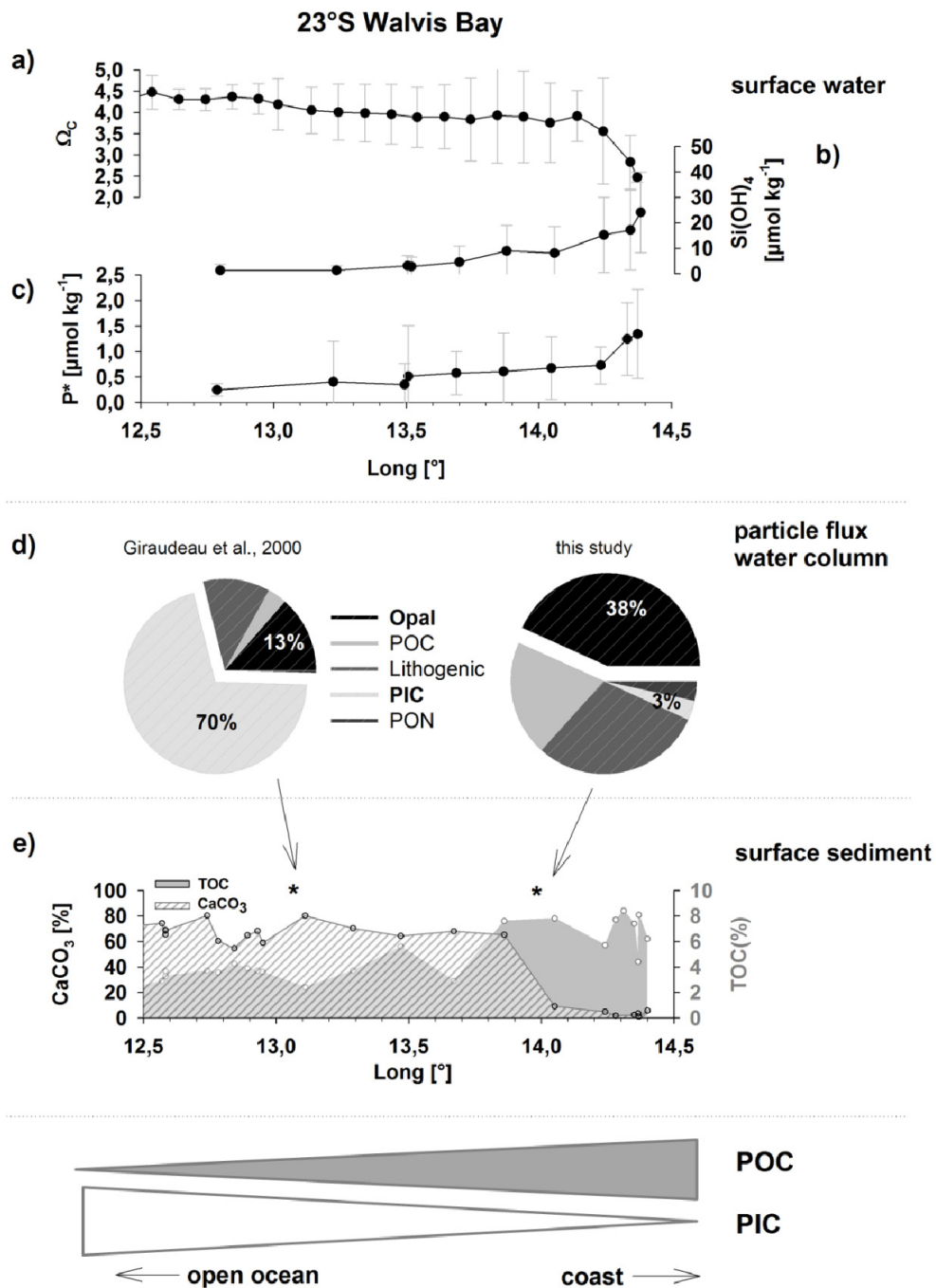


Fig. 7.2.: Composite illustrating the functioning of the biological pump off Walvis Bay (23 °S). (a) Average  $\Omega_{C(\text{CO}_2, \text{DIC})}$  (Flohr et al., unpublished data), average (b)  $\text{Si(OH)}_4$  and (c)  $\text{P}^*$  concentrations (all in  $\mu\text{mol kg}^{-1}$ ) (Chapter I; van der Plas et al., unpublished data) in the surface at 10 m water depth. Composition of the particle fluxes (%) measured on the slope (Giraudeau et al., 2000), and on the shelf (Chapter III); positions of the sediment traps are indicated by the arrows. (e) The TOC and  $\text{CaCO}_3$  (both wt %) of the surface sediment along the 23 °S transect (Inthorn et al., 2006). The triangles on the bottom of the composite illustrate the trend of increasing PIC export with increasing distance from the coast.

The  $p\text{CO}_2$  values of coastal surface water characterise the coastal areas of the BUS as local  $\text{CO}_2$  sources with  $\text{CO}_2$  values of  $>400\text{-}700 \mu\text{atm}$  (Chapter IV). Overall, the spatial and temporal variability of  $\text{CO}_2$  emission patterns in the BUS reveal a clear separation of upwelling areas that are sources and areas that are sinks for atmospheric  $\text{CO}_2$ . The NBUS is a  $\text{CO}_2$  source in the order of  $13.6 \text{ Tg C yr}^{-1}$ , likely reflecting the N deficit in upwelling subsurface water, whereas the SBUS is a significant sink of  $-3.4 \text{ Tg C yr}^{-1}$ . These  $\text{CO}_2$  fluxes exceed previous results, especially with regard to the NBUS: applying earlier estimations on  $\text{CO}_2$  fluxes (González-Dávila et al., 2009; Santana-Casiano et al., 2009) to the spatial extent described in Chapter IV, they correspond to  $1.3 \text{ Tg C yr}^{-1}$  for the NBUS and to  $-2.7 \text{ Tg C yr}^{-1}$  for the SBUS. This emphasises that the importance of the NBUS as  $\text{CO}_2$  source has been largely underestimated so far. Overall, the  $\text{CO}_2$  fluxes in the BUS add up to a net  $\text{CO}_2$  emission of  $\sim 10 \text{ Tg C yr}^{-1}$  to the atmosphere which accounts for  $\sim 27 \%$  of the combined EBUS  $\text{CO}_2$  source of  $\sim 37 \text{ Tg C yr}^{-1}$  (Chen and Borges, 2009).

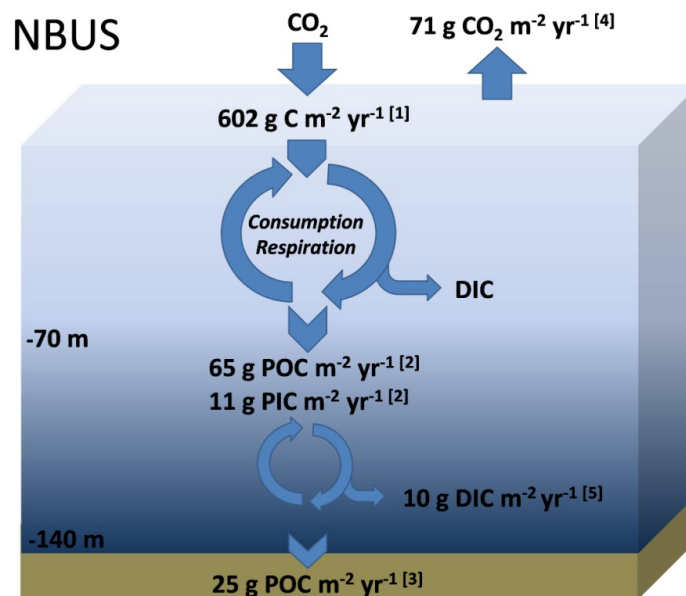


Fig. 7.3.: Composite of carbon pump parameters on the NBUS shelf derived from [1] average phytoplankton productivity off Walvis Bay in summer and winter (Barlow et al., 2009), [2] mean POC and PIC flux from the sediment trap study (Chapter III), [3] accumulation rates estimated for the mud belt region (Meisel et al., 2011b), [4] average  $\text{CO}_2$  flux of the NBUS (Chapter IV) and [5] DIC increase along isopycnal surfaces towards the coast between two stations close to the mooring station (Chapter I; Flohr et al., unpublished data) assuming a residence time of water of 80 days applied by Nagel et al. (2013).

Comparing the POC and PIC export sink of 66 and 11 g C m<sup>-2</sup> yr<sup>-1</sup> measured on the shelf with the CO<sub>2</sub> emissions of the NBUS (i.e. +71 g C m<sup>-2</sup> yr<sup>-1</sup>) indicates that the NBUS is a small net sink of ~6 g C m<sup>-2</sup> yr<sup>-1</sup>. This value represents a lower estimate because the exchange of subsurface water with the atmosphere is amplified in upwelling systems compared to open ocean. Using the amount of POC that is buried in the sediment as POC sink enlarges the NBUS net source to an upper estimate of ~46 g C m<sup>-2</sup> yr<sup>-1</sup>. However, the POC and PIC fluxes are local estimates which are representative for a relatively small spatial area compared to the CO<sub>2</sub> flux estimates. Independent of the total nutrient supply that is higher in the NBUS compared to the SBUS, the contribution of preformed P to the total P accounts for 67 % in the SBUS and for 44 % in the NBUS (Chapter IV) and implies an excess of macronutrients over carbon, and thus the potential to take up additional carbon. The potential POC export driven by preformed P is thus equivalent to the net C uptake of the organic carbon pump and accounts for ~19 Tg C yr<sup>-1</sup> in NBUS and for ~10 Tg C yr<sup>-1</sup> in the SBUS. Overall, the sum of potential C assimilation supported by preformed P exceeds the CO<sub>2</sub> emission in both systems and identifies the BUS as a potential net C sink of ~19 Tg C yr<sup>-1</sup>, making it the strongest potential C sink among the EBUS systems.

## 7.2. IMPACTS OF CLIMATE CHANGE

The GENUS project was established to clarify the ecosystem structure of the BUS in order to provide a basis for a better understanding of how the BUS might respond to climate change.

Upwelling is driven by winds and hence primarily by atmospheric forcing. Although still a matter of debate, an increase in upwelling favourable winds is assumed in the course of climate change due to an intensification of pressure gradients between land and ocean (Bakun, 1990; Bakun et al., 2010). This is supported by regional model studies (Aquad et al., 2006; Garreaud and Falvey, 2008; Goubanova et al., 2010). However, these projections also suggest geographical differences: Under scenarios of increased atmospheric CO<sub>2</sub> concentrations, an intensification of alongshore surface winds and upwelling is predicted

for the region off Chile, whereas a decrease in alongshore wind and upwelling intensity is projected to occur off Peru (Goubanova et al., 2010; Echevin et al., 2011). With respect to the southwest African coast, a trend of increasing temperature on land has been observed (Kruger and Shongwe, 2004), but long-term trends of wind stress data are not available. The coupled general circulation models are also not useful for predictions since they suffer from a strong SST bias (e.g. Richter and Xie, 2008; Zuidema et al., 2011). However, an assumed strengthening of upwelling favourable winds without significant shifts in wind direction would result in a scenario comparable to the austral winter upwelling season. Austral winter is characterised by a well ventilated shelf and enhanced inflow of oxygenated ESACW onto the NBUS shelf (Mohrholz et al., 2008). Furthermore it is characterised by low organic matter fluxes and increased offshore advection of the biomass under increased wind stress, as suggested by the results presented in chapter III. Low POC export to the shelf, along with increased ventilation of the shelf, would lessen the frequency of anoxic events. This in turn would reduce the magnitude of +P\* (= N\* deficiency) generation in bottom water on the shelf and in the surface water and increases the N driven CO<sub>2</sub> drawdown of the biological pump in the NBUS.

The results on the variability of the carbonate saturation state imply that a further invasion of anthropogenic CO<sub>2</sub> could lower  $\Omega_A$  to corrosive levels of <1 within the SACW. This would be reflected in a further uplift of the aragonite saturation horizon to depth levels above Antarctic Intermediate Water (Chapter II). However, in case of a strengthening of upwelling favourable winds, the southward propagation of SACW on the Namibian shelf would be reduced and thus its area of influence.

## 8. PERSPECTIVES

The results presented in this thesis identify research needs that should be addressed in future studies and are briefly outlined below:

### *Processes controlling the variability of $N^*$ excess in SACW*

It was shown that SACW hosts an  $N^*$  excess, varying in magnitude, which is likely controlled by the intensity of  $N_2$  fixation at the surface and is introduced to the thermocline water by the sinking and subsequent decomposition of this organic matter. Compared to phytoplankton, the organic matter of diazotrophic cyanobacteria shows, not only high N/P, but also strongly elevated C/P ratios (Bertillon et al., 2003). These ratios tend to increase under elevated  $pCO_2$  (Barcelos e Ramos et al., 2007) and under P limitation (Sañudo-Wilhemly et al., 2001) implying a stronger C drawdown per mole P used. However,  $N_2$  fixation in the South Atlantic is primarily limited by dissolved iron (dFe) supply (Moore et al., 2009). Moreover,  $N_2$  fixation activity is suggested to also occur under nutrient replete conditions (Foster et al., 2009; Sohm et al., 2011) in the South East Atlantic. Future research on the limiting factors that control the  $N_2$  fixation in the South Atlantic should therefore concentrate on alternative sources for dFe considering, e.g. upwelling of dFe-enriched subsurface waters associated to the oxygen minimum zones in the South East Atlantic (Noble et al., 2012) and should be complemented by investigations on the accompanied variability of C/N/P ratios and  $\delta^{15}N$  ratios of the dissolved and particulate phase within SACW.

### *Contribution of dissolved inorganic matter to the TA variability*

It was shown that TA in the NBUS is highly variable. Especially in bottom waters on the shelf TA increases with increasing DIC concentrations which buffers the carbonate saturation state in upwelling waters along the NBUS coast (Chapter II). A previous study shows that also dissolved organic matter can contribute to TA increase (Kim and Lee,

2009). Our latest results show a high variability of dissolved organic carbon (DOC) in the NBUS (Rixen et al., unpublished data). Future research should therefore focus on the contribution of dissolved organic matter on the observed TA dynamics and should include pore water fluxes between the sediment-water interface.

*Drivers of organic matter export by the carbonate counter pump*

It was shown that export of organic carbon on the shelf is dominated by diatoms (Chapter III), whereas calcifying plankton dominates the POC export on the slope and further offshore (Wefer and Fischer, 1993; Giraudeau et al., 2000). Our results also suggest that the offshore carbonate counter pump is limited by the availability of N (Chapter I, IV). Linking the spatio-temporal variability of nutrients and  $\Omega$  in the surface with the abundance and distribution patterns of calcifying plankton will help to better understand the factors that drive and limit the organic carbon export by the carbonate counter pump with respect to nutritional versus carbonate saturation state preferences of calcifying plankton.

## FIGURE CAPTIONS

Fig. 1.1.: General schematic of the biological (left) and solubility pump (right) (adapted and modified from Chisholm (2000)) maintaining a DIC gradient between the atmosphere and the deep ocean.

Fig. 1.2.: Schematic overview of the the Benguela Current upwelling system located at the southwest African coast. BC, Benguela Current; ESACW, Eastern South Atlantic Central Water; NBUS, northern Benguela upwelling system; SACW, South Atlantic Central Water; SBUS, southern Benguela upwelling system. The  $\text{CaCO}_3$  content (wt %, colour coded) of the surface sediments illustrates the absence of  $\text{CaCO}_3$  deposition over the shelf.  $\text{CaCO}_3$  data provided by Inthorn et al. (2006).

Fig. 3.1.: (a) Schematic overview of the the Benguela upwelling system located at the southwest African coast. Surface currents are represented by solid und subsurface currents by dotted lines. AC, Angola Current; ABFZ, Angola Benguela Frontal Zone; AR, Agulhas Rings; BC, Benguela Current; ESACW, Eastern South Atlantic Central Water; NBUS, northern Benguela upwelling system; SACW, South Atlantic Central Water; SBUS, souhern Benguela upwelling system. (b) Stations sampled during the cruises: MSM07/2b-3 (circles), Afr258 (diamonds) and MSM17/3 (squares). The grey shading refers to the TOC content (wt %) of the surface sediments representing the diatomaceous mud belt (TOC data taken from Inthorn et al. (2006)/10.1594/PANGAEA.351146).

Fig. 3.2.:  $T_{\text{pot}}-S$  diagram of vertical water column profiles measured in the NBUS region during the MSM17/3 cruise. The  $\text{O}_2$  concentration ( $\mu\text{mol kg}^{-1}$ ) is indicated by colour shading and isopycnals ( $\text{kg m}^{-3}$ ) are given by the grey lines. The end points of Eastern South Atlantic Central Water (ESACW, open squares) and South Atlantic Central Water (SACW, open circles) specify the definition source water types given in the text. The  $T_{\text{pot}}-S$  range used to calculate their relative contribution in water samples from  $>100$  m depth is indicated by the black lines.

Fig. 3.3.: Composite of N versus P ( $\mu\text{mol kg}^{-1}$ ) data of the MSM07/2b-3 cruise (circles), Afr258 cruise (diamonds) and MSM17/3 cruise (squares). The data were separated into shelf & slope stations (<500 m bottom depth) indicated by open symbols and offshore stations (>500 m bottom depth) indicated by black filled symbols. The red filling corresponds to data points associated with  $\text{O}_2$  concentrations  $\leq 20 \mu\text{mol kg}^{-1}$ . Positive and negative deviations from the expected N/P correlation of 16/1 (black line) are expressed in  $+N^*$  and  $-N^*$  (Gruber and Sarmiento, 1997). The grey shaded area refers to the range of low N/P (LNP) defined by Tyrrell and Lucas (2002).

Fig. 3.4.: (a) AOU, (b) N, (c) P and (d)  $A_T$  versus  $C_T$  (all in  $\mu\text{mol kg}^{-1}$ ) as measured within the range of 30–500 m water depth during the MSM17/3 cruise. The data were separated into shelf stations (<500 m bottom depth, open circles) and offshore stations (>500 m bottom depth, black circles). The red filling corresponds to data points associated with  $\text{O}_2$  concentrations  $\leq 20 \mu\text{mol kg}^{-1}$ . The correlations observed for the Benguela are given and indicated by the black line. The reported ratios in panel (a) and (b) are derived by excluding the  $\leq 20 \mu\text{mol kg}^{-1}$  data. The open squares in panel (c) represent data from the mud belt region. (d) The dashed black lines indicate the expected correlation caused by aerobic mineralisation  $A_T/C = -16/106 = -0.15$  (Redfield et al., 1963) and N loss, e.g. due to denitrification  $A_T/C = 104/106 = \sim 1$  (Gruber and Sarmiento, 1997).

Fig. 3.5.: Cross-shelf transects off (a) Kunene (17.25 °S) and (b) Walvis Bay (23.0 °S) during MSM17/3 cruise showing the spatial decoupling of N and P maxima expressed in  $N^*$ . The N, P and  $N^*$  concentrations (colour shading, in  $\mu\text{mol kg}^{-1}$ ) are overlain by the  $\text{O}_2$  concentrations (contoured at  $50 \mu\text{mol kg}^{-1}$  intervals, black isolines). The area of low  $\text{O}_2$  concentration ( $\leq 20 \mu\text{mol kg}^{-1}$ ) is marked by the bold black line. The sampled stations used for gridding are indicated by black circles; areas of no data were extrapolated (kriging method).

Fig. 3.6.: Distribution of sea surface temperature (SST) (contoured at  $1^\circ\text{C}$  intervals) at 5 m depth continuously measured along the cruise track during (a) MSM07/2b-3, (b) Afr258

and (c) MSM17/3. Sampled stations (black circles) and cruise track (black line) were used for gridding; areas of no data were extrapolated (kriging method).

Fig. 3.7.: (a-c) Distribution of  $O_2$  ( $\mu\text{mol kg}^{-1}$ ) and (d-f) contribution of SACW and ESACW (%) at 200 m water depth. Note: shelf stations with bottom depths shallower than 200 m were included in the  $O_2$  interpolation and stations with deeper than 100 m were included in the SACW interpolation. The sampled stations used for gridding are marked by black circles; areas of no data were extrapolated (kriging method). 0% SACW is equivalent to 100% ESACW.

Fig. 3.8.: Distribution of  $N^*$  ( $\mu\text{mol kg}^{-1}$ ) (a-c) at 200 m and (d-e) at 5 m water depth (contoured at  $5 \mu\text{mol kg}^{-1}$  intervals). Note: shelf stations with bottom depths shallower than 200 m were included in the  $N^*$  interpolation. The sampled stations used for gridding are marked by black circles; areas of no data were extrapolated (kriging method).

Fig. 3.9.: Vertical profiles of SACW (%),  $O_2$ ,  $N^*$ , P and N (all in  $\mu\text{mol kg}^{-1}$ ) during (a) MSM07/2b-3, (b) Afr258 and (c) MSM17/3 at offshore stations with comparable location offshore of Kunene ( $17.25^\circ\text{S}$ ). The contribution of SACW is indicated by the grey shading.

Fig. 3.10.: Averaged  $P^*$  ( $\mu\text{mol kg}^{-1}$ ) of the euphotic zone (0-20 m) versus distance to the coast (km) during MSM07/2b-3 (black circles), Afr258 (open circles) and MSM17/3 (grey circles) along the Walvis Bay transect ( $23^\circ\text{S}$ ).

Fig. 3.11.: Map of the wind driven large scale circulation (upper 100 m) of the South Atlantic Ocean (adapted from Stramma and England (1999)). The map illustrates the hypothetical advection of  $+P^*$  (red dashed line) via SEC and SECC towards the Angola Gyre where it fuels  $N_2$  fixation and in turn results in  $+N^*$  (blue dashed line) that is introduced to the NBUS. AC, Agulhas Current; BC, Benguela Current; BrC, Brazil Current; CSEC, Central South Equatorial Current; NBrC; North Brazil Current; SAC,

South Atlantic Current; SEC, South Equatorial Current; SECC, South Equatorial Countercurrent; SEUC, South Equatorial Undercurrent.

Fig. 4.1.: Schematic map of the northern Benguela upwelling system (NBUS) off southwest Africa. The  $\text{CaCO}_3$  content (wt %) of surface sediments is indicated by colour shading emphasising the low  $\text{CaCO}_3$  content close to the coast. The stations sampled along transects are indicated by black dots. The open circles, squares, and diamonds denote the stations presented in Fig. 4.4..  $\text{CaCO}_3$  data were obtained from Inthorn et al. (2006). Areas of no data were extrapolated (kriging method).

Fig. 4.2.: Comparison of carbonate system parameters measured in the South Atlantic (SA) and the northern Benguela upwelling system (NBUS) between 0-3000 m depth. (a)  $\text{O}_2$  versus DIC (both in  $\mu\text{mol kg}^{-1}$ ), (b)  $\Omega_C$  and  $\Omega_A$  versus depth, (c)  $\Omega_C$  and  $\Omega_A$  versus DIC ( $\mu\text{mol kg}^{-1}$ ), and (d)  $\Omega_C$  and  $\Omega_A$  versus  $\text{TA}_{35}$  ( $\mu\text{mol kg}^{-1}$ ) measured in the South Atlantic (SA) (grey circles), and the NBUS water column (black circles), and supernatant water of sediment cores (red circles). The SA dataset consists of WOCE Atlantic Ocean sections provided by [cdiac.ornl.gov/oceans/atlantic\\_ODV.html](http://cdiac.ornl.gov/oceans/atlantic_ODV.html) and was filtered for a latitudinal range of 0–40 °S and a depth range of 0-3000 m water depth. The  $\Omega_C$  and  $\Omega_A$  were calculated with CO2SYS programme (Pierrot et al., 2006), and are given for in situ salinity, temperature, and pressure conditions.

Fig. 4.3.: Composite of DIC versus  $\text{TA}_{35}$  (both in  $\mu\text{mol kg}^{-1}$ ) measured in water column samples (black circles, MSM17/3 in 2011), supernatant water of sediment cores (red circles MSM17/3 in 2011) and coastal surface water (Swakopmund time series, blue circles, 2010) of the NBUS. The black dotted lines show  $\Omega_C$  at constant temperature of 15 °C and salinity of 35. The arrows indicate the impact of biogeochemical processes on DIC and  $\text{TA}_{35}$  according to the stoichiometry given in the text.

Fig. 4.4.: Differences of  $\text{TA}_{35}$  production between offshore (a-d) and shelf sites (e-h). Vertical profiles of DIC,  $\text{O}_2$  (both in  $\mu\text{mol kg}^{-1}$ ),  $\Omega_A$  and  $\Omega_C$  are shown. The grey circles, grey squares, and open diamonds denote the location of the stations (refer to Fig. 4.1.). (d,

h) The  $TA_{35}/DIC$  plot involves the supernatant water samples of sediment cores obtained at the respective stations (red edged). (f)  $O_2$  profile for the 26 °S station is not available.

Fig. 4.5.: Vertical distribution of (a)  $\Omega_{A\_obs}$  and (b)  $\Omega_{A\_theor}$  (colour shading) in the water column off Walvis Bay (23 °S); the saturation horizon  $\Omega_A = 1$  is indicated by the black dotted line. The  $\Omega_{A\_obs}$  was calculated for in situ conditions on the basis of observed DIC and  $TA_{35}$  concentrations. The  $\Omega_{A\_theor}$  was calculated for in situ conditions on the basis of observed DIC concentrations. On the basis of the vertical DIC increase the expected rise of nitrate and phosphate, and hence drop of  $TA_{35}$ , was calculated according to Redfield stoichiometry ( $TA/DIC = -17/106$ ).

Fig. 4.6.: Swakopmund time series of coastal surface water. (a) SST (°C), (b)  $TA_{35}$ , (c) DIC (both in  $\mu\text{mol kg}^{-1}$ ), (d)  $pCO_2$  ( $\mu\text{atm}$ ), and (e)  $\Omega_C$  and  $\Omega_A$  in surface water sampled between February and May 2010. The black arrows indicate two main upwelling events with SST <15 °C.

Fig. 5.1.: Study area. The Benguela Current (BC, black line) and locations of our oceanographic (23.0 °S, 14.04 °E) and the sediment trap mooring (23.0 °S, 14.05 °E) our study site (red cross) at a water depth of 140 m. The sediment trap mooring was equipped cylindrical Hydro-Bios sediment trap (MST 12) at a water depth of 70 m. Sampling interval was 21 days during first (December 2009-September 2010) and 12 days during the second deployment period (October 2010-February 2011). The deployed Seabird MircoCat recorded seawater temperature and salinity with a sampling interval of ten minutes at a water depth of 128 m. The oceanographic and the meteorological data presented in Fig. 5.2. were converted into three-weekly means in order to link it to the sediment trap data. Sample and data processing is described in Haake et al. (1993) and Mohrholz et al. (2008). The contribution of lithogenic matter (wt %) in surface sediments (Inthorn et al., 2006) is indicated by colour shading. The position of previous sediment traps sites in the BUS region is marked by filled asterisk (Wefer and Fischer, 1993) and filled diamond (Giraudeau et al., 2000).

Fig. 5.2.: Mooring data. Lithogenic matter fluxes and the C/N ratio measured in the trapped material during the period of observation (a). Sea water temperatures measured by the CTD and the alongshore wind stress ( $\tau$ ). The wind speeds and wind directions used to calculate  $\tau$  were measured at the weather station at the National Marine Information and Research Center (NatMIRC) in Swakopmund that is roughly 62 km away from the mooring site. (b) The fraction of SACW (%) calculated from sea water temperature and the salinity measured at 128 m water depth (Mohrholz et al., 2008),  $\text{PO}_4$  concentration inferred from mixing of SACW and ESACW and the  $\text{C}_{\text{org}}$  flux ( $\text{mg m}^{-2}\text{d}^{-1}$ ) as measured with the sediment trap.

Fig. 6.1.: Organic carbon pump. (a) Schematic view of  $\text{PO}_4^0$  formation by the combination of upwelling at the Antarctic Divergence and subduction of Antarctic Surface Water north of the Antarctic Polar Front (Sarmiento et al., 2004). On its way into the BUS it mixes with SACW that was enriched with regenerated phosphate (indicated by the lighter grey) during its passage through the tropics and subtropics. Excess P that remained unused in the upwelling system is carried into the oligotrophic open ocean where it favours  $\text{N}_2$ -fixation and its export by diazotrophic organisms revealing C/P ratios  $>200$ . (b) An increased productivity and a reduced mode water formation lower the  $\text{PO}_4^0$  formation and the associated  $\text{CO}_2$  release at higher latitudes. Upwelling on the other hand continues to take up  $\text{CO}_2$  by converting  $\text{PO}_4^0$  into  $\text{PO}_4$  in the course of which its reservoir size in the sub-thermocline water shrinks at the expense of expanding OMZs. The declining reservoir size is indicated by the lighter grey and the expanding OMZ by the darker blue.

Fig. 6.2.:  $\text{pCO}_2$  along the southwest African continental margin and the global distribution of the  $\text{PO}_4^0$ . (a)  $\text{pCO}_2$  measured and gridded on  $0.25^\circ$  grid along the cruise tracks (grey lines) and the volunteer observing ship (VOS) lines obtained from Takahashi et al. (2009) (black lines). The VOS data were normalised to the year 2010 by assuming a mean annual increase of  $1.84 \text{ ppm yr}^{-1}$  as seen in the Mauna Loa  $\text{pCO}_2$  data between 1990 and 2013. The Mauna Loa data were obtained from: <http://www.esrl.noaa.gov/gmd/ccgg/trends/mlo.html>. (b) The map shows the interpolated mean  $\text{pCO}_2$  of the entire region. The black line represents a  $\text{pCO}_2$  of 389 and 600  $\mu\text{atm}$ . (c) The mean fugacity of  $\text{CO}_2$  ( $f\text{CO}_2$ ) measured

during all cruises in the ocean (bold red line) and the atmosphere (bold red broken line). The red thin broken line shows the CO<sub>2</sub> concentrations. All data were averaged by 1° x 1° for each cruise and subsequently within latitudinal bands. The arrows show the air-sea CO<sub>2</sub> flux estimates from the Angolan margin (8-16 °S), the NBUS (16-26.6 °S) and the SBUS (26.6-34 °S) whereby the negative values indicate a CO<sub>2</sub> flux from the atmosphere into the ocean (Tab. 6.1.). The water depth was obtained from the ETOPO1 data (<http://www.ngdc.noaa.gov/mgg/global/global.html>). (CT = Cape Town). (d) The fraction of PO<sub>4</sub><sup>0</sup> derived from the World Ocean Atlas 2009 (Garcia et al., 2010) at a water depth of 200 m. The bold line indicates a PO<sub>4</sub><sup>0</sup> of 60 %. The white area in the Sargasso Sea (western Atlantic Ocean) is caused by the fact that the calculated regenerated PO<sub>4</sub> exceeds the total phosphate concentrations. This suggests that the O<sub>2</sub>/P ratio of 175 is too low which might be caused by the high C/P ratio of N<sub>2</sub> fixing bacteria.

Fig. 6.3.: (a) Wind speeds measured on board the research vessels smoothed with a 30 minute moving average (red) versus Julian days. The broken blue line indicates the mean wind speed (WS) of 7.2 m s<sup>-1</sup> obtained from QuickSCAT between 1999 and 2008 along the Namibian and South African coast (Chavez and Messié, 2009). (b) xCO<sub>2</sub> and pCO<sub>2</sub> (only during the RV Meteor cruise) measured in the surface water (black) and the atmosphere (red) averaged minute by minute. Data gaps between the atmospheric data were filled by interpolating linearly between the measured data (red line). The broken red line indicates the mean atmospheric xCO<sub>2</sub> at Mauna Loa in May/June 2008 (388.2 ppm, compare Fig. 6.5.). (c) Sea surface temperatures (SST) measured by the thermosalinograph and the Ferrybox system in May 2008. The black line in the SST plot and the blue line in the WS and xCO<sub>2</sub> plot indicate data obtained from the cruise MSM19/1b.

Fig. 6.4.: pCO<sub>2</sub> measured by the underwater carbon dioxide sensor (PSI CO<sub>2</sub>-Pro) which was integrated into a Ferrybox system (developed at GKSS, Geesthacht, Germany) versus the pCO<sub>2</sub> measured with SUNDANS (developed by Ludger Mintrop; MARIANDA, Germany, [www.marianda.com](http://www.marianda.com)) during the RV Africana cruise. The resulting regression

equation was used to calibrate the  $p\text{CO}_2$  data measured of the RV Meteor M67/2 cruise during which only the Ferrybox was on board.

Fig. 6.5.:  $\text{CO}_2$  concentrations measured at the Mauna Loa Observatory, Hawaii (grey line) at the Namibian Training and Research Center Gobabeb (blue line) and during the cruises with RV M.S. Merian, RV Meteor, RV Africana, RV Discovery in 2008, 2009, 2010 and 2011 (red circles). The standard deviations are indicated by the error bars and the black circle indicates an  $x\text{CO}_2$  of 388.2 ppm which was used to calculate the  $\Delta f\text{CO}_2$  during the RV Meteor cruise in May 2008. The data from the Namibian Training and Research Center in Gobabeb and from the Mauna Loa Observatory were obtained from the NOAA CMDL Carbon Cycle Cooperative Global Air Sampling Network. The low  $p\text{CO}_2$  measured during the cruise MSM17/3 seem to indicate the influence of the  $\text{CO}_2$ -poor air mass which often develops during this time of the year over the southern part of tropical Africa (Buchwitz et al., 2005; Warneke et al., 2005).

Fig. 7.1.: The composite illustrates the NBUS shifting between two states in regional scale nutrient cycling acting as (1) *balanced N & P source* and as (2) *P\* source* mediated by a negative feedback mechanism that is driven by the extent of  $\text{N}^*$  deficiency exported to the South Atlantic. (a) High contribution of SACW favours  $\text{O}_2$  depletion down to anoxic conditions in bottom water on the shelf. This results in elevated  $\text{P}^*$  excess (red arrow) which is exported offshore to the South Atlantic and Angola Gyre where it fuels  $\text{N}_2$  fixation (b) if dissolved iron (dFe) is available in the surface water. The sinking and subsequent remineralisation of this  $\text{N}_2$ -fixed organic matter is reflected in  $\text{N}^*$  excess of subsurface waters (blue arrow) that (c) is transported to the NBUS (blue shaded area) where it replenishes the  $\text{N}^*$  deficiency on the shelf. Thereby the system is shifted towards a more balanced N & P export (black arrow). (d) This is reflected in less  $\text{N}^*$  excess import from the Angola Gyre (blue arrow).

Fig. 7.2.: Composite illustrating the functioning of the biological pump off Walvis Bay (23 °S). (a) Average  $\Omega_{\text{C}(\text{fCO}_2, \text{DIC})}$  (Flohr et al., unpublished data), average (b)  $\text{Si}(\text{OH})_4$  and (c)

P\* concentrations (all in  $\mu\text{mol kg}^{-1}$ ) (Chapter I; van der Plas et al., unpublished data) in the surface at 10 m water depth. Composition of the particle fluxes (%) measured on the slope (Giraudeau et al., 2000), and on the shelf (Chapter III); positions of the sediment traps are indicated by the arrows. (e) The TOC and  $\text{CaCO}_3$  (both wt %) of the surface sediment along the 23 °S transect (Inthorn et al., 2006). The triangles on the bottom of the composite illustrate the trend of increasing PIC export with increasing distance from the coast.

Fig. 7.3.: Composite of carbon pump parameters on the NBUS shelf derived from [1] average phytoplankton productivity off Walvis Bay in summer and winter (Barlow et al., 2009), [2] mean POC and PIC flux from the sediment trap study (Chapter III), [3] accumulation rates estimated for the mud belt region (Meisel et al., 2011b), [4] average  $\text{CO}_2$  flux of the NBUS (Chapter IV) and [5] DIC increase along isopycnal surfaces towards the coast between two stations close to the mooring station (Chapter I; Flohr et al., unpublished data) assuming a residence time of water of 80 days applied by Nagel et al. (2013).

## TABLE CAPTIONS

Table 4.1.: Selection of surface samples of the Swakopmund time series illustrating the impact of increasing  $TA_{35}$  on  $pCO_2$ . The reference station is the coastal most station of the 23 °S transect sampled in 02/2011 (MSM17/3) and closest to Swakopmund. Given  $pCO_2$  values refer to surface (1 bar) at 15 °C.

Table 5.1.: Sampling periods and results of particle fluxes ( $mg\ m^{-2}\ d^{-1}$ ) are listed. The flux calculations refer to the <1 mm size fraction. Columns marked with \* indicate that the amount of sample was insufficient for further analysis. Cup no. 3 was lost during operation and n.d. means non-detectable. Trap position: 23.0 °S, 14.05 °E, trap depth: 70 m, bottom depth: 140 m.

Table 6.1.: Characteristics of major upwelling systems: Area and duration of upwelling, N/P ratios and the contribution of  $PO_4^0$  to the total  $PO_4$  from subsurface water, Ekman transport and pumping as well as nutrient concentrations within the subsurface water that is injected by Ekman transport and pumping into the surface layer. The Redfield C/N/P ratio of 106/16/1 was used to convert nutrient into carbon fluxes. The area of the upwelling regions was derived from the ETOP1 data set, the width, the transport rates, and the nitrate concentration were obtained from (Messié et al., 2009). Data from the Arabian Sea were taken from (Rixen et al., 2000; Rixen et al., 2006). The Arabian Sea upwelling occurs only for four month during the SW monsoon season. The  $CO_2$  flux from the California and the Peruvian upwelling system were obtained from (Friederich et al., 2002; Friederich et al., 2008) whereas the fluxes from the non El Niño years were chosen for the California upwelling system. The  $CO_2$  fluxes from off Mauretania were estimated based on the data presented in (Steinhoff et al., 2012). The contribution of  $PO_4^0$  to the total  $PO_4$  and the N/P ratio were obtained from the (Garcia et al., 2010) at water depths between 75 and 200 m. CUS, California upwelling system; PUS, Peruvian upwelling system; MUS, Mauretanian upwelling system; SBUS, Southern Benguela upwelling system; NBUS, Northern Benguela upwelling system; ASUS; Arabian Sea upwelling system.

Table 6.2.: Cruise details; WB-Walvis Bay, CT-Cape Town.

Table 6.3.: Cruise summary, cruise I.D. and period as well as the mean pCO<sub>2</sub>, SST's, wind speed and direction within the coastal region off Angola, the N- and SBUS. (n.d. - not determined).

Table 6.4.: Subsurface water masses. Properties of the SACW and ESACW (Mohrholz et al., 2008) as well as the PO<sub>4</sub><sup>0</sup> concentration derived from the equation (1) and the contribution of PO<sub>4</sub><sup>0</sup> to the total PO<sub>4</sub> concentration.

## REFERENCES

- Anderson, L. A., and Sarmiento, J. L.: Redfield ratios of remineralization determined by nutrient data analysis, *Global Biogeochemical Cycles*, 8, 65-80, 1994.
- Arrigo, K. R.: Marine microorganisms and global nutrient cycles, *Nature*, 437, 349 - 355, doi:10.1038/nature04158 2005.
- Auad, G., Miller, A., and Di Lorenzo, E.: Long-term forecast of oceanic conditions off California and their biological implications, *Journal of Geophysical Research*, 111, 10.1029/2005JC003219, 2006.
- Bailey, G. W., and Chapman, P.: Short-term variability during an anchor study in the southern Benguela upwelling system: Chemical and physical oceanography, *Progress in Oceanography* 28, 9-37, 1991.
- Baker, A. R., C. Adams, T. G. Bell, Jickells, T. D., and Ganzeveld, L.: Estimation of atmospheric nutrient inputs to the Atlantic Ocean from 50°N to 50°S based on large-scale field sampling: Iron and other dust-associated elements, *Global Biogeochemical Cycles*, 27, 10.1002/gbc.20062., 2013.
- Bakun, A.: Global climate change and intensification of coastal ocean upwelling, *Science*, 247, 1990.
- Bakun, A., Field, D. B., Rodriguez, A. R., and Weeks, S. J.: Greenhouse gas, upwelling-favorable winds, and the future of coastal ocean upwelling ecosystems, *Global Change Biology*, 16, 1213-1228, 2010.
- Barcelos e Ramos, J., GBiswas, H., Schulz, K. G., LaRoche, J., and Riebesell, U.: Effect of rising atmospheric carbon dioxide on the marine nitrogen fixer *Trichodesmium*, *Global Biogeochemical Cycles*, 21, 1-6, 10.1029/2006GB002898, 2007.
- Barker, S., and Elderfield, H.: Foraminiferal calcification response of glacial-interglacial changes in atmospheric CO<sub>2</sub>, *Science*, 297, 833-836, 2002.
- Barlow, R., Louw, D., Balarin, M., and Alheit, J.: Pigment signatures of phytoplankton composition in the northern Benguela ecosystem during spring, *African Journal of Marine Science*, 28, 479-491, 2006.
- Barlow, R., Lamont, T., Mitchell-Innes, B., Lucas, M., and Thomalla, S.: Primary production in the Benguela ecosystem, 1999-2002, *African Journal of Marine Science*, 31, 97-101, 10.2989/AJMS.2009.31.1.9.780, 2009.
- Beaufort, L., Probert, I., de Garidel-Thoron, T., Bendif, E. M., Ruiz-Pino, D., et al.: Sensitivity of coccolithophores to carbonate chemistry and ocean acidification, *Nature*, 476, 80-83, 10.1038/nature10295, 2011.
- Bednarsek, N., Tarling, G. A., Bakker, D. C. E., Fielding, S., Jones, E. M., et al.: Extensive dissolution of live pteropods in the Southern Ocean, *Nature Geoscience*, 5, 881-885, 10.1038/ngeo1635, 2012.
- Behrenfeld, M. J., and Falkowski, P.: Photosynthetic rates derived from satellite-based chlorophyll concentration, *Limnology and Oceanography*, 42, 1-20, 1997.
- Behrenfeld, M. J., O'Malley, R. T., Siegel, D. A., McClain, C. R., Sarmiento, J. L., et al.: Climate-driven trends in contemporary ocean productivity, *Nature*, 444, 752-755, 10.1038/nature05317, 2006a.

- Behrenfeld, M. J., Worthington, K., Sherrell, R., Chavez, F. P., Strutton, P., et al.: Controls on tropical Pacific Ocean productivity revealed through nutrient stress analysis, *Nature*, 442, 1025-1028, 10.1038/nature05083, 2006b.
- Berelson, W. M., Balch, W. M., Najjar, R., Feely, R. A., Sabine, C., et al.: Relating estimates of CaCO<sub>3</sub> production, export, and dissolution in the water column to measurements of CaCO<sub>3</sub> rain into sediment traps and dissolution on the sea floor: A revised global carbonate budget, *Global Biogeochemical Cycles*, 21, 1-15, 10.1029/2006GB002803, 2007.
- Bertillon, S., Berglund, O., Karl, D. M., and Chisholm, S. W.: Elemental composition of marine *Prochlorococcus* and *Synechococcus*: Implications for the ecological stoichiometry of the sea, *Limnology and Oceanography*, 48, 1721-1731, 2003.
- Bijma, J., Hönisch, B., and Zeebe, R. E.: Impact of the ocean carbonate chemistry on living foraminiferal shell weight: Comment on “Carbonate ion concentration in glacial-age deep waters of the Caribbean Sea” by W. S. Broecker and E. Clark, *Geochemistry, Geophysics, Geosystems*, 3, 10.1029/2002GC000388, 2002.
- Boeckel, B., and Baumann, K.-H.: Distribution of coccoliths in surface sediments of the south-eastern South Atlantic Ocean: ecology, preservation and carbonate contribution, *Marine Micropaleontology*, 51, 301-320, 10.1016/j.marmicro.2004.01.001, 2004.
- Boehme, S. E., Sabine, C. L., and Reimers, C. E.: CO<sub>2</sub> fluxes from a coastal transect: a time-series approach *Marine Chemistry*, 63, 49-67, 1998.
- Bograd, S. J., Castro, C. G., Di Lorenzo, E., Palacios, D. M., Bailey, H., et al.: Oxygen declines and the shoaling of the hypoxic boundary in the California Current, *Geophysical Research Letters*, 35, 10.1016/S0967-0645(01)00094-7, 2008.
- Bopp, L., Monfray, P., Aumont, O., Dufresne, J.-L., Le Treut, H., et al.: Potential impact of climate change on marine export production, *Global Biogeochemical Cycles*, 15, 81-99, 2001.
- Bowie, A. R., Whitworth, D. J., Achterberg, E. P., Fauzi, R., Mantoura, C., et al.: Biogeochemistry of Fe and other trace elements (Al, Co, Ni) in the upper Atlantic, *Deep-Sea Research I*, 49, 605-636, 2002.
- Boyd, P. W., Watson, A. J., Law, C. S., Abraham, E. R., Trull, T., et al.: A mesoscale phytoplankton bloom in the polar Southern Ocean stimulated by iron fertilization, *Nature*, 407, 695 - 702, 10.1038/350375500, 2000.
- Brea, S., Alvarez-Salgado, X. A., Alvarez, M., Pérez, F. F., Mémery, L., et al.: Nutrient mineralization rates and ratios in the eastern South Atlantic, *Journal of Geophysical Research*, 109, 1-15, 10.1029/2003JC002051, 2004.
- Bremner, J. M.: Concretionary phosphorite from SW Africa, *The Geological Society*, 137, 773-786, 1980.
- Bremner, J. M.: Sediments on the continental margin off South West Africa between latitudes 17° and 25° S, PhD Thesis, University of Cape Town, 300 pp., 1981.
- Bremner, J. M., and Willis, J. P.: Mineralogy and geochemistry of the clay fraction of sediments from the Namibian continental margin and the adjacent hinterland, *Marine Geology*, 115, 85-116, 1993.
- Broecker, W., Takahashi, T., and Takahashi, T.: Sources and Flow Patterns of Deep-Ocean Waters as Deduced From Potential Temperature, Salinity, and Initial Phosphate Concentration, *Journal of Geophysical Research*, 90, 6925-6939, 1985.

- Broecker, W. S.: Glacial to interglacial changes in ocean chemistry, *Progress in Oceanography*, 2, 151-197, 1982.
- Broecker, W. S., and Peng, T. H.: *Tracers in the sea*, 1982.
- Broecker, W. S., and Takahashi, T.: Sources and flow patterns of deep-ocean waters as deduced from potential temperature, salinity, and initial phosphate concentration, *Journal of Geophysical Research*, 90, 6925-6939, 1985.
- Brüchert, V., Jorgensen, B. B., Neumann, K., Riechmann, D., Schlösser, M., et al.: Regulation of bacterial sulfate reduction and hydrogen sulfide fluxes in the central Namibian coastal upwelling zone, *Geochimica et Cosmochimica Acta*, 67, 4505-4518, 2003.
- Bruland, K. W., Rue, L. E., Smith, G. J., and DiTullio, G. R.: Iron, macronutrients and diatom blooms in the Peru upwelling, *Marine Chemistry*, 93, 81-103, 10.1016/j.marchem.2004.06.011, 2005.
- Buchwitz, M., de Beek, R., Burrows, J. P., Bovensmann, H., Warneke, T., et al.: Atmospheric methane and carbon dioxide from SCIAMACHY satellite data: initial comparison with chemistry and transport models, *Atmos. Chem. Phys.*, 5, 941-962, 10.5194/acp-5-941-2005, 2005.
- Caldeira, K., and Wickett, M., E.: Anthropogenic carbon and ocean pH, *Nature*, 425, 2003.
- Capone, D. G., Burns, J. A., Montoya, J. P., Subramaniam, A., Mahaffey, C., et al.: Nitrogen fixation by *Trichodesmium* spp.: An important source of new nitrogen to the tropical and subtropical North Atlantic Ocean, *Global Biogeochemical Cycles*, 19, 1-17, 2005.
- Capone, D. G., and Hutchins, D. A.: Microbial biogeochemistry of coastal upwelling regimes in a changing ocean, *Nature Geoscience*, 6, 10.1038/NGEO1916, 2013.
- Carpenter, E. J.: Nitrogen fixation by marine Oscillatoria (*Trichodesmium*) in the world's oceans, in: *Nitrogen in the Marine Environment*, edited by: Carpenter, E. J., and Capone, D. G., Academic Press, New York, 65-103, 1983.
- Carr, M.-E.: Estimation of potential productivity in Eastern Boundary Currents using remote sensing, *Deep-Sea Research II*, 49 (2002), 59-80 2002.
- Carr, M.-E., and Kearns, E. J.: Production regimes in four Eastern Boundary Current systems, *Deep-Sea Research II* 50, 3199-3221, 2003.
- Carr, M.-E., Friedrichs, M. A. M., Schmeltz, M., Aita, M. N., Antoine, D., et al.: A comparison of global estimates of marine primary production from ocean color, *Deep-Sea Research II*, 53, 741-770, 2006.
- Chase, Z., Johnson, K. S., Elrod, V. A., Plant, J. N., Fitzwater, S. E., et al.: Manganese and iron distributions off central California influenced by upwelling and shelf width, *Marine Chemistry*, 95, 235-254, 10.1016/j.marchem.2004.09.006, 2005.
- Chavez, F. P., and Messié, M.: A comparison of Eastern Boundary Upwelling Ecosystems, *Progress in Oceanography*, 83, 80-96, 10.1016/j.pocean.2009.07.032, 2009.
- Chavez, F. P., and Toggweiler, J. R.: Physical estimates of global new production: The upwelling contribution, in: *Upwelling in the ocean, modern processes and ancient records*, edited by: Summerhayes, C. P., Emeis, K.-C., Angel, M. V., Smith, R. L., and Zeitschel, B., Chichester, Wiley & Sons, 313-320, 1995.
- Chen, C.-T. A.: Shelf-vs. dissolution-generated alkalinity above the chemical lysocline, *Deep-Sea Research II*, 49, 5365-5375, 2002.

- Chen, C.-T. A., and Borges, A. V.: Reconciling opposing views on carbon cycling in the coastal ocean: Continental shelves as sinks and near-shore ecosystems as sources of atmospheric CO<sub>2</sub>, *Deep Sea Research II*, 56, 578-590, 2009.
- Chester, R., Elderfield, H., Griffin, J. J., Johnson, L. R., and Padgham, R. C.: Eoalial dust along the eastern margins of the Atlantic Ocean, *Marine Geology*, 13, 91-105, 1972.
- Chisholm, S. W.: Stirring times in the Southern Ocean, *Nature*, 407, 685-687, 2000.
- Chung, S.-N., Lee, K., Feely, R. A., Sabine, C. L., Millero, F. J., et al.: Calcium carbonate budget in the Atlantic Ocean based on watercolumn inorganic carbon chemistry, *Global Biogeochemical Cycles*, 17, 2003.
- Codispoti, L. A., Brandes, J. A., Christensen, J. P., Devol, A. H., Naqvi, S. W. A., et al.: The oceanic fixed nitrogen and nitrous oxide budgets: Moving targets as we enter the anthropocene?, *Scientia Marina*, 65, 85-105, 2001.
- del Giorgio, P. A., and Duarte, C. M.: Respiration in the upper ocean, *Nature*, 420, 379-384, 2002.
- Deutsch, C., Sarmiento, J. L., Sigman, D. M., Gruber, N., and Dunne, J. P.: Spatial coupling of nitrogen inputs and losses in the ocean, *Nature*, 445, doi:10.1038/nature05392, 2007.
- Devol, A. H.: Direct measurement of nitrogen gas fluxes from continental shelf sediments, *Nature*, 349, 319-321, 1991.
- Di Lorenzo, E., Miller, A. J., Shneider, N., and McWilliams, J. C.: The warming of the California Current System: dynamics and ecosystem implications, *Journal of Physical Oceanography*, 35, 336-362, 2005.
- Dickson, A. G.: An exact definition of total alkalinity and a procedure for the estimation of alkalinity and total inorganic carbon from titration data, *Deep-Sea Research*, 28 A, 1981.
- Dickson, A. G., Sabine, C. L., and Christian, J. R.: Guide to the best practices for ocean CO<sub>2</sub> measurements, *PICES Special Publication 3*, edited by: Dickson, A. G., Sabine, C. L., and Christian, J. R., UNESCO, 191 pp., 2007.
- Dittmar, T., and Birkicht, M.: Regeneration of nutrients in the northern Benguela Upwelling and the Angola-Benguela Front Areas *South African Journal of Science*, 97, 239-246, 2001.
- Doney, S. C., Fabry, V. J., Feely, R., and Kleypas, J. A.: Ocean Acidification: The Other CO<sub>2</sub> Problem, *Annu. Rev. Mar. Sci.*, 1, 169-192, 10.1146/annurev.marine.010908.163834, 2009.
- Doney, S. C., Ruckelshaus, M., Duffy, J. E., Barry, J. P., Chan, F., et al.: Climate Change Impacts on Marine Ecosystems, *Annu. Rev. Mar. Sci.*, 4, 11-37, 2012.
- Duce, R. A., LaRoche, J., Altieri, K., Arrigo, K. R., Baker, A. R., et al.: Impacts of Atmospheric Anthropogenic Nitrogen on the Open Ocean, *Science*, 893, 10.1126/science.1150369, 2008.
- Duncombe Rae, C. M.: A demonstration of the hydrographic partition of the Benguela upwelling ecosystem at 26°40'S, *African Journal of Marine Science*, 27, 617-628, 2005.
- Dunne, J., Sarmiento, J. L., and Gnanadesikan, A.: A synthesis of global particle export from the surface ocean and cycling through the ocean interior and on the seafloor, *Global Biogeochemical Cycles*, 21, 1-16, 10.1029/2006GB002907, 2007.

- Echevin, V., Goubanova, K., Belmadani, A., and Dewitte, B.: Sensitivity of the Humboldt Current system to global warming: a downscaling experiment of the IPSL-CM4 model, *Climate Dynamics*, 10.1007/s00382-011-1085-2, 2011.
- Eckardt, F. D., and Kuring, N.: SeaWiFS identifies dust sources in the Namib Desert, *International Journal of Remote Sensing*, 26, 4159–4167, 2005.
- Ekau, W., Auel, H., Pörtner, H.-O., and Gilbert, D.: Impacts of hypoxia on the structure and processes in pelagic communities (zooplankton, macroplankton and fish), *Biogeosciences*, 7, 1669-1699, 10.5194/bg-7-1669-2010, 2010.
- Emeis, K.-C., Brüchert, V., Curriec, B., Endler, R., Ferdelman, T., et al.: Shallow gas in shelf sediments of the Namibian coastal upwelling ecosystem, *Continental Shelf Research*, 24, 627-642, 2004.
- Eppley, R. W., and Peterson, B. J.: Particulate organic matter flux and planktonic new production in the deep ocean, *Nature*, 282, 1979.
- Falkowski, P., Scholes, R. J., Boyle, E., Canadell, J., Canadel, D., et al.: The Global Carbon Cycle: A Test of Our Knowledge of Earth as a System, *Science*, 290, 291-296, 2000.
- Falkowski, P. G.: Evolution of the nitrogen cycle and its influence on the biological sequestration of CO<sub>2</sub> in the ocean, *Nature*, 387, 272-275, 1997.
- Fassbender, J. A., Sabine, C. L., Feely, R. A., Langdon, C., and Mordy, C. W.: Inorganic carbon dynamics during northern California coastal upwelling, *Continental Shelf Research*, 31, 1180-1192, 10.1016/j.csr.2011.04.006, 2011.
- Feely, R., Sabine, C. L., Lee, K., Millero, F. J., Lamb, M. F., et al.: In situ calcium carbonate dissolution in the Pacific Ocean, *Global Biogeochemical Cycles*, 16, 91/91-91/12, 10.1029/2002/GB001866, 2002.
- Feely, R., Sabine, C., Lee, K., Berelson, W., Kleypas, J., et al.: Impact of Anthropogenic CO<sub>2</sub> on the CaCO<sub>3</sub> System in the Oceans, *Science*, 305, 362-366, 2004.
- Feely, R., Sabine, C. L., Hernandez-Ayon, J. M., Ianson, D., and Hales, B.: Evidence of upwelling of corrosive "acidified" water onto the continental shelf, *Science*, 320, 10.1126/science.1155676, 2008.
- Fischer, G., Ratmeyer, V., and Wefer, G.: Organic carbon fluxes in the Atlantic and the Southern Ocean: relationship to primary production compiled from satellite radiometer data, *Deep-Sea Research II*, 47, 1961 - 1997, 2000.
- Flohr, A., van der Plas, A. K., Emeis, K.-C., Mohrholz, V., and Rixen, T.: Spatio-temporal patterns of C : N : P ratios in the northern Benguela upwelling system, *Biogeosciences*, 11, 885-897, 10.5194/bg-11-885-2014, 2014.
- Föllmi, K. B.: The phosphorus cycle, phosphogenesis and marine phosphate-rich deposits, *Earth-Science Reviews*, 40, 55-124, 1996.
- Foster, R. A., Subramaniam, A., and Zehr, J. P.: Distribution and activity of diazotrophs in the Eastern Equatorial Atlantic, *Environmental Microbiology*, 11, 741-750, 10.1111/j.1462-2920.2008.01796.x, 2009.
- Friederich, G. E., Walz, P. M., Burczynski, M. G., and Chavet, F. P.: Inorganic carbon in the central California upwelling system during the 1997-1999 El Niño-La Niña event, *Progress in Oceanography*, 54, 185-203, 2002.
- Friederich, G. E., Ledesma, J., Ulloa, O., and Chavez, F. P.: Air-sea carbon dioxide fluxes in the coastal southeastern tropical Pacific. *Progress in Oceanography* 79: 156-166, *Progress in Oceanography*, 79, 156-166, 2008.

- Füssel, J., Lam, P., Lavik, G., Jensen, M. M., Moritz Holtappels, et al.: Nitrite oxidation in the Namibian oxygen minimum zone, *ISME Journal*, 1-10, 2011.
- Garcia, H. E., Locarnini, R. A., Boyer, T. P., Antonov, J. I., Zweng, M. M., et al.: World Ocean Atlas 2009, in: NOAA Atlas NESDIS 71, edited by: Levitus, S., U.S. Government Printing Office., Washington, D.C., 398, 2010.
- Garreaud, R. D., and Falvey, M.: The coastal winds off western subtropical South America in future climate scenarios, *International Journal of Climatology*, 10.1002/joc.1716, 2008.
- Giraudeau, J.: Distribution of recent nannofossils beneath the Benguela system: southwest African continental margin, *Marine Geology*, 108, 219-237, 1992.
- Giraudeau, J.: Planktonic foraminiferal assemblages in surface sediments from the southwest African continental margin, *Marine Geology*, 110, 47-62, 1993.
- Giraudeau, J., Monteiro, P. M. S., and Nikodemus, K.: Distribution and malformation of living coccolithophores in the northern Benguela upwelling system off Namibia, *Marine Micropaleontology*, 22, 93-110, 1993.
- Giraudeau, J., and Bailey, G. W.: Spatial dynamics of coccolithophore communities during an upwelling event in the Southern Benguela system, *Continental Shelf Research*, 15, 1825-1852, 1995.
- Giraudeau, J., Bailey, G. W., and Pujol, C.: A high-resolution time-series analyses of particle fluxes in the Northern Benguela coastal upwelling system: carbonate record of changes in biogenic production and particle transfer processes, *Deep-Sea Research II*, 47, 1999-2028, 2000.
- Glenn, C. R., Follmi, K. B., and Riggs, S. R.: Phosphorus and phosphorites: Sedimentology and environments of formation, *Eclogae Geol. Helv.*, 87, 747-788, 1994.
- Goldhammer, T., Brüchert, V., Ferdelman, T. G., and Zabel, M.: Microbial sequestration of phosphorus in anoxic upwelling sediments, *Nature Geoscience*, 3, 557-561, 10.1038/NGEO913, 2010.
- Goldhammer, T., Brunner, B., Bernasconi, S. M., Ferdelman, T. G., and Zabel, M.: Phosphate oxygen isotopes: Insights into sedimentary phosphorus cycling from the Benguela upwelling system, *Geochimica et Cosmochimica Acta*, 75, 3741-3756, 2011.
- Goldman, J. C., and Brewer, P. G.: Effect of nutrient source and growth rate on phytoplankton-mediated changes in alkalinity, *Limnology and Oceanography*, 25, 352-357, 1980.
- González-Dávila, M., Santana-Casiano, J. M., and Ucha, I. R.: Seasonal variability of  $f\text{CO}_2$  in the Angola-Benguela region, *Progress in Oceanography*, 83, 124-133, j.pocean.2009.07.033, 2009.
- González-Dávila, M., Santana-Casiano, J. M., Fine, R. A., Happell, J., Delille, B., et al.: Carbonate system in the water masses of the Southeast Atlantic sector of the Southern Ocean during February and March 2008, *Biogeosciences*, 8, 1401-1413, 10.5194/bg-8-1401-2011, 2011.
- Gordon, A. L.: South Atlantic thermocline ventilation, *Deep-Sea Research I*, 28A, 1239-1264, 1981.

- Gordon, A. L., Lutjeharms, J. R. E., and Grundlingh, M. L.: Stratification and circulation at the Agulhas Retroflection, Deep Sea Research I - Oceanographic Research Papers, 34, 565-599, 1987.
- Goubanova, K., Echevin, V., Dewitte, B., Codron, F., Takahashi, K., et al.: Statistical downscaling of sea-surface wind over the Peru-Chile upwelling region: diagnosing the impact of climate change from IPSL-CM4 model, Climate Dynamics, 10.1007/s00382-010-0824-0, 2010.
- Grasshoff, K., Kremling, K., and Ehrhardt, M.: Methods of seawater analysis, Third edition ed., edited by: Grasshoff, K., Kremling, K., and Ehrhardt, M., Verlag Chemie, 419 pp., 1999.
- Großkopf, T., Mohr, W., Baustian, T., Schunck, H., Gill, D., et al.: Doubling of marine dinitrogen-fixation rates based on direct measurements, Nature, 488, 10.1038/nature11338, 2012.
- Gruber, N., and Sarmiento, J. L.: Global patterns of marine nitrogen fixation and denitrification Global Biogeochemical Cycles, 11, 235-266, 1997.
- Gruber, N.: Anthropogenic CO<sub>2</sub> in the Atlantic Ocean, Global Biogeochemical Cycles, 12, 165-191, 1998.
- Gruber, N., Gloor, M., Fletcher, S. E. M., Doney, S. C., Dutkiewicz, S., et al.: Oceanic sources, sinks, and transport of atmospheric CO<sub>2</sub>, Global Biogeochemical Cycles, 23, 1-21, 2009.
- Haake, B., Ittekkot, V., Rixen, T., Ramaswamy, V., Nair, R. P., et al.: Seasonality and interannual variability of particle fluxes to the deep Arabian Sea, Deep Sea Research I, 40, 1323-1344, 1993.
- Hales, B., Takahashi, T., and Bandstra, L.: Atmospheric CO<sub>2</sub> uptake by a coastal upwelling system, Global Biogeochemical Cycles, 19, 1-11, 10.1029/2004GB002295, 2005.
- Hall, C., and Lutjeharms, J. R. E.: Cyclonic eddies identified in the Cape Basin of the South Atlantic Ocean, Journal of Marine Systems, 85, 1-10, 10.1016/j.jmarsys.2010.10.003, 2011.
- Hansen, A., Ohde, T., and Wasmund, N.: Succession of micro- and nanoplankton groups in ageing upwelled waters of Namibia, Journal of Marine Systems, in press, 2014.
- Harris, K. E., DeGrandpre, M. D., and Hales, B.: Aragonite saturation state dynamics in a coastal upwelling zone, Geophysical Research Letters, 40, 1-6, 10.1002/grl.50460, 2013.
- Hauri, C., Gruber, N., Plattner, G.-K., Alin, S., Feely, R. F., et al.: Ocean acidification in the California Current System, Oceanography, 22, 2009.
- Heinze, C., Maier-Reimer, E., and Winn, K.: Glacial pCO<sub>2</sub> Reduction by the World Ocean: Experiments with the Hamburg Carbon Cycle Model, Paleoceanography, 6, 395-430, 1991.
- Henderiks, J., Winter, A., Elbrächter, M., Fesitel, R., van der Plas, A., et al.: Environmental controls on *Emiliana huxleyi* morphotypes in the Benguela coastal upwelling system (SE Atlantic), Marine Ecology Progress Series, 448, 51-56, 10.3354/meps09535, 2012.
- Henson, S. A., Sanders, R., Madsen, E., Morris, P. J., LeMoigne, F., et al.: A reduced estimate of the strength of the ocean's biological carbon pump, Geophysical Research Letters, 38, 1-5, 10.1029/2011GL046735, 2011.

- Hernández-Ayon, M. J., Zirino, A., Dickson, A. G., Camiro-Vargas, T., and Valenzuela-Espinoza, E.: Estimating the contribution of organic bases from microalgae to the titration alkalinity in coastal seawaters, *Limnology and Oceanography: Methods*, 5, 225-232, 2007.
- Hofmann, G. E., Barry, J. P., Edmunds, P. J., Gates, R. D., Hutchins, D. A., et al.: The Effect of Ocean Acidification on Calcifying Organisms in Marine Ecosystems: An Organism to Ecosystem Perspective, *Annu. Rev. Ecol. Evol. Syst.*, 41, 127-147, 10.1146/annurev.ecolsys.110308.120227, 2010.
- Honjo, S., Manganini, S. J., Krishfield, R. A., and Francois, R.: Particulate organic carbon fluxes to the ocean interior and factors controlling the biological pump: A synthesis of global sediment trap programs since 1983, *Progress in Oceanography*, 76, 217-285, 2008.
- Hutchings, L., van der Lingen, C. D., Shannon, L. J., Crawford, R. J. M., Verheye, H. M. S., et al.: The Benguela Current: An ecosystem of four components, *Progress in Oceanography*, 83, 15-32, 2009.
- Hutchins, L., Fu, F.-X., Zhang, Y., Warner, M. E., Feng, Y., et al.: CO<sub>2</sub> control of *Trichodesmium* N<sub>2</sub> fixation, photosynthesis, growth rates, and elemental ratios: Implications for past, present, and future ocean biogeochemistry, *Limnology and Oceanography*, 52, 1293-1304, 2007.
- Inthorn, M., Birch, G. F., Bremner, J. M., Calvert, S. E., and Rogers, J.: Compilation of organic carbon distribution and sedimentology in the surface sediments on the continental margin offshore southwestern Africa. Supplement to: Inthorn, M., Wagner, T., Scheeder, G., Zabel, M. (2006): Lateral transport controls distribution, quality and burial of organic matter along continental slopes in high-productivity areas, *Geology*, 34(3), 205-208, DOI: 10.1130/G22153.1, 10.1594/PANGAEA.351146, 2006.
- Ito, T., Follows, M. J., and Boyle, E. A.: Is AOU a good measure of respiration in the oceans?, *Geophysical Research Letters*, 31, 1-4, 10.1029/2004GL020900, 2004.
- Ito, T., and Follows, M. J.: Preformed phosphate, soft tissue pump and atmospheric CO<sub>2</sub>, *Journal of Marine Research*, 63, 813-839, 2005.
- Jickells, T. D., An, Z. S., Andersen, K. K., Baker, A. R., Bergametti, G., et al.: Global Iron Connections Between Desert Dust, Ocean Biogeochemistry, and Climate, *Science*, 308, 10.1126/science.1105959, 2005.
- Johnson, K. S., Chavez, F. P., Elrod, V. A., Fitzwater, S. E., Pennington, J. T., et al.: The annual cycle of iron and the biological response in central California coastal waters, *Geophysical Research Letters*, 28, 1247-1250, 2001.
- Kalvelage, T., Jensen, M. M., Contreras, S., Revsbech, N. P., Lam, P., et al.: Oxygen Sensitivity of Anammox and Coupled N-Cycle Processes in Oxygen Minimum Zones, *PLoS ONE* 6, 1-12, 10.1371/journal.pone.0029299, 2011.
- Karl, D. M., Church, M. J., Dore, J. E., Letelier, R. M., and Mahaffey, C.: Predictable and efficient carbon sequestration in the North Pacific Ocean supported by symbiotic nitrogen fixation, *PNAS*, 109, 1842-1849, doi/10.1073/pnas.1120312109, 2012.
- Keeling, C. D., and Whorf, T. P.: Atmospheric CO<sub>2</sub> concentrations (ppmv) derived from in situ air samples collected at Mauna Loa Observatory, Hawaii, Scrips Institution of Oceanography, University of California La Jolla, California USA 92093 - 04444, 2005.

- Kim, H.-C., and Lee, K.: Significant contribution of dissolved organic matter to seawater alkalinity, *Geophysical Research Letters*, 36, 1-5, 10.1029/2009GL040271, 2009.
- Knapp, A. N.: The sensitivity of marine N<sub>2</sub> fixation to dissolved inorganic nitrogen, *Front. Microbiol.*, 3, 1-14, 10.3389/fmicb.2012.00374, 2012.
- Knapp, A. N., Dekaezemacker, J., Bonnet, S., Sohm, J. A., and Capone, D. G.: Sensitivity of *Trichodesmium erythraeum* and *Crocospaera watsonii* abundance and N<sub>2</sub> fixation rates to varying NO<sub>3</sub> and PO<sub>4</sub> concentrations in batch cultures, *Aquat. Microb. Ecol.*, 66, 223-236, 10.3354/ame01577, 2012.
- Koeve, W., and Kähler, P.: Heterotrophic denitrification vs. autotrophic anammox - quantifying collateral effects on the oceanic carbon cycle, *Biogeosciences*, 7, 2327-2337, 10.5194/bg-7-2327-2010, 2010.
- Körtzinger, A., Duinker, J. C., and Mintrop, L.: Strong CO<sub>2</sub> emissions from the Arabian Sea during south-west monsoon, *Geophysical Research Letters*, 24, 1763-1766, 1997.
- Krauk, J. M., Villareal, T. A., Sohm, J. A., Montoya, J. P., and Capone, D. G.: Plasticity of N:P ratios in laboratory and field populations of *Trichodesmium* spp., *Aquat Microb Ecol*, 42, 243-253, 2006.
- Kroeker, K. J., Kordas, R. L., Crim, R., Henderiks, I. E., Ramajo, L., et al.: Impacts of ocean acidification on marine organism: quantifying sensitivities and interaction with warming, *Global Change Biology*, 19, 1884-1896, 10.1111/gcb.12179, 2013.
- Kruger, A. C., and Shongwe, S.: Temperature trends in South Africa: 1960-2003, *International Journal of Climatology*, 24, 1929-1945, 10.1002/joc.1096, 2004.
- Kuypers, M. M. M., Lavik, G., Woebken, D., Schmid, M., Fuchs, B. M., et al.: Massive nitrogen loss from the Benguela upwelling system through anaerobic ammonium oxidation, *PNAS* 102, 6478-6483, 2005.
- Lam, P., and Kuypers, M. M.: Microbial nitrogen cycling processes in oxygen minimum zones, *Annual Review in Marine Science*, 3, 317-345, 10.1146/annurev-marine-120709-142814, 2010.
- Langer, G., Nehrke, G., Probert, I., Ly, J., and Ziveri, P.: Strain-specific responses of *Emiliana huxleyi* to changing seawater carbonate chemistry, *Biogeosciences*, 6, 2637-2646, 2009.
- Larouelle, G. G., Dürr, H. H., Slomp, C. P., and Borges, A. V.: Evaluation of sinks and sources of CO<sub>2</sub> in the global coastal ocean using spatially-explicit typology of estuaries and continental shelves, *Geophysical Research Letters*, 37, 1-6, 10.1029/2010GL043691, 2010.
- Lavik, G., Stührmann, T., Brüchert, V., Plas, A. V. d., Mohrholz, V., et al.: Detoxification of sulphidic African shelf waters by blooming chemolithotrophs, *Nature Letters*, 457, 581-585, doi:10.1038/nature07588, 2009.
- Le Quéré, C., Peters, G. P., Andres, R. J., Andrew, R. M., VBooden, T. A., et al.: Global carbon budget 2013, *Earth System Science Data*, 6, 235-263, 10.5194/essd-6-235-2014, 2014.
- Lee, C., and Cronin, C.: The vertical flux of particulate organic nitrogen in the sea: decomposition of amino acids in the Peru upwelling area and the equatorial Atlantic, *Journal of Marine Research*, 40, 227-251, 1982.

- Leinweber, A., Gruber, N., Frenzel, H., Friederich, G. E., and Chavez, F. P.: Diurnal carbon cycling in the surface ocean and lower atmosphere of Santa Monica Bay, California, *Geophysical Research Letters*, 36, 1-5, 2009.
- Lewis, E., and Wallace, D. W. R.: Program developed for CO<sub>2</sub> system calculations. ORNL/CDIAC-105a. Carbon dioxide Information Analysis Center, Oak Ridge National Laboratory, U.S. Department of Energy, Oak Ridge, Tennessee, 1998.
- Li, Y.-H., and Peng, T.-H.: Latitudinal change of remineralization ratios in the oceans and its implication for nutrient cycles, *Global Biogeochemical Cycles*, 16, 1130, 10.1029/2001GB001828, 2002.
- Longhurst, A., Sathyendranath, S., Platt, T., and Caverhill, C.: An estimate of global primary production in the ocean from satellite radiometer data, *Journal of Plankton Research*, 17, 1245-1271, 1995.
- Loucaides, S., Tyrrell, T., Achterberg, E. P., Torres, R., Nightingale, P. D., et al.: Biological and physical forcing of carbonate chemistry in an upwelling filament off northwest Africa: Results from a Lagrangian study, *Global Biogeochemical Cycles*, 26, 1-13, 10.1029/2011GB004216, 2012.
- Lutz, M., Dunbar, R., and Caldeira, K.: Regional variability in the vertical flux of particulate organic carbon in the ocean interior, *Global Biogeochemical Cycles*, 16, 10.1029/2000BG001383, 2002.
- Lutz, M., Caldeira, K., Dunbar, R., and Behrenfeld, M. J.: Seasonal rhythms of net primary production and particulate organic carbon flux describe biological pump efficiency in the global ocean, *Journal of Geophysical Research*, 112, 1-26, 10.1029/2006JC003706, 2007.
- Mahaffey, C., Williams, R. G., Wolff, G. A., Mahowald, N., Anderson, W., et al.: Biogeochemical signatures of nitrogen fixation in the eastern North Atlantic, *Geophysical Research Letters*, 30, 33/31-33/34, 10.1029/2002GL016542, 2003.
- Mahaffey, C., Michaels, A. F., and Capone, D. G.: The conundrum of marine N<sub>2</sub> fixation, *American Journal of Science*, 305, 546-595, 2005.
- Mahowald, N. M., Engelstaedter, S., Luo, C., Sealy, A., Artaxo, P., et al.: Atmospheric Iron Deposition: Global Distribution, Variability, and Human Perturbations, *Annu. Rev. Mar. Sci.*, 1, 245-278, 10.1146/annurev.marine.010908.163727, 2009.
- Manabe, S., and Stouffer, R. J.: Century-scale effects of increased atmospheric CO<sub>2</sub> on the ocean-atmosphere system, *Nature*, 364, 215-218, 1993.
- Martin, J. H., Knauer, G. A., Karl, D. M., and Broenkow, W. W.: VERTEX: carbon cycling in the northeast Pacific, *Deep-Sea Research*, 34, 267-285, 1987.
- McElroy, M. B.: Marine biological controls on atmospheric CO<sub>2</sub> and climate, *Nature*, 302, 328-329, 1983.
- Meeuwis, J. M., and Lutjeharms, J. R. E.: Surface thermal characteristics of the Angola-Benguela Front, *South African Journal of Marine Science*, 9, 261-279, 1990.
- Meisel, S., Emeis, K.-C., Struck, U., and Kristen, I.: Nutrient regime and upwelling in the northern Benguela since the middle Holocene in a global context – a multi-proxy approach, *Fossil Record*, 14, 171-193, 10.1002/mmng.201100006, 2011b.
- Messié, M., Ledesma, J., Kolber, D. D., Michisaki, R. P., Foley, D. G., et al.: Potential new production estimates in four eastern boundary upwelling ecosystems, *Progress in Oceanography*, 83, 151–158, 2009.

- Middelburg, J. J., and Levin, L. A.: Coastal hypoxia and sediment biogeochemistry *Biogeosciences*, 6, 1273-1293, 2009.
- Mills, M. M., Ridame, C., Davey, M., La Roche, J., and Geider, R. J.: Iron and phosphorus co-limit nitrogen fixation in the eastern tropical North Atlantic, *Nature*, 429, 10.1038/nature02550, 2004.
- Mintrop, L., Körtzinger, A., and Duinker, J. C.: The carbon dioxide system in the northwestern Indian Ocean during south-west monsoon, *Marine Chemistry* 64, 315-336, 1999.
- Mintrop, L.: The Versatile Instrument for the Determination of Titration Alkalinity: Manual for version 3s and 3c, Marianda 2, 2005.
- Mitchell-Innes, B., and Winter, A.: Coccolithophores: a major phytoplankton component in mature upwelled waters off the Cape Peninsula, South Africa, *Marine Biology*, 95, 25-30, 1987.
- Mohr, W., Großkopf, T., Wallace, D. W. R., and La Roche, J.: Methodological underestimation of oceanic nitrogen fixation rates, *PLoS ONE*, 5, 10.1371/journal.pone.0012583, 2010.
- Mohrholz, V., Bartholomae, C. H., Plas, A. K. v. d., and Lass, H. U.: The seasonal variability of the northern Benguela undercurrent and its relation to the oxygen budget on the shelf, *Continental Shelf Research* 28, 424-441, 2008.
- Moisander, P. H., Beinart, R. A., Hewson, I., White, A. E., Johnson, K. S., et al.: Unicellular Cyanobacterial Distributions Broaden the Oceanic N<sub>2</sub> Fixation Domain, *Science*, 327, 10.1126/science.1185468, 2010.
- Mollenhauer, G., Schneider, R. R., Müller, P. J., Spieß, V., and Wefer, G.: Glacial/interglacial variability in the Benguela upwelling system: Spatial distribution and budgets of organic carbon accumulation, *Global Biogeochemical Cycles*, 16, 10.1029/2001GB001488, 2002
- Monteiro, P. M. S., Plas, A. v. d., Mohrholz, V., Mabilhe, E., Pascall, A., et al.: Variability of natural hypoxia and methane in a coastal upwelling system: Oceanic physics or shelf biology?, *Geophysical Research Letters*, 33, L16614, doi:10.1029/2006GL026234, 2006.
- Monteiro, P. M. S.: The Benguela Current System, in: Carbon and nutrient fluxes in continental margins - A global synthesis, edited by: Liu, K.-K., Atkinson, L., Quinones, R. A., and Talaue-McManus, L., *Global Change - The IGBP Series*, Springer, 2010.
- Moore, C. M., Mills, M. M., Achterberg, E. P., Geider, R. J., LaRoche, J., et al.: Large-scale distribution of Atlantic nitrogen fixation controlled by iron availability, *Nature Geoscience*, 2, 867-871, 10.1038/NGEO667, 2009.
- Moore, C. M., Mills, M. M., Arrigo, K. R., Berman-Frank, I., Bopp, L., et al.: Processes and patterns of oceanic nutrient limitation, *Nature Geoscience*, 6, 701-710, 10.1038/ngeo1765, 2013.
- Moy, A. D., Howard, W. R., Bray, S. G., and Trull, T. W.: Reduced calcification in modern Southern Ocean planktonic foraminifera, *Nature Geoscience*, 2, 276-280, 2009.
- Muller-Karger, F.-E., Varela, R., Thunell, R., Luerssen, R., Hu, C., et al.: The importance of continental margins in the global carbon cycle, *Geophysical Research Letters*, 32, 10.1029/2004GL021346, 2005.

- Muller, F. L. L., and Bleie, B.: Estimating the organic acid contribution to coastal seawater alkalinity by potentiometric titrations in a closed cell, *Analytica Chimica Acta*, 619, 183-191, 10.1016/j.aca.2008.05.018, 2008.
- Nagel, B., Emeis, K.-C., Flohr, A., Rixen, T., Schlarbaum, T., et al.: N-cycling and balancing of the N-deficit generated in the oxygen minimum zone over the Namibian shelf - an isotope-based approach, *Journal of Geophysical Research: Biogeosciences*, 118, 361-371, 10.1002/jgrg.20040, 2013.
- Nathan, Y., Bremner, J. M., E., R., Loewenthal, and Monteiro, P.: Role of bacteria in phosphorite genesis, *Geomicrobiology Journal*, 11, 69-76, 10.1080/01490459309377935, 1993.
- Nelson, G., and Hutchings, L.: The Benguela Upwelling Area, *Progress in Oceanography* 12, 333-356, 1983.
- Noble, A. E., Lamborg, C. H., Ohnemus, D. C., Lam, P. J., Goepfert, T. J., et al.: Basin-scale inputs of cobalt, iron, and manganese from the Benguela-Angola front to the South Atlantic Ocean, *Limnol. Oceanogr.*, 57, 989-1010 10.4319/lo.2012.57.4.0989, 2012.
- Oschlies, A., Schulz, K. G., Riebesell, U., and Schmittner, A.: Simulated 21st century's increase in oceanic suboxia by CO<sub>2</sub>-enhanced biotic carbon export, *Global Biogeochemical Cycles*, 22, 10.1029/2007GB003147, 2008.
- Pauly, D., and Christensen, V.: Primary production required to sustain global fisheries, *Nature*, 374, 255-257, 1995.
- Pierrot, D., Lewis, E., and Wallace, D. W. R.: MS Excel program developed for CO<sub>2</sub> System Calculations. ORNL/CDIAC-105a. Carbon dioxide Information Analysis Center, Oak Ridge National Laboratory, U.S. Department of Energy, Oak Ridge, Tennessee, 10.3334/DCIAC/otg.CO2SYS\_XLS\_CDIAC105a, 2006.
- Pitcher, G. C., Brown, P. C., and Mitchell-Innes, B. A.: Spatio-temporal variability of phytoplankton in Southern Benguela Upwelling System, *South African Journal of Marine Science*, 12, 439-456, 1992.
- Poole, R., and Tomczak, M.: Optimum multiparameter analysis of the water mass structure in the Atlantic Ocean thermocline, *Deep-Sea Research I*, 46, 1895-1921, 1999.
- Redfield, A. C., Ketchum, B. H., and Richards, F. A.: The influence of organisms on the composition of seawater, *The Sea*, edited by: Hill, M. N. E., Wiley - Interscience New York, 1963.
- Rhein, M., Rintoul, S. R., Aoki, S., Campos, E., Chambers, D., et al.: Observations: Ocean, in: *Climate Change 2013: The Physical Science Basis. Contribution of Working Group I to the Fifth Assessment Report of the Intergovernmental Panel on Climate Change*, edited by: Stocker, T. F., Qin, D., Plattner, G.-K., Tignor, M., Allen, S. K., Boschung, J., Nauels, A., Xia, Y., Bex, V., and Midgley, P. M., Cambridge University Press, Cambridge, United Kingdom and New York, NY, USA, 2013.
- Richter, I., and Xie, S.-P.: On the origin of equatorial Atlantic biases in coupled general circulation models, *Climate Dynamics*, 31, 587-598, 10.1007/s00382-008-0364-z, 2008.
- Riebesell, U., Zondervan, I., Rost, B., Tortell, P. D., Zeebe, R. E., et al.: Reduced calcification of marine plankton in response to increased atmospheric CO<sub>2</sub>, *Nature*, 407, 364-367, 2000.

- Riebesell, U., Schulz, K. G., Bellerby, R. G. J., Botros, M., Fritsche, P., et al.: Enhanced biological carbon consumption in a high CO<sub>2</sub> ocean, *Nature*, 450, 545-549, 10.1038/nature06267, 2007.
- Rixen, T., Haake, B., and Ittekkot, V.: Sedimentation in the western Arabian Sea: the role of coastal and open-ocean upwelling, *Deep Sea Research II*, 47, 2155-2178, 2000.
- Rixen, T., Guptha, M. V. S., and Ittekkot, V.: Deep ocean fluxes and their link to surface ocean processes and the biological pump, *Progress in Oceanography*, 65 240-259, 2005.
- Rixen, T., and Ittekkot, V.: Nitrogen deficits in the Arabian Sea, implications from three component mixing analysis, *Deep Sea Research II*, 52, 1879-1891, 2005.
- Rixen, T., Goyet, C., and Ittekkot, V.: Diatoms and their influence on the biologically mediated uptake of atmospheric CO<sub>2</sub> in the Arabian Sea upwelling system, *Biogeosciences*, 3, 1-13, 2006.
- Rixen, T., Jiménez, C., and Cortés, J.: Impacts of upwelling events on the sea water carbonate chemistry and dissolved oxygen concentration in the Gulf of Papagayo (Culebra Bay), Costa Rica: Implications for coral reefs, *Revista de Biología Tropical*, 60, 187-195, 2012.
- Rixen, T., Flohr, A., Lahajnar, N., Schmidt, M., Mohrholz, V., et al.: Upwelling lowering carbon export in the Benguela upwelling system off Namibia, in prep.
- Roberts, D., Howard, W. R., Moy, A. D., Roberts, J. L., Trull, T. W., et al.: Interannual pteropod variability in sediment traps deployed above and below the aragonite saturation horizon in the Sub-Antarctic Southern Ocean, *Polar Biology*, 34, 1739-1750, 10.1007/s00300-011-1024-z, 2011.
- Romero, O., Boeckel, B., Donner, B., Lavik, G., Fischer, G., et al.: Seasonal productivity dynamics in the pelagic central Benguela System inferred from the flux of carbonate and silicate organisms, *Journal of Marine Systems*, 37, 259-278, 2002.
- Ryther, J. H.: Photosynthesis and fish production in the Sea, *Science*, 166, 72-76, 1969.
- Sabine, C. L., Feely, R. A., Gruber, N., Key, R. M., Lee, K., et al.: The Oceanic Sink for Anthropogenic CO<sub>2</sub>, *Science*, 305, 367-371, 2004.
- Saito, M. A., Moffet, J. M., Chisholm, S. W., and Waterbury, J. B.: Cobalt limitation and uptake in *Prochlorococcus*, *Limnol. Oceanogr.*, 47, 1629-1636, 2002.
- Saito, M. A., Moffet, J. M., and DiTullio, G. R.: Cobalt and Nickel in the Peru upwelling region: A major flux of labile cobalt utilized as a micronutrient, *Global Biogeochemical Cycles*, 18, 10.1029/2003GB002216, 2004.
- Santana-Casiano, J. M., González-Dávila, M., and Ucha, I. R.: Carbon dioxide fluxes in the Benguel upwelling system during winter and spring: A comparison between 2005 and 2006, *Deep Sea Research II*, 56, 533-541, 2009.
- Sañudo-Wilhemý, S. A., Kustka, A. B., Gobler, C. J., Hutchins, D. A., Yang, M., et al.: Phosphorous limitation of nitrogen fixation by *Trichodesmium* in the central Atlantic, *Nature*, 411, 66-69, 2001.
- Sañudo-Wilhemý, S. A., Tovar-Sanchez, A., Fu, F.-X., Capone, D. G., Carpenter, E. J., et al.: The impact of surface-adsorbed phosphorous on phytoplankton Redfield stoichiometry, *Nature*, 897-901, 2004.
- Sarmiento, J. L., Dunne, J., Gnanadesikan, A., Key, R. M., Matsumoto, K., et al.: A new estimate of the CaCO<sub>3</sub> to organic carbon export ratio, *Global Biogeochemical Cycles*, 16, 10.1029/2002GB001919, 2002.

- Sarmiento, J. L., Gruber, N., Brzezinski, M. A., and Dunne, J. P.: High-latitude controls of thermocline nutrients and low latitude biological productivity, *Nature*, 427, 56-60, 2004.
- Sarmiento, J. L., and Gruber, N.: *Ocean Biogeochemical Dynamics*, edited by: Sarmiento, J. L., and Gruber, N., Princeton University Press, 2006.
- Sarthou, G., Baker, A. R., Blain, S., Achterberg, E. P., Boye, M., et al.: Atmospheric iron deposition and sea-surface dissolved iron concentrations in the eastern Atlantic Ocean, *Deep-Sea Research I*, 50, 10.1016/S0967-0637(03)00126-2, 2003.
- Schiebel, R.: Planktic foraminiferal sedimentation and the marine calcite budget, *Global Biogeochemical Cycles*, 16, 13/11-13/21, 2002.
- Schneider, B., Schlitzer, R., Fischer, G., and Nöthig, E.-M.: Depth-dependent elemental compositions of particulate organic matter (POM) in the ocean, *Global Biogeochemical Cycles*, 17, 10.1029/2002GB001871, 2003.
- Schulz, H. N., and Schulz, H. D.: Large Sulfur Bacteria and the Formation of Phosphorite, *Science*, 307, 416-418, 2005.
- Shannon, L. V.: The Benguela Ecosystem: 1. Evolution of the Benguela, physical features and processes, *Oceanography and Marine Biology*, 23, 105-182, 1985.
- Shillington, F., Reason, C. J. C., Duncombe Rae, C. M., Florenchie, P., and Penven, P.: Large scale physical variability of the Benguela Current Large Marine Ecosystem (BCLME), in: *Benguela: predicting a large marine ecosystem*, edited by: Shannon, V., Hempel, G., Malanotte-Rizzoli, P., Moloney, C., and Woods, J., Large marine ecosystems Elsevier, Amsterdam, 2006.
- Sigman, D. M., and Boyle, E. A.: Glacial/interglacial variations in atmospheric carbon dioxide, *Nature*, 407, 859-869, 2000.
- Sigman, D. M., Hain, M. P., and Haug, G. H.: The polar ocean and glacial cycles in the atmospheric CO<sub>2</sub> concentration, *Nature*, 466, 47-55, 10.1038/nature09149, 2010.
- Singh, A., Lomas, M. W., and Bates, N. R.: Revisiting N<sub>2</sub> fixation in the North Atlantic Ocean: Significance of deviations from the Redfield Ratio, atmospheric deposition and climate variability, *Deep-Sea Research II*, 93, 148-158, 10.1016/j.dsr2.2013.04.008, 2013.
- Sohm, J. A., and Capone, D. G.: Emerging patterns of marine nitrogen fixation, *Nature Reviews Microbiology*, 9, 499-508, 10.1038/nrmicro2594, 2011.
- Sohm, J. A., Hilton, J. A., Noble, A. E., Zehr, J. P., Saito, M. A., et al.: Nitrogen fixation in the South Atlantic Gyre and the Benguela Upwelling System, *Geophysical Research Letters*, 38, 1-6, 10.1029/2011GL048315, 2011.
- Staal, M., te Lintel Hekkert, S., Brummer, G. J., Veldhuis, M., Sikkens, C., et al.: Nitrogen fixation along a north-south transect in the eastern Atlantic Ocean, *Limnol. Oceanogr.*, 52, 1305-1316, 2007.
- Steinhoff, T., Bange, H. W., Kock, A., Wallace, D. W. R., and Körtzinger, A.: Biological productivity in the Mauretanian upwelling estimated with a triple gas approach, *Biogeosciences Discuss.*, 9, 10.5194/bgd-9-4853-2012, 2012.
- Stramma, L., and England, S.: On the water masses and mean circulation of the South Atlantic Ocean, *Journal of Geophysical Research*, 104, 20,863-820,883, 1999.
- Subramaniam, A., Mahaffey, C., Johns, W., and Mahowald, N.: Equatorial upwelling enhances nitrogen fixation in the Atlantic Ocean, *Geophysical Research Letters*, 40, 1766-1771, 10.1002/grl.50250, 2013.

- Swap, R., Garstang, M., Macko, S. A., Tyson, P. D., Maenhaut, W., et al.: The long-range transport of southern African aerosols to the tropical South Atlantic, *Journal of Geophysical Research*, 101, 23777-23791, 1996.
- Takahashi, T., Broecker, W., and Langer, S.: Redfield Ratio Based on Chemical Data from Isopycnal Surfaces, *Journal of Geophysical Research*, 90, 6907-6924, 1985.
- Takahashi, T.: The Fate of Industrial Carbon Dioxide, *Science*, 305, 352-353, 2004.
- Takahashi, T., Sutherland, S. C., Wanninkhof, R., Sweeney, C., Feely, R. A., et al.: Climatological mean and decadal change in surface ocean pCO<sub>2</sub>, and net sea-air CO<sub>2</sub> flux over the global oceans, *Deep-Sea Research II*, 56, 554-577, 2009.
- Thomas, H., Schiettecatte, L.-S., Suykens, K., Kone, Y. J. M., Shadwick, E. H., et al.: Enhanced ocean carbon storage from anaerobic alkalinity generation in coastal sediments, *Biogeosciences*, 6, 267-274, 2009.
- Toggweiler, J. R., Gnanadesikan, A., Carson, S., Murnane, R., and Sarmiento, J. L.: Representation of the carbon cycle in box models and GCMs: 1. Solubility pump, *Global Biogeochemical Cycles*, 17, 1026, 10.1029/2001GB001401, 2003.
- Torres, R., Turner, D. R., Silva, N., and Rutllant, J.: High short-term variability of CO<sub>2</sub> fluxes during an upwelling event off the Chilean coast at 30°S, *Deep-Sea Research I*, 46, 1161-1179, 1999.
- Trimborn, S., Langer, G., and Rost, B.: Effect of calcium concentration and irradiance on calcification and photosynthesis in the coccolithophore *Emiliania huxleyi*, *Limnol. Oceanogr.*, 52, 2285-2293, 2007.
- Tyrrell, T., and Law, C. S.: Low nitrate:phosphate ratios in the global ocean, *Nature*, 387, 793-796, 1997.
- Tyrrell, T., and Lucas, M. I.: Geochemical evidence of denitrification in the Benguela upwelling system, *Continental Shelf Research*, 22, 2497-2511, 2002.
- Tyrrell, T., Maranon, E., Poulton, A. J., Bowie, A. R., and Harbour, D. S.: Large-scale latitudinal distribution of *Trichodesmium* spp. in the Atlantic Ocean, *Journal of Plankton Research*, 25, 405-416, 2003.
- Tyson, P. D., Garstang, M., Swap, R., Kallberg, P., and Edwards, M.: An air transport climatology for subtropical southern Africa, *International Journal of Climatology*, 16, 1996.
- van der Plas, A. K., Monteiro, P. M. S., and Pascall, A.: Cross-shelf biogeochemical characteristics of sediments in the central Benguela and their relationship to overlying water column hypoxia, *African Journal of Marine Science*, 29, 37-47, 2007.
- van Mooy, B. A. S., Keil, R. G., and Devol, A. H.: Impact of suboxia on sinking particulate organic carbon: Enhanced carbon flux and preferential degradation of amino acids via denitrification, *Geochimica et Cosmochimica Acta*, 66, 457-465, 2002.
- Volk, T., and Hoffert, M.: Ocean carbon pumps: analysis on the relative strengths and efficiencies in ocean-driven atmospheric CO<sub>2</sub> changes, in: *The carbon cycle and atmospheric CO<sub>2</sub>: Natural variations Archean* edited by: Sandquist, E. T., and Broecker, W. S., Washington, D. C., 99-110, 1985.
- Wang, M., Overland, J. E., and Bond, N. A.: Climate projections for selected large marine ecosystems, *Journal of Marine Systems*, 79, 258-266, 10.1016/j.marsys.2008.11.028, 2010.

- Wanninkhof, R.: Relationship between gas exchange and wind speed over the ocean, *Journal of Geophysical Research*, 97, 7373-7381, 1992.
- Wanninkhof, R., and McGillis, W. M.: A cubic relationship between gas transfer and wind speed, *Geophysical Research Letters*, 26, 1889-1983, 1999.
- Warneke, T., Yang, Z., Olsen, S., Korner, S., Notholt, J., et al.: Seasonal and latitudinal variations of column averaged volume-mixing ratios of atmospheric CO<sub>2</sub>, *Geophysical Research Letters*, 32, 10.1029/2004gl021597, 2005.
- Watson, A. J., Bakker, D. C. E., Ridgwell, A. J., Boyd, P. W., and Law, C. S.: Effect of iron supply on Southern Ocean CO<sub>2</sub> uptake and implications for glacial atmospheric CO<sub>2</sub>, *Nature*, 407, 730-733, 2000.
- Weber, T. S., and Deutsch, C.: Ocean nutrient ratios governed by plankton biogeography, *Nature*, 467, 550-554, doi:10.1038/nature09403, 2010.
- Weeks, S. J., Currie, B., and Bakun, A.: Massive emissions of toxic gas in the Atlantic, *Nature*, 415, 2002.
- Wefer, G., and Fischer, G.: Seasonal patterns of vertical particle flux in equatorial and coastal upwelling areas of the eastern Atlantic, *Deep Sea Research I* 40, 1613-1645, 1993.
- Weiss, R. F.: The solubility of nitrogen, oxygen and argon in water and seawater, *Deep Sea Research*, 17, 721-735, 1970.
- Wolf-Gladrow, D. A., Zeebe, R. E., Klaas, C., Körtzinger, A., and Dickson, A. G.: Total alkalinity: The explicit conservative expression and its application to biogeochemical processes, *Marine Chemistry*, 106, 287-300, 2007.
- Zeebe, R. E., and Wolf-Gladrow, D. A.: CO<sub>2</sub> in seawater: Equilibrium, Kinetics, Isotopes, Elsevier Oceanography Series, edited by: Halpern, D., 2001.
- Zehr, J. P.: Nitrogen fixation by marine cyanobacteria, *Trends in Microbiology*, 19, 162-173, 10.1016/j.tim.2010.12.004, 2011.
- Zuidema, P., Chang, P., Mechoso, C. R., and Terray, L.: Coupled ocean-atmosphere-land processes in the tropical Atlantic, Joint edition of the newsletter of the Climate Variability and Predictability Project (CLIVAR) exchanges and the CLIVAR variability of the American Monsoon System Project (VAMOS), 16, 12-14, 2011.

## LIST OF CO-AUTHOR PUBLICATIONS

- Nagel, B., Emeis, K.-C., **Flohr, A.**, Rixen, T., Schlarbaum, T., Mohrholz, V., and v. d. Plas, A. (2013). N-cycling and balancing of the N-deficit generated in the oxygen minimum zone over the Namibian shelf - an isotope-based approach, 2013. *Journal of Geophysical Research: Biogeosciences* *Journal of Geophysical Research: Biogeosciences*, 118, 361-371, 10.1002/jgrg.20040.
- Gutknecht, E., Dadou, I., Le Vu, B., Cambon, G., Sudre, J., Garçon, V., Machu, E., Rixen, T., Kock, A., **Flohr, A.**, Paulmier, A., and Lavik, G. (2013). Coupled physical/biogeochemical modeling including O<sub>2</sub>-dependent processes in the Eastern Boundary Upwelling Systems: application in the Benguela. *Biogeosciences*, 10, 3559 – 3591, 10.5194/bg-10-3559-2013.
- Gutknecht, E., Dadou, I., Marchesiello, P., Cambon, G., Le Vu, B., Sudre, J., Garçon, V., Machu, E., Rixen, T., Kock, A., **Flohr, A.**, Paulmier, A., and Lavik, G. (2013). Nitrogen transfers off Walvis Bay: a 3-D coupled physical/biogeochemical modeling approach in the Namibian upwelling system. *Biogeosciences*, 10, 4117 – 4135, 10.5104/bg-10-4117-2013.



## CURRICULUM VITAE

Entfällt aus datenschutzrechtlichen Gründen.

## DANKSAGUNG

Hiermit möchte ich mich bei allen Personen bedanken, die an der erfolgreichen Fertigstellung meiner Doktorarbeit beteiligt waren.

Herrn Dr. Tim Rixen möchte ich für die Betreuung und die Begutachtung der Doktorarbeit, für die kontinuierliche und vertrauensvolle Unterstützung während der Doktorandenphase und darüber hinaus für die konstruktiven Gespräche und die mitreißende Begeisterung an den großen Zusammenhängen danken.

Herrn Prof Dr. Kay-Christian Emeis danke ich für die Betreuung, für die schnelle Durchsicht meiner Manuskripte und für die Begutachtung meiner Doktorarbeit. Darüber hinaus bedanke ich mich für die sofortige Unterstützung während des Wechsels meines Promotionsverfahrens an die Universität Hamburg.

Für die erstklassige Kooperation, die Unterstützung und Hilfsbereitschaft, die ich in Vorbereitung auf und während meines Aufenthaltes in Swakopmund erfahren habe, möchte ich mich besonders bei Dr. Anja van der Plas bedanken. Großer Dank gilt auch Suzi Christof, die mir in vielen Angelegenheiten zur Seite stand und mir den Laboralltag versüßt hat. Vielen Dank auch an Nadine Moroff für die Unterstützung bei meinen Visumsproblemen und für das Bekanntmachen mit Land und Leuten.

Der GENUS-Gemeinde danke ich für die ausgeprägte Teamarbeit und die vielen erfolgreichen und schönen Expeditionen, die ich in guter Erinnerung behalten werde. Besonderer Dank gilt meinen GENUS Kollegen Anna, Lena, Simon, Thorsten und Karo, denen ich für die freundschaftliche Zusammenarbeit und die vielen unvergesslichen Erlebnisse danke. Ein großer Dank gilt auch den Kapitänen und den Crews der Forschungsschiffe Africana, Discovery, M. S. Merian und Meteor für die Zusammenarbeit und Unterstützung während der Expeditionen.

Vielen Dank an die Techniker des ZMT, Dorothee Dasbach, Dieter Peterke, Matthias Birkicht, Christina Staschok, Stefanie Bröhl, Conny von Waldhausen und Epiphane Yéyi für die vielen Ratschläge und die Unterstützung bei den Vorbereitungen für die Expeditionen aber auch bei den Probennahmen und den Analysen. Dem Team aus der Bibliothek, Christina und Hanna, danke ich für die schnelle Beschaffung diverser Artikel.

Bei unseren studentischen Hilfskräften Csilla Kovacs, Laura Lehnhoff, Katharina Pilgram und Claas Steigüber möchte ich mich für die Unterstützung bei der Probenahme während der Expeditionen und der sich anschließenden Analysen bedanken.

Mein großer Dank geht auch an alle Kollegen/innen des ZMT, die zu einem freundschaftlichen und vertrauensvollen Arbeitsklima beigetragen haben, allen voran Antje, Luci, Claire, Corinna, Astrid, Swati, Shilly, Sven, Marc, Francisca und Celeste.

Ich bedanke mich bei allen, die mir in den letzten Zügen meiner Doktorarbeit mit Ratschlägen und aufmunternden Worten zur Seite gestanden haben und diese Dissertation von ellenlangen Schachtelsätzen befreit haben – Antje, Luci, Lena, Simon und Anna – besten Dank an Euch!!

Meiner Familie und Hendrik gilt besonderer Dank für die stetige Unterstützung auf meinem bisherigen Weg und für alles was neben der Arbeit im Leben wichtig ist.



## ERKLÄRUNG

Eidesstattliche Erklärung  
(Gem. §7 (4) MIN-PromO)

Hiermit erkläre ich, Anita Flohr, geboren am 06.06.1982 in Eisenhüttenstadt, an Eides statt, dass ich die vorliegende Dissertation mit dem Titel:

*Carbon pumps in the Benguela Current upwelling system*

abgesehen durch die Beratung meiner Betreuer selbstständig ausgearbeitet und verfasst habe und keine anderen als die angegebenen Quellen und Hilfsmittel verwendet habe bzw. die benutzten Quellen als solche kenntlich gemacht habe. Ich habe die vorliegende Arbeit weder gänzlich noch in Teilen in einem anderen Fachbereich im In- oder Ausland im Rahmen eines Prüfungsverfahrens vorgelegt.

Hamburg, den

---

Anita Flohr